Biochimica et Biophysica Acta, 1019 (1990) 171–224
Elsevier

BBABIO 43257

Biothermokinetics of processes and energy conversion

Dieter Walz

Biozentrum, University of Basel, Basel (Switzerland)

(Received 8 March 1990)

Key words: Biothermokinetics; Energy conversion; Thermodynamics; Kinetics

Contents

Correspondence: D. Walz, Biozentrum, University of Basel, Klingelbergstrasse 70, CH-4056 Basel, Switzerland.

I. Introduction

One characteristic of living systems is a continuous running of processes, and an equilibrium state for *all* processes occurs only when the system is dead. Therefore, life has to be supported by a regular input of energy in form of nutrients or light which is converted into other forms of energy needed by the system. Energy conversion between processes thus plays a vital role in biology and has attracted the interest of many researchers over the years.

One would expect that thermodynamics is the tool best suited for an assessment of energy conversion since after all the principal and fundamental laws of thermodynamics relate to energies. Unfortunately, and despite of its name, thermodynamics provides us with definite rules only for that state of the system which is of least interest, viz. the equilibrium state after death. The statements of thermodynamics pertaining to the living state are also universally applicable but cannot be exploited without further information about the processes, in particular the rate at which they proceed. It thus appears that a kinetic description of the processes would be the most appropriate. However, such a description requires a detailed mechanism which is often not known, particularly in the early stage of investigation of a system.

Attempts to overcome this dilemma came first from an extension of thermodynamics into the domain near equilibrium [1–3], and the so-called non-equilibrium thermodynamics (NET) arrived at is still independent of any particular mechanism as is thermodynamics. Energy conversion can be elegantly taken into account by NET [4,5], but its applicability to biological processes which occur far from equilibrium was severely disputed (see, for example, Ref. 6). Nevertheless, many systems

were investigated by means of NET (for a review see Ref. 7) and were found to comply with this formalism. Evidence that relations similar to those predicted by NET can exist under certain constraints and thus would explain these findings was presented by Rottenberg [8] and later by Van der Meer et al. [9] on the basis of simple enzyme kinetics. This approach was vastly extended by Westerhoff and Van Dam [10], which eventually led to what these authors call 'mosaic non-equilibrium thermodynamics' [11].

On the other hand, there is a constant progress in elucidating the molecular mechanisms underlying the processes of energy conversion. A sufficiently detailed mechanistic scheme then provides us with all we need for a consistent description as done by Hill [12–14] which automatically takes care of thermodynamics. The qualification 'sufficiently detailed' in the above statement expresses the actual problems inherent in this approach because the characterization of an enzyme-catalyzed process the way it is commonly done (i.e., by means of the so-called Michaelis-Menten parameters, see e.g., Segel [15]) does in most cases not include the required amount of detail. Moreover, the knowledge about different parts of the system may be quite differently detailed, which prevents a description of the whole system on the same level.

This review, then, attempts to illuminate the different facets of processes in biological systems from the thermodynamic as well as the kinetic point of view, as should be expressed by the notation 'biothermokinetics'. After collecting together the principal aspects of thermodynamics in Section II, we shall consider in some detail interfacial phenomena and in particular the electrical surface potentials which are sometimes mistaken for an 'energy storage device' (Section III). We then turn to the kinetics of as yet uncoupled chemical reactions and transport processes (Section IV) in order to learn how kinetic schemes are translated into relations which allow us to link kinetics and thermodynamics, as done in Section V. Thus equipped, we can enter the large field of coupled processes in Section VI and discuss the different modes of coupling as well as possible means for their description. Before starting, however, I would like to add some comments.

The presentation of the subjects is in more general terms and only occasionally is a particular system addressed. As a consequence, many colleagues will not find their work mentioned here, which should by no means be misinterpreted as meaning that their contributions are not appreciated. But, in order to limit this review to a reasonable length, I had to refrain from going into detail, which is also legitimate because the literature has been comprehensively reviewed by Westerhoff and Van Dam [11]. I am aware of the fact that not every reader may be so fond of a mathematical notation, hence I have tried to cut the number of equations in the text as much as possible and to find the best intelligible presentation for them. Additional equations are collected in the Appendix for purpose of reference.

II. Thermodynamics

II.A. Systems, phases and compartments

The first step in the biothermokinetic description of a given experimental system is the definition of a suitable thermodynamic system. The goal of this step is to obtain an isolated system, i.e., a system which does not exchange heat or matter with its surroundings. To this end, the elements of the experimental system are substituted by equivalent elements of the thermodynamic system which have well-defined thermodynamic parameters and properties in terms of exchange of heat and matter. The actual topology of the experimental system need not be retained. In fact it is often advantageous to combine physically disconnected spaces in the experimental system, which are expected to have identical composition due to the same processes occurring in and around them, into one space in the thermodynamic system.

Suppose we have a suspension of membrane vesicles (e.g., isolated mitochondria, thylakoids or vesicles obtained from a reconstitution of a purified protein with lipids) in a suspending medium of known composition. In order to eliminate effects of a varying ambient temperature we place the vessel containing the suspension in a thermostat, which should guarantee a constant temperature in the system. Moreover, an effective stirring of the suspension will prevent the formation of gradients in the suspending medium. Since the reaction vessel is open, the atmospheric pressure acts as a barostat, i.e., the suspension is under constant pressure (see Fig. 1A).

When translating such an experimental system into a thermodynamic system, we first define a heat reservoir whose heat capacity is assumed to be so large that it can act as a heat sink or heat source, i.e., heat supplied to or absorbed from the rest of the system does not change the temperature (see Fig. 1B). Similarly, we define a 'reservoir for mechanical work' which provides the energy for the stirring device. Next we recognize that the system contains two *phases*, a phase being defined by the chemical nature of its major constituent. One phase is constituted by the membranes of the vesicles, while the other is the aqueous phase in the suspending medium and in the internal space of the vesicles. If we assume that the vesicles are identical in composition, we can combine all membranes into one extended and, for example, plane membrane. In doing so we have implicitly assumed that the aqueous phases in the internal spaces of the vesicles can also be collected and placed

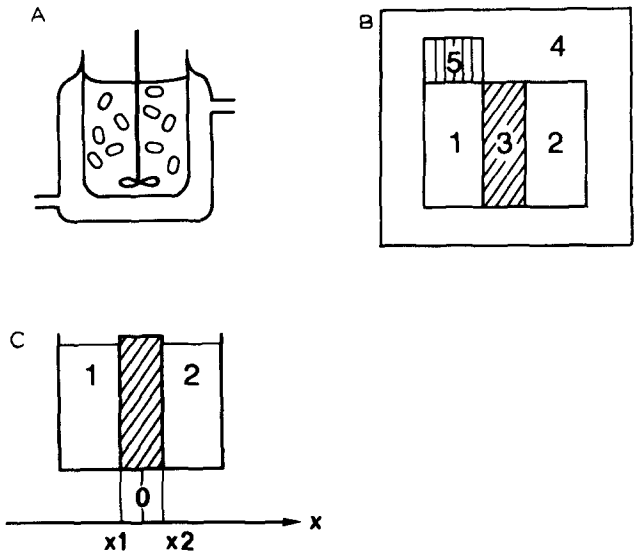

Fig. 1. Translation of an experimental system (A) into a thermodynamic system (B). In (B) two compartments with an aqueous phase (1, 2) are separated by a membrane (3) and surrounded by two reservoirs for heat (4) and mechanical work (5), respectively. The two-compartment system in (C) is the part of (B) in which the processes of interest take place. The x-axis is used as a space coordinate. For further explanation see text.

into one *compartment*. This compartment is separated by the membrane from another compartment which contains the aqueous phase constituted by the suspending medium (see Fig. 1B).

The thermodynamic system thus constructed is totally isolated from its surroundings and comprises all elements of the experimental system. Neither energy nor matter needs to be supplied from the outside world during the experiment. The walls between the reservoirs and the compartments are selectively permeable to heat and mechanical energy. Note that the heat formed by the stirring of the sample is absorbed by the heat reservoir. The aqueous phases are homogeneous, i.e., temperature, composition and electrical potential are the same throughout a given compartment. This is achieved by stirring for the suspending medium. The internal spaces of the vesicles are obviously not stirred. However, due to the small dimension of these spaces, diffusion of matter and heat is usually much faster than the processes which cause a change in composition and give rise to a production of heat. Hence, we can treat the compartment representing the combined internal spaces as if it were stirred. Finally, we assume a constant pressure throughout the system * due to the barostatic effect of the atmospheric pressure.

* This implies that the movement of solutes between the compartments is accompanied by a flow of water which annihilates osmotic pressure differences. Since the change in volume of the internal space of the vesicles can be rather limited, we have to expect severe interferences from this phenomenon unless it is carefully controlled.

When constructing the thermodynamic system, we have neglected the analytical devices needed to follow the processes in the experimental system. This is legitimate, since monitoring the parameters of the system should not disturb the processes. Although no information can be obtained without some interaction of an analytical device with the component to be assessed, the effect of this interaction should be negligibly small. Thus, the light intensity of a spectroscopic device should not give rise to photochemical processes, or the current through a pair of electrodes should be so small that it does not change the composition.

II.B. Thermodynamic potentials

The state of a system is uniquely defined by its internal energy, U, which is the sum of all sorts of energies present such as mechanical energy, heat or chemical energy. The internal energy $U(S, V, L, N_i)$ is a unique function of the state parameters volume V, elongation L (which is taken as a measure for performing mechanical work), chemical composition as indicated by the mole numbers N_i of the ith species, and a potential called entropy S [1–3,16]. It is important to note that U and S are potentials, i.e., their value is uniquely defined for a given state of the system independent of the path on which this state was reached. The parameters V, L, and N_i which define the state are implicitly independent of such paths. In a thermodynamic system like that depicted in Fig. 1B, the internal energy U_k can be defined separately for the kth part of the system (the parts being the reservoirs, the compartments and the membrane). The internal energy of the whole system is then

$$U = \sum_k U_k(S_k, V_k, L_k, N_{i,k}) \tag{1}$$

where the sum has to be taken over all parts.

The processes occurring in a system cause a transition of the system from one state to another. In the following discussion we dissect this transition into small increments which allows us to apply differentials for the variations of the parameters of the system. The change in internal energy of a given part of the system due to such an incremental transition amounts to

$$\mathrm{d}U_k = T\,\mathrm{d}S_k - P\,\mathrm{d}V_k + X_k\,\mathrm{d}L_k + \sum_i \tilde{\mu}_{i,k}\,\mathrm{d}N_{i,k} \tag{2}$$

where P and T denote, respectively, the pressure and the absolute temperature in the system, which are both constant as discussed in the preceding section. When writing Eqn. 2 we have made use of the Gibbs-Duhem relation, $\mathrm{d}TS_k - \mathrm{d}PV_k + \mathrm{d}X_kL_k + \Sigma d\tilde{\mu}_{i,k}N_{i,k} = 0$. Moreover, we have introduced the *electrochemical poten-*

tial of the ith species as the partial derivative of U_k with respect to $N_{i,k}$ at constant S, V and L,

$$\tilde{\mu}_{i,k} = [\partial U_k / \partial N_{i,k}]_{S,V,L} \tag{3}$$

and the potential X_k for mechanical work similarly defined as $\partial U_k / \partial L_k$. Again, as indicated by their names, $\tilde{\mu}_{i,k}$ and X_k are potentials like U and S.

The first law of thermodynamics states that energy cannot be created or annihilated, but only converted from one form into another. Since the total system is isolated (see preceding section), it does not exchange energy or matter with its surroundings; therefore, $U =$ constant or $\mathrm{d}U = 0$ for an incremental transition. It then follows from Eqns. 1 and 2 that

$$\sum_k \left[T\,\mathrm{d}S_k - P\,\mathrm{d}V_k + X_k\,\mathrm{d}L_k + \sum_i \tilde{\mu}_{i,k}\,\mathrm{d}N_{i,k} \right] = 0 \tag{4}$$

Since the total volume of the system is constant, $\Sigma P\,\mathrm{d}V_k = 0$. No change in chemical composition occurs in the reservoirs shown in Fig. 1B, i.e., $\mathrm{d}N_{i,4} = \mathrm{d}N_{i,5} = 0$. Moreover, $\mathrm{d}L_i \neq 0$ only for $k = 5$. Hence, for the system in Fig. 1B, Eqn. 4 reads

$$T \sum_k \mathrm{d}S_k + \sum_{k=1}^{3} \left[\sum_i \tilde{\mu}_{i,k}\,\mathrm{d}N_{i,k} \right] + X_5\,\mathrm{d}L_5 = 0 \tag{4a}$$

If temperature and pressure are constant, a new potential, G, called *Gibbs free energy* can be defined as

$$G = U - TS + PV \tag{5}$$

It measures the system's capability to perform useful work from either a mechanical potential, X, or the electrochemical potentials, $\tilde{\mu}_i$. Its change in the kth part of the system becomes (cf. Eqn. 2)

$$\mathrm{d}G_k = \mathrm{d}U_k - T\,\mathrm{d}S_k + P\,\mathrm{d}V_k = X_k\,\mathrm{d}L_k + \sum_i \tilde{\mu}_{i,k}\,\mathrm{d}N_{i,k} \tag{6}$$

It is important to realize that $\mathrm{d}G_k$ in Eqn. 6 merely indicates how much the free energy changes in a transition. The actual fate of $\mathrm{d}G_k$ is considered in the following section.

II.C. The dissipation function

The second law of thermodynamics states that the change in entropy of a system has to be positive (or zero in a special case, see below) when the system changes from one state to another. Rearranging Eqn. 4a and introducing Eqn. 6 yields

$$T\,\mathrm{d}S_{\mathrm{tot}} = T \sum_k \mathrm{d}S_k = -X_5\,\mathrm{d}L_5 - \sum_{k=1}^{3} \left[\sum_i \tilde{\mu}_{i,k}\,\mathrm{d}N_{i,k} \right] = -\mathrm{d}G_{\mathrm{tot}} \tag{7}$$

where $\mathrm{d}S_{\mathrm{tot}}$ and $\mathrm{d}G_{\mathrm{tot}}$ are the change in entropy and Gibbs free energy, respectively, for the total system. Thus, the compulsory increase in entropy is covered by a decrease in free energy. But we are interested in energy conversion and now Eqn. 7 tells us that all of the free energy is 'lost in entropy'. This is only an apparent contradiction, since the energy conversion we are interested in is hidden in the statement that the system changes its state. In fact, we have not considered how this change is brought about or, in other words, what relations exist between the $\mathrm{d}N_{i,k}$.

In a more detailed treatment, it is possible to analyze further the entropy changes $\mathrm{d}S_k$ for each part of the system [1–3,5,11]. It is then recognized that $\mathrm{d}S_k = \mathrm{d}_e S_k + \mathrm{d}_i S_k$, where $\mathrm{d}_e S_k$ and $\mathrm{d}_i S_k$ are called the 'exchange' and the 'internal' contribution, respectively *. The exchange contribution is 'compulsory' and is present even if the transition of the system is conceptually made to occur from one equilibrium state (or very close to it) to another, i.e., if all changes in the system associated with the transition are brought about by so-called *reversible processes*. In contrast, the internal contribution arises only if *irreversible processes* are involved in the transition. It is found that $\Sigma\,\mathrm{d}_e S_k = 0$ which means that $\mathrm{d}S_{\mathrm{tot}} = 0$ for a reversible transition. Thus, no free energy has to be spent for an entropy change (cf. Eqn. 7) in a reversible transition and all can be used in the energy conversion referred to above. However, *reversible transitions are hypothetical borderline cases hardly realized in practice because they imply that the processes associated with them occur at an infinitely small rate.* Processes of interest proceed at finite rates and therefore give always rise to an expenditure of free energy and an increase of entropy which amounts to $\mathrm{d}S_{\mathrm{tot}} = \Sigma\,\mathrm{d}_i S_k$. As a consequence, the free energy available for the energy conversion is always less in real processes than expected from the corresponding hypothetical reversible transitions.

The change in entropy $\mathrm{d}S_{\mathrm{tot}}$ in Eqn. 7 includes a contribution arising from the irreversible process of stirring of the sample which is driven by the term $X_5\,\mathrm{d}L_5$. This contribution is of no relevance for the processes we are interested in because a partial conversion of mechanical energy invested in stirring into the energy involved in these processes can be excluded **. Therefore, in what follows we consider only the entropy change, $\mathrm{d}S$, due to the processes of interest, which is equivalent to singling out the two-compartment system shown in Fig. 1C from the total thermodynamic system.

---

* A more appropriate notation for $\mathrm{d}_e S_k$ and $\mathrm{d}_i S_k$ would be $\delta_e S_k$ and $\delta_i S_k$, respectively, since exchange and internal entropy change are not total differentials as is their sum $\mathrm{d}S_k$.

** Such a conversion would occur only when the viscous drag created by the stirring affects the electrochemical potentials $\tilde{\mu}_{i,k}$.

When taking the time derivative of dS, we obtain from Eqn. 7:

$$\Phi = T\,dS/dt = -\sum_{k=1}^{3}\left[\sum_i \tilde{\mu}_{i,k}\,dN_{i,k}/dt\right] \geq 0 \tag{8}$$

The quantity Φ is called the '*dissipation function*' and indicates the rate of the loss (or dissipation) of free energy due to irreversible processes other than stirring. For a comment on the notion of 'dissipating free energy' see Westerhoff and Van Dam [11]. According to the second law of thermodynamics, Φ has to be positive and vanishes for the hypothetical case of reversible processes or when the equilibrium state is reached (see subsection II.E).

II.D. Flows and forces

In order to determine the dissipation function in Eqn. 8 at any state of the system in the course of an experiment, it suffices to estimate the electrochemical potentials $\tilde{\mu}_{i,k}$ and the pertinent time derivatives $dN_{i,k}/dt$ for the constituents of the system. No knowledge of the actual processes which take place in the system and cause $dN_{i,k}/dt \neq 0$ is required. This allows us to define these processes in any convenient form with the only limitation that a given set of definitions has to comply with the dissipation function. In what follows, we assume that the processes in the membrane phase (index $k = 3$ in Eqn. 8) have reached a steady state (see subsection II.E-2) so that $dN_{i,3}/dt = 0$. We then are only concerned with the processes occurring in the two compartments of Fig. 1C.

II.D-1. Chemical reactions and redox reactions

We first consider a chemical reaction which occurs in one of the compartments. It is given the index j (in order to distinguish it from other reactions) and is represented by

$$\sum_s \nu_{Sj,s} S_{j,s} \rightleftarrows \sum_p \nu_{Pj,p} P_{j,p} \tag{9}$$

The reaction converts the substrates $S_{j,s}$ with stoichiometric coefficients $\nu_{Sj,s}$ into the products $P_{j,p}$ with stoichiometric coefficients $\nu_{Pj,p}$ and vice versa. Mass balance imposes a strict relation on the mole numbers of substrates and products of a reaction. It is most conveniently expressed by means of a quantity called degree of advancement, ξ_j, defined as [3]:

$$\xi_j = [N_{Sj,s}(0) - N_{Sj,s}(t)]/\nu_{Sj,s}$$

$$= [N_{Pj,p}(t) - N_{Pj,p}(0)]/\nu_{Pj,p} \tag{10}$$

where the arguments t and 0 indicate the mole numbers, respectively, at time t and at the beginning ($t = 0$) of the experiment. Note that the expression for substrates in Eqn. 10 becomes identical with that for products if we adopt the convention that the *stoichiometric coefficients for substrates have a negative sign and those for products a positive sign*. Moreover, as already implied with the notation substrates and products, we have introduced a *positive direction for the reaction* when going from substrates to products in the sense that $d\xi_j \geq 0$. Taking the time derivative of ξ_j in Eqn. 10 yields a measure for the rate of the chemical reaction which we denote by the *flow of the reaction*

$$J_j = d\xi_j/dt = [dN_{Rj,r}/dt]/\nu_{Rj,r} \tag{11}$$

where reactant $R_{j,r}$ now stands as an abbreviation for substrates $S_{j,s}$ or products $P_{j,p}$ which need no longer be distinguished if the above sign convention is used. When introducing the time derivatives for the mole numbers in Eqn. 11 into Eqn. 8, the corresponding $\tilde{\mu}_{Rj,r}$ can be collected and abbreviated by a quantity known as the *affinity*, A_j, of the jth reaction [3]

$$A_j = -\sum_r \nu_{Rj,r}\tilde{\mu}_{Rj,r} \tag{12}$$

The quantity A_j is an example of a *thermodynamic force*, in this case of the jth reaction.

A redox reaction consists of just an electron transfer between substrates whereby the products are formed. Such a reaction is more appropriately formulated in terms of redox couples [17]. The ith redox couple in the system is represented by

$$R_{i,o} + n_i e \rightleftarrows R_{i,r} \tag{13}$$

where $R_{i,o}$ and $R_{i,r}$ denote the oxidized and the reduced species, respectively, while n_i is the number of electrons which the couple can exchange. Let us arbitrarily select one of the redox couples in the jth redox reaction as being the electron donating couple and denote its reduced and oxidized species by $D_{r,j}$ and $D_{o,j}$, respectively; the other redox couple is then the electron accepting couple with species $A_{r,j}$ and $A_{o,j}$. This notation also defines the positive direction of the redox reaction which reads

$$n_{A,j}D_{r,j} + n_{D,j}A_{o,j} \rightleftarrows n_{A,j}D_{o,j} + n_{D,j}A_{r,j} \tag{14}$$

where $n_{D,j}$ and $n_{A,j}$ are the n_i values (see Eqn. 13) of the donating and accepting redox couple, respectively. The flow in Eqn. 11 is then equivalent to a flow of electrons, J_{ej}, associated with the redox reaction, while the force in Eqn. 12 is equivalent to the affinity of the electron

$$A_{e,j} = (\tilde{\mu}_{Dr,j} - \tilde{\mu}_{Do,j})/n_{D,j} + (\tilde{\mu}_{Ao,j} - \tilde{\mu}_{Ar,j})/n_{A,j} \tag{15}$$

II.D-2. Transport processes

When dealing with transport of species across the membrane, it is necessary to arbitrarily choose a *positive direction of transport which has to be the same for all transport processes*. Here we choose the direction from compartment 1 to compartment 2 (Fig. 1C) as positive. We then define the *flow for the transport* of the ith species as

$$J_i = -\mathrm{d}N_{i,1}/\mathrm{d}t = \mathrm{d}N_{i,2}/\mathrm{d}t \tag{16}$$

where the second part of Eqn. 16 arises from mass balance. Introducing the time derivatives into Eqn. 8 again shows that the $\tilde{\mu}_{i,k}$ can be collected. This results in the difference in electrochemical potential between the compartments

$$\Delta\tilde{\mu}_i = \tilde{\mu}_{i,1} - \tilde{\mu}_{i,2} \tag{17}$$

which is the *thermodynamic force* for a transport process.

II.D-3. Flows and forces in the dissipation function

Chemical reactions and transport processes are connected by the effect of their respective flows on the mole number of the species involved. Thus, for the ith species, which is transported and takes part as reactant $\mathrm{R}_{j,\mathrm{r}}$ or $\mathrm{R}_{k,\mathrm{r}}$ in the jth chemical reaction in compartment 1 or the kth reaction in compartment 2, respectively,

$$\mathrm{d}N_{i,1}/\mathrm{d}t = -J_i + \sum_j \nu_{\mathrm{R}j,r} J_j \tag{18a}$$

and

$$\mathrm{d}N_{i,2}/\mathrm{d}t = J_i + \sum_k \nu_{\mathrm{R}k,r} J_k \tag{18b}$$

The changes in mole number given by Eqns. 18 have to be identical with those in the dissipation function, and the chosen set of definitions of transport and reactions is then appropriate. In terms of flows and forces, the dissipation function (see Eqn. 8) reads

$$\Phi = \sum_i J_i \Delta\tilde{\mu}_i + \sum_j J_j A_j = \sum_k J_k X_k \geq 0 \tag{19}$$

where the sums have to be taken over all transported species and all chemical reactions occurring in both compartments. We recognize that the dissipation function is a sum of products of flows, J_k, and conjugated thermodynamic forces, X_k. The flow of a process has the same sign as its force when it runs 'downhill', i.e., when it occurs spontaneously, and the product of flow and conjugated force is positive. If flow and conjugated force have opposite signs the flow-force product is negative and the process is driven 'uphill' by another process (or processes). This is the thermodynamic expression of the energy conversion we are interested in. It is possible because only the sum of all flow-force products has to be positive according to Eqn. 19 and not each product by itself.

We have arrived at the above conclusion in most general terms without considering any mechanisms by which transport or chemical reactions are brought about. This is the great advantage of thermodynamics but, at the same time, its severe limitation. Thermodynamics cannot tell us how flows are related to their conjugated forces and, in the case of energy conversion, to the forces of other processes. Answers to this question can in general only be obtained on the basis of molecular or kinetic schemes (see Sections IV and VI). However, as we shall see in subsection VI.D, a phenomenological description of how flows depend on forces is possible. The only additional information to be invested is the assignment of coupling between the processes in the system.

II.E. Steady states and equilibrium state

There are particular states of a system which find their expression in the dissipation function. Typical for them is that the time derivatives of the mole number of all species vanish, which lets the dissipation function attain a minimal value. Depending on the flows at these states, we distinguish the *steady states* where flows in general do not vanish from the *equilibrium state where all flows are zero.*

II.E-1. The equilibrium state and equilibrium constants

This state is characterized by $\Phi = 0$ with the corollary that all processes have ceased and none of the parameters of the system changes anymore. It also implies that all flows vanish because *either a process is under a constraint or its force is zero* [18]. The latter condition allows us to introduce the equilibrium constants. Before doing so, we expand the electrochemical potential of the ith species in the kth compartment or phase into three terms *,

$$\tilde{\mu}_{i,k} = \mu^{\circ}_{i,k} + RT \ln\{f_{i,k} c_{i,k}\} + z_i F\psi \tag{20}$$

Here R and F denote the gas constant and the Faraday constant, respectively. The standard chemical potential, $\mu^{\circ}_{i,k}$, is a substance specific constant which also depends on the type of phase (hence index k retained) and, in general, on P and T, which, however, are constant in

* The symbols ln and log are used for the logarithm with respect to base e (natural logarithm) and 10 (decadic logarithm), respectively.

our system. The next term in Eqn. 20 comprises the concentration of the species defined as

$$c_{i,k} = N_{i,k}/V_k \tag{21}$$

where V_k denotes the volume of the compartment or phase. The factor $f_{i,k}$ is called the activity coefficient and comprises the interaction of the ith species with all other constituents of the phase. We shall assume throughout this review that activity coefficients can be set to unity. This is certainly a simplification, yet does not cause a loss in generality. The reader can easily rewrite the pertinent equations with $f_{i,k}$ included if he or she wishes to do so. The sum of the standard chemical potential and the concentration-dependent term is usually abbreviated by

$$\mu_{i,k} = \mu^{\circ}_{i,k} + RT \ln\{ f_{i,k} c_{i,k} \} \tag{22}$$

and called the chemical potential of the species. The last term in Eqn. 20 expresses the contribution of an electrical potential ψ of the phase * to $\tilde{\mu}$ and includes the valence (or charge number) z_i of the species.

This author has shown [17] that an electrochemical potential, $\tilde{\mu}_e$, can be formally assigned to the electron although this species does not exist as a free entity. The assignment is based on the presence of redox couples (see Eqn. 13), and the electrochemical potential of the electron associated with the ith couple is defined as

$$\tilde{\mu}_{e,i} = \mu_{e,i} - F\psi = \mu^{\circ}_{e,i} + (RT/n_i) \ln \rho_i - F\psi \tag{23a}$$

where $\mu_{e,i}$ is the chemical potential of the electron, and

$$\rho_i = c_{Rr,i}/c_{Ro,i} \tag{23b}$$

is called the reduction state of the couple. Activity coefficients were set equal to 1 in Eqn. 23b in line with the policy adopted here (see above). The standard chemical potential of the electron is

$$\mu^{\circ}_{e,i} = (\mu^{\circ}_{Rr,i} - \mu^{\circ}_{Ro,i})/n_i = -FE^{\circ}_i \tag{23c}$$

where the quantity E°_i is known as the standard redox potential of the couple. Each couple in the system thus determines its own $\tilde{\mu}_e$, which, however, poses no problems if consistently dealt with. This and other aspects, including the case of ligand binding, in particular H^+ ions, to the redox species, is discussed in Ref. 17.

The vanishing force for transport at equilibrium means $\Delta\tilde{\mu}_i = 0$ or $\tilde{\mu}_{i,1} = \tilde{\mu}_{i,2}$ (see Eqn. 17). We can generalize this condition and state that, *at equilibrium*, $\tilde{\mu}_i$ *has the same value in all phases and compartments into which the ith species can move*. The qualification of movement in this statement is important, although at equilibrium nothing moves. As discussed by Walz and Caplan [18] an element in the system which sets a restriction to the movement of the species (e.g., an impermeable membrane) may cause different electrochemical potentials at equilibrium in the phases or compartments separated by the restrictive element. It is therefore important to specify which possible constraints exist in a given equilibrium state.

The condition of equal electrochemical potential applied to the partitioning of a species between the membrane (index $k = 3$) and the aqueous phase in one of the compartments (index $k = 1$ or 2) yields by virtue of Eqn. 20

$$K_{pi} = \exp\left[\frac{\mu^{\circ}_{i,k} - \mu^{\circ}_{i,3}}{RT}\right] = \left[\frac{c_{i,3}}{c_{i,k}}\right]_{eq} \exp\{ z_i(\phi_3 - \phi_k) \} \tag{24}$$

where ϕ denotes the reduced electrical potential defined as

$$\phi = \psi F/RT \tag{25}$$

The quantity K_{pi} is the equilibrium constant for partitioning of a species called *partition coefficient*. It relates the concentrations of the species in the two phases at equilibrium. Note that these concentrations are affected by a possible difference in electrical potential between the phases. Obviously, $K_{pi} = 1$ for partitioning of a species between two equal phases (e.g., between the aqueous phases in the two compartments).

The condition $A_j = 0$ for the jth chemical reaction at equilibrium is transformed by means of Eqn. 20 into

$$K_{cj} = \exp\{ -\Delta G^{\circ}_j/RT \} = \left[\prod_r c^{\nu_{Rj,r}}_{Rj,r}\right]_{eq} \tag{26a}$$

where ΔG°_j is called the standard free energy of the reaction defined as

$$\Delta G^{\circ}_j = \sum_r \nu_{Rj,r} \mu^{\circ}_{Rj,r} \tag{26b}$$

K_{cj} is the *equilibrium constant* * for the reaction which determines the ratio of product and substrate concentrations at equilibrium, as indicated by the law of mass action on the right-hand side of Eqn. 26a. Similarly, for a redox reaction by virtue of Eqns. 23

$$K_{cj} = \exp\{ F(E^{\circ}_{A,j} - E^{\circ}_{D,j})/RT \} = [\rho^{1/n_{A,j}}_{A,j}/\rho^{1/n_{D,j}}_{D,j}]_{eq} \tag{26c}$$

It has to be stressed that equilibrium constants which emerge from standard chemical potentials are always

* For a comment on the controversy and legitimacy of the electrical term $z_i F\Psi$ in Eqn. 20 see [17]. Note the following printing errors in [17]: replace RT by RT/n in Eqn. 11; multiply the argument of ln by r in Eqn. 32; drop m in front of the sum in Eqn. 37.

* Note that equilibrium constants (if not dimensionless) have to be given in concentration units of M.

valid, irrespective of the state of the system. The term equilibrium in their name merely refers to the fact that they relate the concentrations of reactants at equilibrium.

II.E-2. Steady states, and the chemical capacity

As is evident from Eqns. 18, the mole number of the ith species in the kth compartment is constant when the flows in which the species takes part balance each other. Hence, it is not necessary for $dN_{i,k}/dt = 0$ that all flows vanish but, in order for this situation to persist longer than just for a short instant, the flows should be constant. As we shall see in Section IV flows are determined by the concentration of species rather than their mole numbers. We therefore would like to have negligibly small variations in concentrations. This leads us to the chemical capacity, $C_{ci,k}$, for species i in compartment or phase k, defined as

$$C_{ci,k} = dN_{i,k}/dc_{i,k} \tag{27}$$

which relates the change in concentration $dc_{i,k}$ in response to $dN_{i,k}$.

Some of the chemical reactions in which the species takes part may be just binding to another component(s) of the system without further chemical modification. We shall call such a component a 'buffer' for species i and assume that the binding reaction is always very close to equilibrium due to large kinetic constants and because the binding is not part of a reaction sequence (cf. subsection IV.A). With dissociation being the positive direction of the binding reaction, it then follows from Eqn. 26a

$$K_{Bi,k} = c_{i,k}(c_{Bt,k} - c_{ib,k})/c_{ib,k} \tag{28}$$

where $c_{i,k}$ and $c_{ib,k}$ denote the concentration of free and bound species i, respectively, while $c_{Bt,k}$ and $K_{Bi,k}$ are the total concentration of buffer and the dissociation constant for the binding of the species to the buffer B in compartment or phase k, respectively. Solving Eqn. 28 for $c_{ib,k}$ and recognizing that $dN_{i,k} = d[V_k(c_{i,k} + c_{ib,k})]$ we obtain

$$C_{ci,k} = V_k\left\{1 + \frac{c_{Bt,k}K_{Bi,k}}{(c_{i,k} + K_{Bi,k})^2} + \frac{d(\ln V_k)}{d(\ln c_{i,k})}\left[1 + \frac{c_{Bt,k}}{c_{i,k} + K_{Bi,k}}\right]\right\} \tag{29}$$

Let us assume that $V_k \approx$ constant which cancels the last term in curly brackets of Eqn. 29. We then realize that $C_{ci,k}$ is simply the volume of the phase or compartment, which is formally increased by the term due to binding of the species to a buffer. Note that for $c_{i,k} \ll K_{Bi,k}$ this term simplifies to $c_{Bt,k}/K_{Bi,k}$. According to Eqn. 27, $dc_{i,k}$ for a given $dN_{i,k}$ is the smaller the larger $C_{ci,k}$, which explains the notion of B being a buffer. The chemical capacity for a particular species, viz. the H^+ ion, is well known under a different name and slightly modified. For this species the logarithm of its activity called pH and defined as

$$pH_k = -\log\{f_{H,k}c_{H,k}\} \tag{30}$$

for an *aqueous phase* is more frequently used. Its chemical capacity is therefore defined with respect to pH and termed buffer capacity,

$$\beta_k = -(1/V_k)\, dN_{H,k}/dpH_k = -(C_{cH,k}/V_k)\, dc_{H,k}/dpH_k \tag{31}$$

Evidently, the contribution of V_k to the chemical capacity is eliminated in the definition of β. When applying Eqn. 31, we have to take into account that water itself is a 'buffer' for H^+ ions according to the reaction $OH^- + H^+ \rightleftarrows H_2O$ with the 'dissociation constant'

$$K_w = (f_{H,k}c_{H,k})(f_{OH,k}c_{OH,k}) \tag{32}$$

where K_w ($\approx 10^{-14}$ at room temperature) is equal to the actual dissociation constant multiplied by the concentration of water, which is assumed to be constant. We then obtain from Eqns. 29–31 with the assumption of $f_{i,k} = 1$

$$\beta_k = \ln 10\left[10^{-pH} + 10^{pH}/K_w + c_{Bt,k}\frac{K_{BH}10^{pH}}{(K_{BH}10^{pH} + 1)^2}\right] \tag{33}$$

Note that a variable volume, V_k, does not cause a term like that in Eqn. 29 for C_c because V_k is included in the definition of β. However, it would alter $c_{Bt,k}$, which is the total concentration of an H^+-buffer present in the kth compartment, and whose dissociation constant is K_{BH}.

Let us now return to the discussion of steady states. By means of the chemical capacity, we can assess the change in concentration of a given species due to the flows. We then have to compare this change to the concentration present in a given phase or compartment in order to decide whether this concentration can be considered as approximately constant. We realize that the chemical capacities for the membrane phase are by far the smallest in the system because of the rather small volume of this phase compared to that of the compartments. This is true even if the membrane contains constituents which effectively bind species (e.g., the membrane-bound enzymes to be discussed in Sections IV and VI). We therefore conclude that the concentrations in the membrane change the fastest, but also that the membrane is the first part of the system which reaches a steady state in terms of a balancing of flows as mentioned at the beginning of this subsection. An equivalent statement is that the relaxation times of the processes in the membrane are the shortest. The next part of the system to attain a steady state due to

balanced flows is compartment 2, which represents the internal space of the vesicles (see Fig. 1). Its volume is considerably smaller than that of compartment 1, and so are most likely the corresponding relaxation times. Since the relaxation times for the processes in the membrane are still substantially smaller than those for compartment 2, the membrane remains in a steady state while compartment 2 relaxes to it. The faster relaxing membrane processes almost immediately adapt to the changing conditions in compartment 2. We are thus left with compartment 1 representing the suspending medium as that part of the system which eventually determines whether the whole system reaches a steady state. A suitable design of the experiment in terms of substrates and products of the overall process, which results as a sum of all individual processes in the system, will allow compartment 1 to reach a steady state, at least approximately. Appropriate measures to this end include large enough concentrations and, if necessary and/or possible, addition of buffers. Alternatively, the crucial concentrations could be clamped.

Finally, it should be added that the qualification steady state pertains only to the system and not to all processes occurring in the system. It is therefore possible that certain processes in a system at steady state are very close to equilibrium because their kinetic parameters (see Section IV) are much larger than those of the other processes. A frequently encountered example is the binding of H^+ ions in acid/base pairs. It is then legitimate to approximate the force of such processes by zero because the offset of the force from zero, which generates the finite flow at the steady state, is negligibly small.

III. Interfaces and electrical potential profiles

III.A. Interfacial domains

The homogeneity of the aqueous phases discussed in subsection II.A applies to the bulk of the phases in the compartments. It is no longer true for the small domains adjacent to the boundary between two phases which are called interfaces. These domains correspond to the unstirred layers formed in a stirred viscous medium on its boundaries. Many processes in biological energy conversion are catalyzed by enzymes residing in membranes with substrates and products originating from the adjacent aqueous phases. The relevant concentration of these reactants is then not the bulk phase concentration but the one close to the membrane surfaces, i.e., in the unstirred interfacial domains.

In the case of uncharged reactants, substantial differences between bulk phase and surface concentration are unlikely because the enzyme catalyzed reactions usually cannot effectively compete with diffusion of substrates and products through the unstirred layers. A situation like that of a polarographic electrode in the saturation region (e.g., a Clarke-type oxygen electrode) does not occur. In the case of charged reactants, however, differences between bulk and surface concentration can exist irrespective of the rate of the enzyme-catalyzed reactions, provided that the membrane surfaces are charged. It is therefore appropriate to investigate more closely what governs the concentration profiles in the interfacial domains.

III.B. Electrical surface potentials

III.B-1. A Gedankenexperiment

The electrical potential on the surface of a charged membrane differs from that in the bulk of the adjacent aqueous phase, and the difference between the two values is called surface potential. Why this is so can be intuitively understood by the following Gedankenexperiment. Suppose we have a charged membrane in its 'dry state' in air. The fixed charges on the membrane surfaces are then neutralized by counter-ions which sit close to the fixed charges as in a crystal of salt. Upon immersion of the membrane into an aqueous phase, the fixed charges remain on the surfaces but the counter-ions, if not tightly bound, start to diffuse into the newly accessible phase. This movement is aided by the electrostatic repulsion between ions of equal sign but counteracted by the attraction between ions of opposite sign. The attraction prevents the counter-ions from eventually becoming equally distributed in the aqueous phase, but a diffuse layer of counter-ions close to the membrane surfaces is formed. If the aqueous phase also contains ionic species, those with the same sign as a given fixed charge on the membrane are expelled from the diffuse layer near this charge, while those with the opposite sign are accumulated and partially or fully replace the original counter-ions.

The Gedankenexperiment clearly shows that no input of energy is required in order to form the diffuse layers. The 'driving force' for their formation is an increase in entropy on expense of the electrostatic interaction energies which are reduced when going from a phase with low dielectric constant (air) to one with a high dielectric constant (water). In other words, despite of the ions' concentrations deviating from those in the bulk phase, *the diffuse layers are not a storage device for useful energy, and the surface potential is a 'dead' potential in this respect.* The diffuse layers represent a case of a restricted equilibrium [18] with the fixed surface charges constituting the restriction. According to this view, a new equilibrium state can be attained if the restriction is removed, i.e., if the surface charges are neutralized, e.g., by binding or release of H^+-ions. Again, the energy associated with the then no longer equilibrated ions is lost as entropy, which increases upon equilibration of the ions. A suitable device which could

make use of this energy is hard to conceive and seems not to exist in nature.

III.B-2. The Gouy-Chapman theory of diffuse layers

A quantitative description of diffuse layers was first worked out independently by Gouy and Chapman; it is still a useful approach, despite of its limitations [19]. Only plane membranes are considered which shall also serve as an approximation for the curved membranes of vesicles. (A rigorous treatment of the case of spherical vesicles is rather tedious.) Geometry then reduces to one dimension and can be assessed by the x-coordinate shown in Fig. 1C. The discrete charges of both signs on the membrane surface facing the kth compartment are represented by a surface charge density, σ_k. This means that the actual charges are replaced by a fictitious charge equal to the sum of all charges and evenly smeared over the whole surface.

Since the ions in the diffuse layers are equilibrated, their electrochemical potential has to be constant from the bulk of the phase up to the membrane surface. Hence from Eqn. 20 for the concentration $c_{i,k}$ of the ith ionic species in compartment k at position x

$$c_{i,k}(x) = c_{io,k} \exp\{-z_i(\phi(x) - \phi_k)\} \tag{34}$$

where ϕ is the reduced electrical potential (see Eqn. 25), while $c_{io,k}$ and ϕ_k denote the pertinent concentration and the reduced potential in the bulk phase, respectively. A charge density $\rho_k(x)$ results from the uneven distribution of ions in the kth diffuse layer which is related to the electrical potential according to Poisson's equation

$$\rho_k(x) = F\sum_i z_i c_{i,k}(x) = -(\epsilon_o D_a RT/F)\, d^2\phi/dx^2 \tag{35}$$

where ϵ_o and D_a denote the absolute permittivity and the dielectric constant of the aqueous phase, respectively. After substitution of $c_{i,k}(x)$ from Eqn. 34, Eqn. 35 can be readily integrated, which yields

$$d\phi/dx = s_k/\delta_k \left[\sum_i (c_{io,k}/c_{t,k})[\exp\{-z_i(\phi(x) - \phi_k)\} - 1]\right]^{1/2} \tag{36}$$

Here, $s_1 = \mathrm{sgn}(\sigma_1)$ and $s_2 = -\mathrm{sgn}(\sigma_2)$ [or $s_1 = s_2 = \mathrm{sgn}(\phi_2 - \phi_1)$ if $\sigma_k = 0$]; $c_{t,k}$ is a measure for the total concentration of ions also known as ionic strength

$$c_{t,k} = \tfrac{1}{2}\sum_i z_i^2 c_{io,k} \tag{37}$$

The quantity δ_k is the so-called Debye-Hückel length defined as

$$\delta_k = [RT\epsilon_o D_a/(2F^2 c_{t,k})]^{1/2} \tag{38}$$

The membrane does not contain movable charges, since the partition coefficient for ions into a hydrophobic phase is rather small. Hence $\rho(x) = 0$, and Poisson's equation (cf. Eqn. 35) can be easily integrated to yield $d\psi/dx = E_m = \text{constant}$, which means a constant electric field within the membrane, and (cf. Fig. 1C)

$$\psi(x) = \psi(x1) + E_m x \quad \text{for } x1 \le x \le x2 \tag{39}$$

The surface charge densities come into play via boundary conditions for the electric field at the membrane surfaces

$$D_a\, d\psi/dx|_{x=x1} - D_m E_m = -\sigma_1/\epsilon_o \tag{40a}$$

and

$$D_m E_m - D_a\, d\psi/dx|_{x=x2} = -\sigma_2/\epsilon_o \tag{40b}$$

where D_m denotes the dielectric constant of the membrane.

Eqn. 36 can be integrated only for special cases, e.g., if the aqueous phases contain only one symmetrical salt [19,20]. Alternatively, the exponentials could be expanded into Taylor series, but the resulting equation would still be transcendental in $\phi(x)$. Therefore, the electrical potential profile across the membrane in a given system can be obtained only numerically, and Eqns. 36–40 are sufficient for this purpose *. Fig. 2 then presents some typical examples of such profiles.

III.B-3. Characteristics of diffuse layers and surface potentials

The features of diffuse layers and of the surface potentials associated with them to be learned from the examples given in Fig. 2 can be summarized as follows. (i) Surface potentials decrease with increasing salt concentration. (ii) Divalent ions, particularly with sign opposite to that of the surface charge, are more effective than monovalent ions. (iii) The bulk to bulk potential difference, i.e., the membrane potential, has only minor effects on the surface potentials. Under no circumstances can the surface potential be inferred from the membrane potential. (iv) The surface potentials strongly affect the slope of the linear potential profile within the membrane. Under certain circumstances, the sign of the slope can even be opposite to that expected from the polarity of the membrane potential.

The concentration of any charged reactant follows the electrical potential in the diffuse layers according to

* In an iterative procedure, a value is assigned to $\phi(x_1)$ which yields $d\phi/dx|_{x=x1}$ (Eqn. 36) and in turn E_m as well as $\phi(x2)$ (Eqns. 40a and 39, together with 25). The derivative $d\phi/dx|_{x=x2}$ is then determined by two independent relations (Eqns. 36 and 40b), and the value of $\phi(x1)$ is varied until the two values for $d\phi/dx|_{x=x2}$ agree within a preset accuracy.

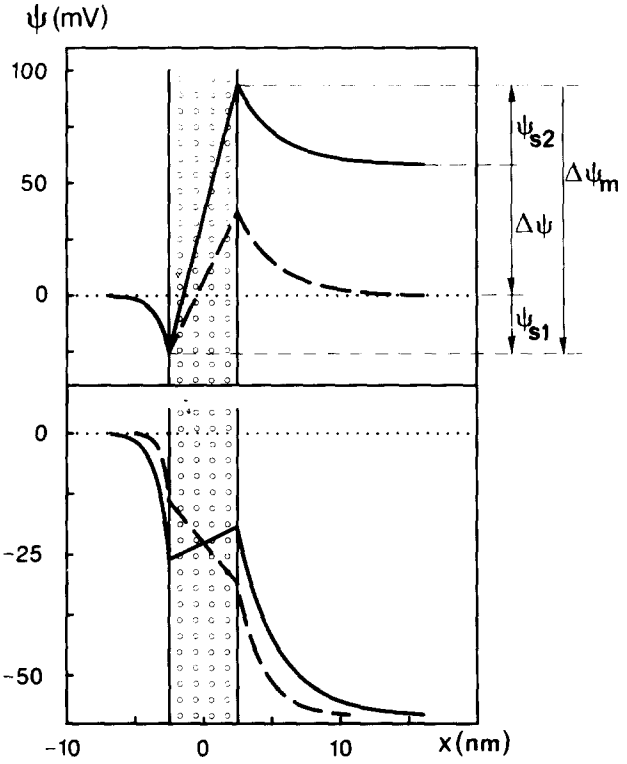

Fig. 2. Surface potentials calculated according to the Gouy-Chapman theory of diffuse layers. The membrane with thickness $d = 5$ nm has surface charge densities $\sigma_1 = -0.02$ C/m^2 and $\sigma_2 = 0.01$ C/m^2; dielectric constants are 80 and 5 for aqueous phase and membrane, respectively, temperature 20 °C. Bulk phase concentrations of salt are $c_{o,1} = 100$ mM and $c_{o,2} = 10$ mM (for geometry and indices see Fig. 1C). The upper panel pertains to a univalent salt and $\Delta\Psi = -58.2$ mV (solid line) or 0 mV (broken line). The lower panel is for $\Delta\psi = 58.2$ mV and a univalent salt (solid line) or a salt with divalent cations (broken line).

Eqn. 34. Moreover, if such a reactant is a major ionic species in the aqueous phases, the potential profile can change in the course of an experiment due to the varying concentration of the reactant. In order to avoid such a phenomenon and to minimize the effect of surface potentials it is advisable to include, whenever possible, an 'inert' electrolyte in actual experiments whose concentration should not change appreciably during the experiment and should be high enough to depress the surface potentials as much as possible. In addition, such electrolytes help to keep activity coefficients constant (cf. subsection II.E-1).

III.C. Electrical capacitance of membranes

The formation of a membrane potential requires the transfer of charges from one compartment to the other. These charges appear in the diffuse layers or, if no surface charges are present, form the diffuse layers. The membrane is thus electrically equivalent to a capacitor; the hydrophobic part of the membrane constitutes the dielectric and the diffuse layers together with that part of the membrane into which ions penetrate represent the metal plates of the capacitor *. The overall charge per membrane area in the kth diffuse layer, q_k, is obtained by integrating $\rho_k(x)$ from the surface of the membrane to the bulk. Eqn. 35 then yields, in view of Eqn. 36,

$$q_k = -(1/\delta_k)\left[\sum_i (c_{io,k}/c_{i,k})[\exp\{-z_i(\phi(x_k)-\phi_k)\}-1]\right]^{1/2} \tag{41}$$

The capacitance per unit area, C, of a capacitor whose plates have an area A is defined as

$$C(U) = (1/A)\,\mathrm{d}Q/\mathrm{d}U \tag{42a}$$

where $\mathrm{d}U$ is the increment in voltage across the capacitor generated by the increment of charge $\mathrm{d}Q$ withdrawn from one plate and added to the other. Note that $C(U) =$ constant for an ideal electrical capacitor. When applied to the capacitance of the membrane, C_m, this definition reads

$$C_m(U, c_{i,k}, \sigma_k) = -\mathrm{d}q_1/\mathrm{d}U = \mathrm{d}q_2/\mathrm{d}U \tag{42b}$$

where the voltage is equal to the membrane potential, $U = \psi_1 - \psi_2$. Total concentrations and surface charge densities have been included as arguments of C_m because these parameters determine the surface potentials and therefore are likely to affect C_m.

It is found that membranes behave as almost ideal capacitors with respect to the voltage (or membrane potential), i.e., C_m is essentially independent of U. However, a dependence on $c_{i,k}$ is observed for membranes without surface charge densities σ_k. This dependence is gradually reduced with increasing σ_k. For $\sigma_k \approx 0$, the diffuse layers arise entirely from the charges transferred between the compartments due to U. In the presence of large enough surface charge densities, the diffuse layers are predominantly determined by σ_k, and the charges due to U play only a minor role. Since biological membranes almost invariably carry charges at physiological pH values, we can assume as a reasonable approximation that $C_m \approx$ constant and has a value between 0.7 and 1.1 μF/cm^2 [21]. It should be kept in mind, however, that an effective change in C_m of a given membrane may occur when the ionic strength is substantially altered.

* Strictly speaking, a membrane with diffuse layers is electrically equivalent to three capacitors in series, one consisting of the membrane with its surface charges and two associated with the diffuse layers. Since the latter two capacitors cannot be used for energy storage (see subsection III.B-1), it is appropriate to unite the three capacitors into one, which then can serve as a storage device for electrical energy.

III.D. Relevance of membrane topology to potential profiles

The Debye-Hückel length, δ_k, is a measure for the thickness of the kth diffuse layer, which roughly extends over $3\delta_k$. This means that beyond this distance bulk phase properties for electrical potential and ion concentrations can be assumed (although theoretically these properties are only asymptotically reached at an infinite distance from the membrane surface). Typical values for 3δ are of the order of nanometers for tenth to hundredth molar ionic strengths.

The membranes of energy converting (or signal transducing) organelles often display a complex topology, a typical example being the closely spaced membranes of thylakoids in chloroplasts which are separated by only a few nanometers. Other examples are the cristae of mitochondria or the disks in the outer segments of retinal rods. In such systems the diffuse layers of neighboring membranes can start to overlap. They are still described by Eqns. 34–40, but a simple addition of the two layers calculated for the membranes spaced far enough apart is not permissible because of the non-linearity in Eqn. 36. An analytical solution to Eqns. 36–40 can be found for special cases which is rather complex [19,22,23] and therefore is not given here. Instead, examples for the electrical potential profile across a thylakoid stack are presented in Fig. 3 which demonstrate that, depending on conditions, a domain with bulk phase properties between the membranes does no longer exist.

According to the features of diffuse layers summarized in subsection III.B-3 one could think of choosing a high enough ionic strength in order to create or broaden the bulk phase region between the membranes. Such a measure may not always work as desired because of the effect of surface charges on the spacing of the membranes. At least for thylakoids, it is now accepted that stacking results from an interplay between Van der Waals attraction and electrostatic repulsion [24], and a similar mechanism is to be expected for the formation of the flat thylakoids with essentially plane and parallel membranes. A decreased electrostatic repulsion due to a better shielding of the surface charges by a higher ionic strength causes a shortening of the distances between membranes which in turn brings the diffuse layers closer together.

The situations depicted in Fig. 3 are hard to reconcile with the concept introduced in subsection II.A, which states that the concentration of a given species and the

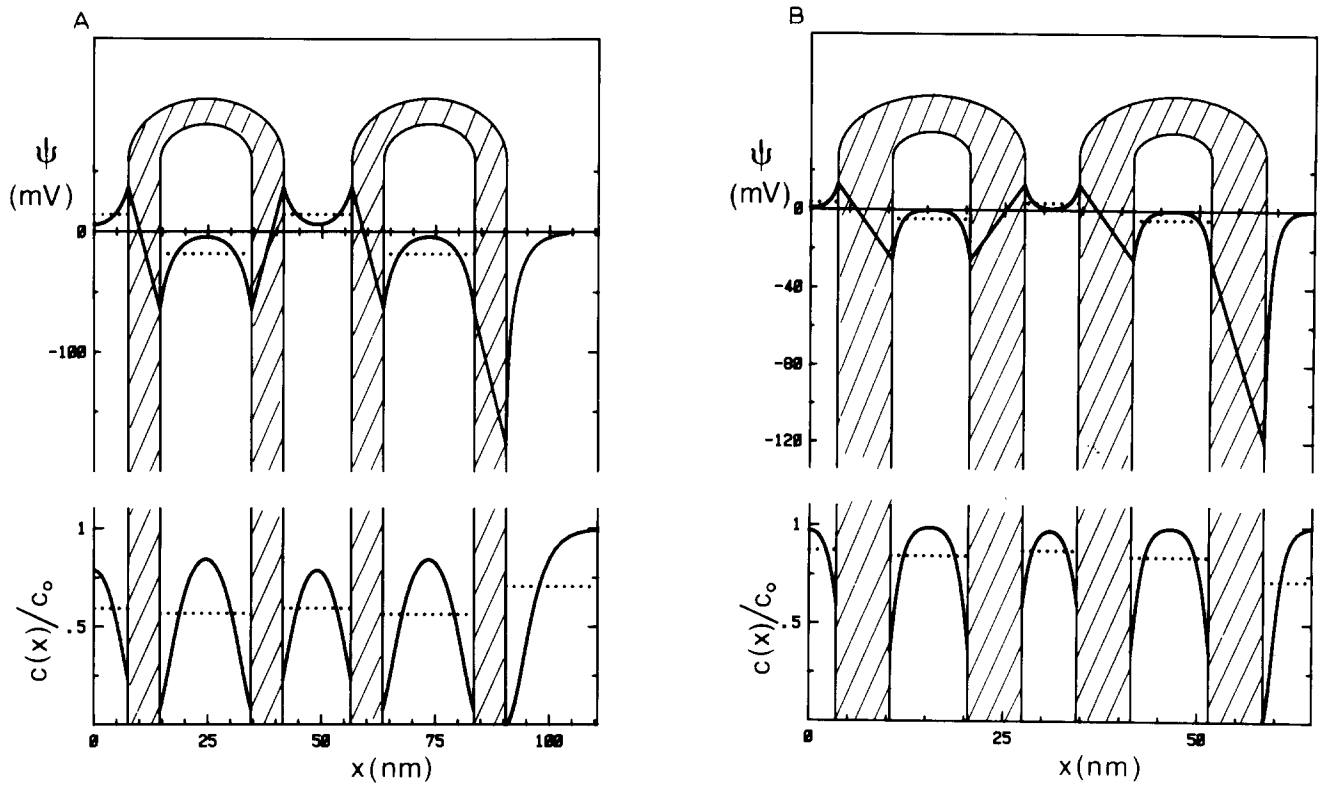

Fig. 3. Profiles of electrical potential and concentration of monovalent ions in a thylakoid stack. The upper panel in A and B shows the profile of the electrical potential and the lower panel the profiles for the concentration of those ions (with respect to the bulk phase concentration) whose valence has the same sign as the charges on the adjacent membrane surfaces. Surface charge densities (in C/m^2) are -0.02 and 0.01 on luminal and outer surface of thylakoid membranes, respectively, and -0.2 on the surface of the stack. Membrane thickness 7 nm, dielectric constants 5 and 80 for membrane and aqueous phase, respectively, temperature 20 °C. The concentration of ions in the bulk phase, and the distances of the membranes in and between thylakoids are, respectively, 10 mM, 20 nm and 15 nm (A); 100 mM, 10 nm and 7.5 nm (B).

electrical potential are constant in the major part of a compartment. The sum of the two, i.e., the electrochemical potential, of course is always constant. Average potentials can be defined which allow to retain the aforementioned concept (Walz, in preparation); however, their estimation requires a more complex procedure than that usually applied [25]. One major source of error is the assumption that any deviation of a marker's concentration from that in the suspending medium occurs uniquely in the inner space of organelles and is due solely to energization. Fig. 3 clearly shows that, even in non-energized thylakoids, the concentration deviates from the bulk phase concentration in and between the thylakoids. This has to be taken into account in order to arrive at thermodynamically meaningful data for the electrochemical potentials determined by means of marker distributions.

III.E. Limitations, refinements, and comments

III.E-1. Limitations of the Gouy-Chapman theory

The ionic species are treated as point charges which can attain unlimited high concentrations, and the chemical nature of the ions is not considered. The interaction of the ions with the membrane surface due to binding or adsorption can be included via the surface charge densities. Binding (or adsorption) is described by a dissociation constant (or a partition coefficient), and σ_k is adjusted according to the amount of bound ions, calculated with the surface concentration for the free ion. In order to prevent unrealistically high concentrations near the surface, a layer of adsorbed ions on the membrane can be defined (the Helmholtz layer) which is assumed to occur above a critical concentration [19]. Since the ions in this layer are no longer mobile, the potential drops linearly across the layer as determined by the dielectric constant being different from that of water and the membrane.

Due to the replacement of discrete charges on the membrane surface by a surface charge density, the Gouy-Chapman theory can yield only an 'average' diffuse layer, which is identical for any place on the membrane surface. Similarly, the constant D_w assumed for water disregards the fact that the water structure close to the membrane surface and particularly in the neighborhood of charges differs from that of bulk phase water. Ice-like structures in hydration shells require a dependence of D_w on the amount of charges present [26]. The refinement of discrete charges instead of σ considerably complicates the treatment of diffuse layers and requires detailed knowledge of the membrane structure, as does the inclusion of a variable D_w. It is worth doing only if the refined picture provides a possible explanation for an experimentally observed phenomenon (for an example see Ref. 27).

III.E-2. The electrical potential within the membrane

Neither fixed nor mobile charges were assumed to occur in the interior of the membrane. If transport of ions across the membrane takes place it should create only negligibly small concentrations of ions in the membrane, or it will be confined to special devices such as pores or carriers which occupy only a small fraction of the membrane area. These assumptions lead to the constant field approximation and the linear potential profile (cf. Eqn. 39) within the membrane.

Fixed charges in a membrane (e.g., due to acidic or basic amino acid residues in proteins) are likely to occur particularly if they are 'neutralized' by similar charges with opposite sign residing in the neighborhood. In addition, they can be formed upon energization of the membrane as exemplified by the charge separation created by redox processes in the primary reactions of the photosystems in thylakoid membranes [28]. Such charges greatly modify the electric field and the potential in a fairly large domain surrounding them and hence should be taken into account when the processes under investigation occur within this domain. This task can become very heavy depending on the level of approximation and details chosen for the description. A low level of approximation was chosen by this [17,29] and other authors [30] when evaluating the effect of such charges on the behavior of membrane-bound redox couples. A more realistic treatment of charges within the membrane was given by Duniec et al. [31] while the evolvement of the electrical potential profile following a charge separation in the membrane was investigated by Zimanyi and Garab [32]. The most comprehensive procedure was worked out by Klapper et al. [33]. The computational time and the amount of information required increases considerably when going to more detailed description, and one or both of these factors usually limits the feasibility.

A kind of a mixed view was adopted by Kamp et al. [34]. These authors assumed the H^+-binding groups in protein type layers adjacent to the hydrophobic core of the membrane to be so abundant that the charges associated with them can be treated as if they were mobile. Real diffusible ions were allowed to enter these layers according to given partition coefficients. Additional 'diffuse layers' thus arise which belong to the membrane and are interspersed between the diffuse layers in the aqueous phases and the core of the membrane. The equations corresponding to Eqn. 36 were linearized and surface charge densities were excluded in order to obtain an analytical solution for this system. A substantial potential drop in the additional layers was found which thus can serve as a storage device for H^+ ions. As a consequence, not all of these ions pumped in a pulse experiment with an H^+-translocating enzyme may appear in the aqueous phase, which could explain the 'missing H^+ ions' observed under certain conditions

(see, for example, Ref. 35). It should be noted, however, that the ions in such storage devices still have the same electrochemical potential as those in the aqueous phase (the description of diffuse layers relies on this very fact). Moreover, the linearization of Eqn. 36 causes a vast overestimation of the potential profile and thus the storage capacity of the protein layers for H^+ ions if the potential difference across these layers exceeds a few millivolts (compare Fig. 7 in Ref. 34).

The constant value assigned to D_m is another approximation. The domains of the membrane adjacent to the aqueous phases are more polar than the hydrophobic core. A dependence of D_m on position would therefore be more appropriate. Attempts to include the variable polarizability in a membrane exist but do not exceed the level of empirical approximations [36], one exception being the comprehensive treatment of charges mentioned above [33].

III.E-3. Some comments

In the above considerations, we have assumed a membrane potential to exist without specifying what determines its value. In the systems of interest in the present context, it is determined by the transfer characteristics of the membrane for ions and the concentrations of these ions in the bulk aqueous phases on both sides of the membrane (see subsection VI.A). A discussion of other conditions as well as a review on surface phenomena can be found in the paper of McLaughlin [37].

In most investigations (including this review) the constant field (or linear potential profile) approximation within the membrane is used, and surface phenomena are described by the classical Gouy-Chapman theory (in some cases even with a linearization of Eqn. 36). This is for good reasons because the refinements discussed above almost invariably increase the complexity of the equations to such an extent that the efforts required to arrive at a tractable solution seem not to be justified in view of the improvements to be gained. Quite frequently, the result of a refinement may introduce some ambiguity. In addition, it may turn out to be not so much different from the unrefined result in terms of experimentally assessable parameters that its validity can be tested.

IV. Kinetics of chemical reactions and transport

IV.A. First- and second-order chemical reactions

The rate laws for chemical reactions emerge from the view of activation and collision. The molecules of a species, M_i, are stable over a certain period of time because transitions to other conformations which they may adopt or the event of breaking into fragments are hampered by energy barriers. A molecule has to gain sufficient energy either due to thermal fluctuations or by collisions with other molecules in order to surmount these activation energy barriers [16,38]. These features can be condensed into a temperature-dependent rate constant, k_{Mi}, which determines the change in concentration of M_i, c_{Mi}, with time

$$dc_{Mi}/dt = -k_{Mi}c_{Mi}(t) \text{ (1st order)} \tag{43}$$

If two molecules M_1 and M_2 are ligated in a reaction, they have to collide in the right orientation and with sufficient energy for the bond between them to be formed. Again, a rate constant, k_{M12}, can be found which governs the time-course of this reaction

$$dc_{M1}/dt = dc_{M2}/dt = -k_{M12}c_{M1}(t)c_{M2}(t) \text{ (2nd order)} \tag{44}$$

Eqns. 43 and 44 pertain only to *unidirectional processes*. The fate of the molecular species M_i' formed by these processes was not yet considered.

Conservation of mass requires that $dc_{Mi'}/dt = -dc_{Mi}/dt$ and $dc_{Mi'}/dt = -dc_{M1}/dt$ due to the process described by Eqns. 43 and 44, respectively. The species M_i' can always undergo a reaction which yields back the species M_i from which they were formed. Hence, the net change in concentration of a species M_i caused by a given reaction is the sum of the changes arising from two unidirectional processes: one being the process in which the species itself takes part usually called the 'forward reaction', and the other called 'backward reaction' being the inverse of this process. This net change can then be used for assigning the flow to the given reaction (cf. Eqns. 11 and 16). Thus, the flow, J_i, pertinent to the ith reaction where, say, two substrates, S_{i1} and S_{i2}, are converted into the product P_i,

$$S_{i,1} + S_{i,2} \rightleftarrows P_i \tag{45}$$

becomes

$$J_i = V[k_i c_{Si,1}c_{Si,2} - k_{-i}c_{Pi}] \tag{46}$$

Here k_i and k_{-i} denote, respectively, the (unidirectional) rate constant for the second-order forward and the first-order backward reaction. Note that, in this case, 'forward' and 'backward' refer to the direction (arbitrarily) introduced when assigning the attributes 'substrates' and 'products' to the reacting species M_i and M_i' (cf. subsection II.D-1).

The product(s) of the ith reaction can in turn become the substrate(s) of the jth, kth,... reaction, or they may be also formed as products of other reactions. The change in concentration of any species M involved in one or several of such reactions is then given by

$$dc_M/dt\left[\sum_k \nu_k J_k\right]/V \tag{47}$$

where the sum has to be taken over all reactions in which M participates, and ν_k is its stoichiometric coefficient in the kth reaction (sign of ν_k according to the convention introduced in subsection II.D-1).

Suppose the product P_i in the reaction of Eqn. 45 is the substrate $S_{j,1}$ of the subsequent reaction

$$S_{j,1} + S_{j,2} \rightleftarrows P_{j,1} + P_{j,2} \tag{48}$$

then

$$dc_{P_i}/dt = k_i c_{S_{i,1}} c_{S_{i,2}} - (k_{-i} + k_j c_{S_{j,2}}) c_{P_i} + k_{-j} c_{P_{j,1}} c_{P_{j,2}} \tag{49}$$

When a *steady state* for P_i is attained (see subsection II.E-2), $dc_{P_i}/dt = 0$ and from Eqn. 49

$$c_{P_i} = (k_i c_{S_{i,1}} c_{S_{i,2}} + k_{-j} c_{P_{j,1}} c_{P_{j,2}})/(k_{-i} + k_j c_{S_{j,2}}) \tag{50}$$

Introducing Eqn. 49 into Eqn. 47 written for $M = P_{j,1}$ yields

$$dc_{P_{j,1}}/dt = \frac{k_i k_j c_{S_{i,1}} c_{S_{i,2}} - k_{-i} k_{-j} c_{P_{j,1}} c_{P_{j,2}}}{k_{-i} + k_j c_{S_{j,2}}} \tag{51}$$

The same procedure repeated for $M = P_{j,2}$, $S_{i,1}$, $S_{i,2}$ and $S_{j,2}$ always yields the right-hand side of Eqn. 51 for $dc_{P_{j,2}}/dt$, $-dc_{S_{i,1}}/dt$, $-dc_{S_{i,2}}/dt$ and $-dc_{S_{j,2}}/dt$. If $k_{-i} \gg k_j c_{S_{j,2}}$ for all reasonable values of $c_{S_{j,2}}$ the denominator in Eqn. 51 can be approximated by k_{-i}, and the two consecutive reactions in Eqns. 45 and 48 can be combined into one overall reaction

$$S_{i,1} + S_{i,2} + S_{j,2} \rightleftarrows P_{j,1} + P_{j,2} \tag{52}$$

with

$$J_{ij} = V[(k_i k_j / k_{-i}) c_{S_{i,1}} c_{S_{i,2}} c_{S_{j,2}} - k_{-j} c_{P_{j,1}} c_{P_{j,2}}] \tag{53}$$

which mimics a third-order reaction in the forward direction. Note that the steady state for P_i ($= S_{j,1}$) is reached the faster the larger k_{-i} is with respect to $k_i c_{S_{i,1}} c_{S_{i,2}}$ and $k_{-j} c_{P_{j,1}} c_{P_{j,2}}$. By the same token, the concentration c_{P_i} attained in this state (Eqn. 50) decreases and may become negligibly small.

It is generally accepted that unidirectional reactions with order higher than 2 are rather unlikely, since they would require a simultaneous collision of three or more species. However, depending on the rate constants of sequential reaction steps and the actual concentrations of certain reactants, the formulation of higher order reactions may be legitimate as outlined above.

IV.B. Enzyme-catalyzed reactions

A catalyst reduces the activation energy of a reaction and thus increases the rate constants for both directions. In second-order processes, it can also increase the collision probability and promote the proper orientation of the reactants. In order to fulfill this task, the catalyst has to interact with the reactants and even may undergo chemical reactions. However, after completion of the catalyzed reaction, the original state of the catalyst has to be regenerated so that it can start a new cycle. A third aspect of catalysis concerns specificity. The interaction of the catalyst with different members of a group of reactants all being able to perform the same type of reaction can greatly vary, which causes a variable extent of acceleration for the reaction of the different members. An enzyme is a specialized protein optimally tailored to act as a catalyst for a particular reaction (or reactions) of a selected number of reactants and thus displays all aspects of a catalyst outlined above. The interaction gives rise to binding of the reactants to the enzyme and lowers the activation energies for the reactions of bound reactants.

IV.B-1. Chemical kinetics and the cycle diagram method for the description of enzyme catalysis

In terms of kinetics, the enzyme can be considered as if it were an additional reactant which, however, is present at a much lower concentration than the real reactants and which is restored at the end of a sequence of reactions. Thus, the simplest scheme for the enzyme-catalyzed reaction of S_1 plus S_2 to P (cf. Eqn. 61) is obtained when the following substitutions are made in Eqns. 45, 48 and 52: S_1 for $S_{i,1}$, the free enzyme E for $S_{i,2}$ and $P_{j,2}$, the enzyme-substrate complex ES_1 for P_i, S_2 for $S_{j,2}$, and P for $P_{j,1}$.

Due to the low concentration of the enzyme, the steady-state condition dc_{P_i}/dt ($= dc_{ES1}/dt$) $= 0$ is soon reached and independent of the condition $k_{-i} \gg k_j c_{S_{j,2}}$. The rate of the reaction is then given by Eqn. 51. It is found to be proportional to the free enzyme concentration c_E, which can be replaced by the total enzyme concentration, $c_{E,tot}$, by means of c_{ES1} ($= c_{P_i}$) given in Eqn. 50 and the mass balance for the enzyme, $c_{E,tot} = c_E + c_{ES1}$. Following this procedure, King and Altman [39] have worked out an algorithm for deriving the rate of enzyme-catalyzed reactions, which was used by Cleland [40], Segel [15] and others to treat a large number of different kinetic schemes.

A substantial extension of the algorithm according to King and Altman was presented by Hill [12–14]. This author focuses attention on the enzyme whose role is considerably upgraded from just being an additional reactant. Moreover, the cyclic behavior of the enzyme appears explicitly. A short outline of Hill's cycle diagram method can be found in the Appendix A.I, it suffices here to summarize its essential points.

The enzyme is considered to adopt different states during catalysis. Hence, binding of a reactant to the enzyme causes a transition to a new state in which the

bound reactant becomes an integral part of the enzyme. Further transitions can occur due to changes in enzyme conformation. A chemical reaction between bound reactants also gives rise to a change in conformation, since bound reactants are taken as integral parts of the enzyme. An appropriate sequence of transitions has to end at the state from which it started, thus constituting a given catalytic cycle of the enzyme. Moreover, dead-end branches may start off a given state which evidently do not contribute to catalysis but modify the overall activity of the enzyme.

A remark on the definition (or recognition) of different states in an enzyme diagram is in place. An enzyme being a protein can adopt a multitude of conformations even in its native state, i.e., without bound reactants. These conformations are usually not identical to those best adapted to a bound reactant (cf. the notion of induced fit). Moreover, the conformations best adapted to a given set of bound reactants are usually no longer adapted to a new set of bound reactants formed in a chemical reaction. As a consequence, a whole sequence of conformational changes may set in, which eventually relaxes the constraints exerted on the enzyme due to binding or alteration of reactants [41]. In general, these transitions are much faster than the processes of binding or chemical transformation of reactants. A discernible state in an enzyme cycle thus appears as a collection of conformational states (or, strictly speaking, substates) which, however, are in equilibrium among each other and therefore need not be discriminated [12]. For a further discussion (including a case which does not comply with this condition) the reader is referred to the papers of Welch et al. and Kamp et al. [42–44].

The fast relaxation of unfavorable conformations evoked by reactants should not be mistaken for an argument that true conformational changes of an enzyme need not be considered at all. In fact, a transition between two sets of substates may occur only at a rate comparable to the rates of binding and chemical reactions if it is associated with a substantial rearrangement of protein moieties. As an example, one could think of a transition which shifts the accessibility of a binding site to a different domain on the protein.

IV.B-2. The isomerization reaction, and the effect of enzyme inhibitors

The simplest chemical reaction is the isomerization of a substrate, S, to a product, P:

$$S \rightleftarrows P \tag{54}$$

The minimal diagram of an enzyme catalyzing this reaction consists of three states as depicted in Fig. 4A. Three additional states are also shown which are dead-end branches and arise from binding of an inhibitor, I, to the enzyme in the three states of the catalytic cycle.

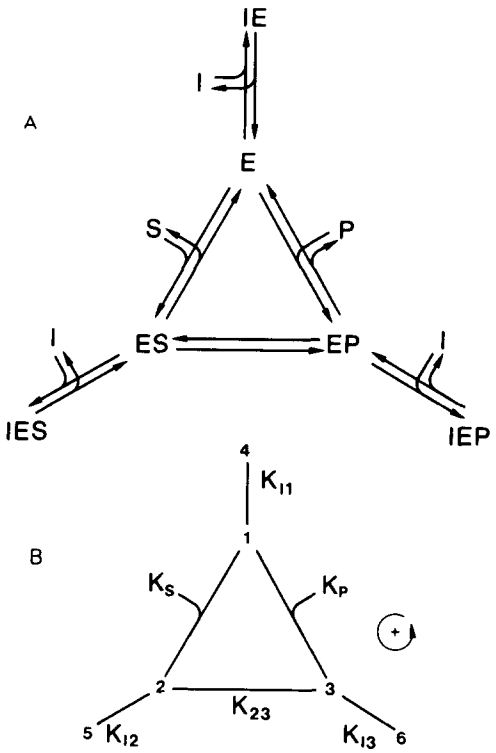

Fig. 4. Kinetic scheme (A) and diagram (B) for the enzyme-catalyzed isomerization reaction. E, S, P and I in (A) denote the enzyme, the substrate, the product, and an inhibitor, respectively. In (B) the different states of the enzyme in the kinetic scheme are numbered. K_S, K_P, and K_{Ii} are the dissociation constants for binding of substrate, product, and inhibitor to the ith state, respectively, while K_{23} is the equilibrium constant for the transition $2 \rightleftarrows 3$. The positive direction for the cycle is indicated.

Analysis of this diagram (see Appendix A.II-1) yields for the flow of the reaction

$$J = N_e \frac{\alpha_{32}}{\Sigma_{r1}} \left[K_{23} \frac{c_S}{K_S} - \frac{c_P}{K_P} \right] \tag{55}$$

The quantity Σ_{r1} is a function of substrate (c_S), product (c_P) and inhibitor (c_I) concentration, as evident from Eqn. A18 in the Appendix. N_e denotes the mole number of enzyme. K_{23} is the equilibrium constant for that transition in the enzyme cycle where the actual isomerization takes place, while α_{32} is its transition probability (see Appendix A.I-1) from state 3 to state 2. K_S, K_P and K_{Ii} are the dissociation constants for the binding of S, P and I to the ith state, respectively.

In terms of the Michaelis-Menten parameters as defined in the Appendix (Eqns. A20 and A21), Eqn. 55 reads

$$J = N_e \frac{k_{catS} c_S / K_{mS} - k_{catP} c_P / K_{mP}}{1 + c_S / K_{mS} + c_P / K_{mP}}$$

$$= N_e \left[\frac{k_{catS} c_S}{c_S + K_{mS}(1 + c_P / K_{mP})} - \frac{k_{catP} c_P}{c_P + K_{mP}(1 + c_S / K_{mS})} \right] \tag{56}$$

The Michaelis-Menten parameters are conveniently estimated from the initial flow of the reaction, i.e., when

only substrate ($c_P \approx 0$) or only product ($c_S \approx 0$) is present. Then, Eqn. 56 is reduced to the form

$$|J| = N_e k_{catX} c_X / (K_{mX} + c_X), \quad X = S \text{ or } P \tag{56a}$$

Performing such experiments for different substrate (product) concentrations yields K_{mS} and k_{catS} (K_{mP} and K_{catP}) by well-known techniques based on linear plots (see, for example, Segel [15]).

In the *absence of an inhibitor* the ratio

$$k_{catS}(0)/K_{mS}(0) = \alpha_{23}/[K_S(1 + \tau_1 K_{23} + \tau_2)] \tag{57}$$

(or the corresponding ratio for P) is taken as a measure for the 'catalytic activity' of the enzyme in the sense that the larger the ratio the better the catalysis. In Eqn. 57, the argument for k_{cat} and K_m indicates that $c_I = 0$, while τ_1 and τ_2 are given in Eqn. A19. The optimal value for the ratio in Eqn. 57 is obtained for $\tau_2 \approx 0$ and amounts to $k_{catS}(0)/K_{mS}(0) = \alpha_{12}^{\circ}/[1 + 1/(\tau_1 K_{23})]$ which becomes the larger the larger $\tau_1 K_{23}$. In other words, the catalytic activity for the unidirectional process S → P is maximal if the dissociation of S and P is, respectively, much slower and much faster than the transition P → S, and if the equilibrium for the isomerization is very much in favor of P_i. In the limit, $k_{catS}(0)/K_{mS}(0) \approx \alpha_{12}^{\circ}$, which itself is limited by the diffusion of S. It should be kept in mind, however, that Eqn. 57 applies only to the unidirectional process S → P, but the actual flow of the reaction includes also the inverse process and thus may be considerably smaller, depending on c_P and $k_{catP}(0)/K_{mP}(0)$. It is evident from Eqns. A20 and A21 that $K_{mS}(0)$ and $K_{mP}(0)$ become equal to the respective true dissociation constants K_S and K_P only if $\tau_2 \approx \tau_3$. Then $k_{catS}(0)/k_{catP}(0) = K_{23}$, which is the equilibrium constant for the isomerization of *bound S* to *bound P*.

The *effect of an inhibitor on the enzyme* is usually categorized according to its effect on the Michaelis-Menten parameters. By virtue of Eqns. A20 and A21, we can trace these categories back to a differential binding of the inhibitor to the three states of the enzyme, as expressed by the dissociation constants K_{I1}, K_{I2}, and K_{I3}. Let us first assume that an inhibitor binds only to the free enzyme, then

$$\begin{aligned} &K_{mX}(c_I) = K_{mX}(0)(1 + c_I/K_{I1}) \quad \text{and} \\ &k_{catX}(c_I) = k_{catX}(0) \quad \text{for } K_{I2} = K_{I3} = \infty, \quad X = S \text{ or } P \end{aligned} \tag{58}$$

Since the inhibitor cannot bind to the enzyme when S or P is bound, it most likely competes with S and P for the same binding site, a condition known as *competitive inhibition*. On the other hand, if the inhibitor binds equally well to all states,

$$\begin{aligned} &k_{catX}(c_I) = k_{catX}(0)/(1 + c_I/K_I) \quad \text{and} \\ &K_{mX}(c_I) = K_{mX}(0) \quad \text{for } K_I \equiv K_{I1} = K_{I2} = K_{I3}, \quad X = S \text{ or } P \end{aligned} \tag{59}$$

The inhibitor merely decreases the number of active enzyme molecules and therefore decreases k_{catX} without affecting K_{mX}, which is typical for a *non-competitive inhibition*. If the inhibitor binds equally well to the states with bound S and P, but not to the free enzyme,

$$\begin{aligned} &K_{mX}(c_I) = K_{mX}(0)/(1 + c_I/K_{I2}) \quad \text{and} \\ &k_{catX}(c_I) = k_{catX}(0)/(1 + c_I/K_{I2}) \\ &\qquad \text{for } K_{I1} = \infty, \; K_{I2} = K_{I3}, \quad X = S \text{ or } P \end{aligned} \tag{60}$$

In this case, which is known as *uncompetitive inhibition*, K_m and k_{cat} vary with c_I, but the ratio of the two is constant. $K_{I1} = \infty$ implies that the binding site for the inhibitor becomes accessible only after a conformational change of the enzyme due to binding of S or P. In the most general case, i.e., all K_{Ii} are different and finite, K_m and k_{cat} are both dependent on c_I (see Eqns. A20 and A21), as is the ratio K_m/k_{cat}, in contrast to uncompetitive inhibition. No special notation seems to exist for this case, maybe because it is rarely encountered, although its occurrence cannot be excluded a priori.

The terms $K_{mS}(1 + c_P/K_{mP})$ and $K_{mP}(1 + c_S/K_{mS})$ in the denominators of the fractions in square brackets of Eqn. 56 are reminiscent of the dependence of K_m on c_I for competitive inhibition (see Eqn. 58). This has led to the rather unfortunate notion that "the reaction S → P is inhibited by the product" (which, by the same token, could also read "the reaction P → S is inhibited by the substrate") [15,40]. In fact, if and only if $k_{catP} \approx 0$, the flow of the reaction is uniquely determined by the first term comprising $K_{mS}(1 + c_P/K_{mP})$ and P behaves as if it were a competitive inhibitor for S. In all other cases, however, the slowing down of the net rate of the reaction with increasing c_P is due to an increasing back-reaction, P → S, which counteracts the forward reaction S → P and eventually balances it at equilibrium. Hence, the above statement should be avoided, and the notion of a product (or substrate) inhibition should be restricted to those possible cases where P (or S), in addition to being the product (or the substrate) of the reaction, indeed takes over the role of an inhibitor. Such cases are adequately described by Eqns. 58–60 rewritten with index P (or S) instead of I.

IV.B-3. Formation of one product from two substrates

An additional aspect of enzyme-catalysis pops up if two or more substrates (or products) take part in a reaction. The simplest of such a reaction is the condensation of two substrates to one product,

$$S_1 + S_2 \rightleftarrows P \tag{61}$$

The general diagram for an enzyme catalyzing this reaction is shown in Fig. 5A. There are two branches which lead from state 1, which is the free enzyme, to

state 4 where both substrates are bound to the enzyme. When both branches are operative, we have the situation of *random binding of substrates* according to Cleland's terminology [40], and the flow of the reaction in Eqn. 61 is (see Appendix A.II-2)

$$J = N_e \frac{\alpha_{54}}{\Sigma_{r2}} \left[K_{45} \frac{c_{S1} c_{S2}}{K_{S1} K_{S2}} - \frac{c_P}{K_P} \right] (1 + B_r) \qquad (62)$$

The quantity Σ_{r2} (see Eqn. A23) is a sum of six terms comprising also the concentrations of the substrates (c_{S1}, c_{S2}) and of the product (c_P). N_e denotes the mole number of enzyme. K_{45} is the equilibrium constant of the transition where the formation of bound P from bound S_1 and S_2 occurs, while α_{54} is the transition probability (see Appendix A.I-1) from state 5 to state 4. K_{S1} and K'_{S1} are the dissociation constants for binding of S_1 in transitions $1 \rightleftarrows 2$ and $3 \rightleftarrows 4$, while K_{S2} and K_P are the corresponding constants for S_2 and P in transition $2 \rightleftarrows 4$ and $1 \rightleftarrows 5$, respectively. The term abbreviated by B_r (see Eqn. A24) determines the relative contributions of the two branches involving binding of S_1 and S_2 to the reaction flow.

An attempt to cast Eqns. 62 and A23 into the 'Michaelis-Menten' form (compare Eqn. 56a) for the condition $c_P \approx 0$ and c_{S2} = constant fails because B_r comprises c_{S1}, which gives rise to terms with c_{S1}^2. The same argument holds for S_2, and only in the case $c_{S1} = c_{S2} \approx 0$ is the procedure straightforward, yielding K_{mP} and k_{catP} (see Eqn. A28). At sufficiently low concentrations c_{S1} or c_{S2}, i.e., if the conditions in Eqns. A26 hold, the quadratic terms can be neglected and relations like that in Eqn. 56a can be obtained with the Michaelis-Menten parameters given in Eqns. A27. With increasing concentrations, however, the conditions in Eqn. A26 no longer hold and the quadratic terms give rise to an increasing deviation from the relation like that in Eqn. 56a. Hence, the statement that Eqn. 56a can always be obtained provided that a reaction is unimolecular with respect to the varied reactant [11] is in general not correct. On the contrary, if an enzyme-catalyzed reaction as specified in Eqn. 61 fails to comply with the simple 'Michaelis-Menten law' over an extended concentration range this is a good evidence (although not necessarily a proof) for random binding of S_1 and S_2. On the other hand, compliance with this law does not prove the absence of random binding, as we shall see next.

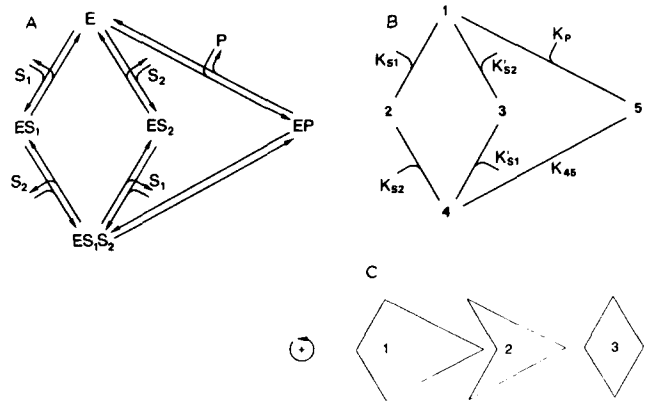

Fig. 5. Kinetic scheme (A), diagram (B) and cycles (C) for the enzyme-catalyzed formation of one product P from two substrates S_1 and S_2. For an explanation of symbols see legend to Fig. 4.

Provided that all transitions involving binding are much faster than the transition due to the chemical reaction, i.e., all $\tau_i \approx 0$ in Eqn. A25a, the term $(1 + B_r)$ cancels and thus the terms with c_{Si}^2 disappear. The reader who takes the effort to rewrite Eqns. A27 with all $\tau_i = 0$ will realize that $K_{mP} = K_P$ and $k_{catP} = \alpha_{54}$. He or she will also find that $K_{mS1}(0) = K_{S1}$ and $K_{mS2}(0) = K_{S2} K_{S1} / K'_{S1}$ ($= K'_{S2}$, cf. Eqn. 77b) while $k_{catSi}(0) = 0$. In the absence of one substrate, no reaction can occur and the other substrate simply binds to the enzyme in that transition which is independent of the missing substrate, i.e., $1 \rightleftarrows 2$ and $1 \rightleftarrows 3$ for S_1 and S_2, respectively. K_{mS1} and K_{mS2} approach K'_{S1} and K_{S2} with increasing c_{S2} and c_{S1}, respectively, while k_{catSi} approaches $\alpha_{54} K_{45}$ for both substrates.

The transition probabilities, α_{ij}, in one of the branches pertinent to binding of S_1 and S_2 could be so small compared to those of all other transitions that the cycle flows (see Appendix A.I-2) of all cycles comprising this branch become negligibly small. The enzyme then operates along a *predominant cycle*, and the branch with the small α_{ij} values can be omitted in the diagram. We thus arrive at the situation of *ordered binding of substrates*. However, there are less stringent conditions which also lead to ordered binding. It suffices that $B_r \approx 0$ in order to let the branch 1-3-4 become inoperative. This condition is achieved if $\beta_1 \approx 0$ (see Eqn. A24), which means that the dissociation of S_1 is much slower in the transition $4 \rightarrow 3$ than in $2 \rightarrow 1$, then also $K'_{S1}/K_{S1} \approx 0$. Alternatively, $K'_{S1} \approx 0$ due to a very slow association of S_1 in the transition $3 \rightarrow 4$ (note that $K'_{S1} \approx 0$ causes $K'_{S2} \rightarrow \infty$, cf. Eqn. 77b for finite K_{S1} and K_{S2}).

The flow of the chemical reaction in Eqn. 61 with the ordered binding of S_1 before S_2 is given by Eqn. 62 with $B_r = 0$. Then, no terms with c_{S1}^2 and c_{S2}^2 arise for $c_P \approx 0$ and the reaction complies with the 'Michaelis-Menten law' over the whole concentration range. The pertinent Michaelis-Menten parameters can be obtained from Eqns. A27 by setting $B_{rj} = 0$ and $K'_{S1}/K_{S1} = 0$.

IV.B-4. Redox reactions

Two cases can be distinguished for redox reactions (cf. Eqn. 14) catalyzed by an enzyme. If the enzyme itself cannot undergo a redox reaction, its role is restricted to bringing the reactants together and lowering the activation barrier for the electron exchange. In this

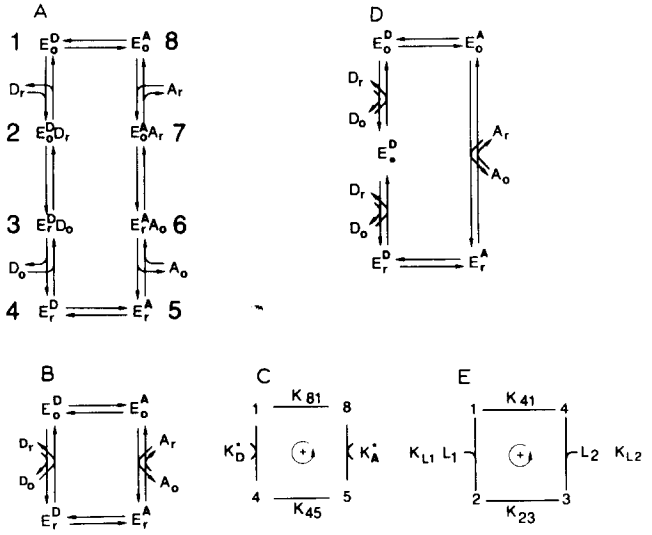

Fig. 6. Kinetic schemes (A, B, D) and diagram (C) for enzyme-catalyzed redox reactions as well as diagram (E) for a carrier-mediated transport. E, D and A represent the redox enzyme, the electron donating and the electron accepting redox couple, respectively, while indices r and o indicate the reduced and oxidized species of each couple, respectively. The redox enzyme can adopt different conformations which react only with either D or A as indicated by the corresponding superscripts. The dot on E in (D) means 'half-reduced' enzyme (semiquinoid form). The scheme in (B) and its diagram in (C) are obtained from the scheme in (A) by a reduction of states as explained in the text. The diagram in (E) pertains to a carrier-mediated transport of species L between the compartments indicated by the indices 1 and 2 (cf. Fig. 1C). States 1 and 2 represent the carrier whose binding site is accessible only from compartment 1 without and with bound species, respectively, while states 4 and 3 are the corresponding states for the carrier facing compartment 2.

case, redox reactions do not differ from any other reaction in which two substrates are formed from two products. If the enzyme itself is a redox couple, D_r can bind to the enzyme, transfer its electron(s) to the enzyme and leave it as D_0 (see Fig. 6A, which pertains to a redox reaction with $n_D = n_A$). In a subsequent sequence of transitions, A_o can then bind to the enzyme and get the electron(s) whereby A_r is formed which dissociates from the enzyme. The scheme in Fig. 6A includes an additional feature, viz. a transition for the oxidized and reduced enzyme which represents an adaptation of the enzyme's conformation to the binding of D and A.

Electron transfer reactions in a complex of redox couples are usually much faster than ordinary chemical reactions or binding [45]. As a consequence, the probabilities of the states 2, 3, 6, and 7 become rather small, which allows us to condense the sequence of transitions $1 \rightleftarrows 2 \rightleftarrows 3 \rightleftarrows 4$ and $5 \rightleftarrows 6 \rightleftarrows 7 \rightleftarrows 8$ into *one* transition, $1 \rightleftarrows 4$ and $5 \rightleftarrows 8$, respectively (see Appendix A.I-4). The analysis of the resulting scheme (Fig. 6B) yields for the flow of electrons (see Appendix A.II-3)

$$J_e = N_e n_e \alpha_{54} (K_{45} K_{81} \rho_D / K_D^* - \rho_A / K_A^*) / \Sigma_{rd} \qquad (63)$$

N_e and n_e denote, respectively, the mole number of the enzyme and the total number of electrons which it exchanges with D (or A) in the cycle; ρ_D and ρ_A indicate the redox state (see Eqn. 23b) of the donating and accepting redox couple, respectively. K_{45} and K_{81} are the true equilibrium constants for the conformational change of the reduced and the oxidized enzyme, while K_A^* and K_D^* are defined in Eqn. A32a. Inspection of the quantity Σ_{rd} given in Eqn. A31 reveals that an enzyme-catalyzed redox reaction behaves like a carrier-mediated transport (compare Eqn. 72) if $\tau_1 = \tau_2 \approx 0$ or if $c_{Do}/K_{Do} \gg 1$ and $c_{Ao}/K_{Ao} \gg 1$. Electrons are transported between two 'concentrations' which are expressed by the reduction states ρ_D and ρ_A. It should be noted that this analogy is complete for a membrane-bound redox enzyme with the donating redox couple being in a compartment different from that occupied by the accepting couple (compare diagrams in Fig. 6C and 6E). The complexity encountered with the transport of a charged species across the membrane to be discussed in subsection IV.C-3 then applies to the transport of electrons as well.

A redox enzyme catalyzing the reaction where $n_D \neq n_A$ has to be able to exchange n_D and n_A electrons in the conformations adapted to D and A, respectively. A scheme describing such a situation for $n_D = 1$ and $n_A = 2$ is depicted in Fig. 6D. Obviously, two sequential transitions with $D_r \rightleftarrows D_0$ are required in order to collect the two electrons subsequently transferred to A_o. The analysis of this scheme is fully analogous to the analysis of the scheme for ordered binding of two (identical) substrates yielding one product, and hence need not be repeated. Alternatively, the enzyme may be able to transfer only one electron in all transitions. Two redox centers in the enzyme are then required, and A must be able to accept electrons in a sequence of two transitions each transferring one electron. The corresponding scheme can be converted to the scheme in Fig. 6D by possible reduction of states. The situation becomes more complicated if the half-reduced enzyme created in the first transition involving D_r can change to a conformation which binds D_r as well as A_o. Additional branches are then introduced which yields a diagram with four cycles. Its analysis, though straightforward, will be omitted, since it results in relations too complex to be reproduced here.

IV.C. Transport

Transport of species within the aqueous phases need not be considered because of stirring or rapid diffusion in the internal unstirred spaces (see subsection II.A). It is worth mentioning, however, that certain membrane topologies such as tight folding may lead to unequal distributions of solutes despite of stirring [46]. The transport through membranes is usually assumed to

occur by diffusion. If present, pores formed by specialized proteins or carriers which bind and transfer selected species can substantially increase the transport rates.

IV.C-1. Permeation through membranes

The flow of the ith species, J_i, in the membrane arises from a unidirectional gradient in its electrochemical potential, $\tilde{\mu}_i$ (Nernst-Planck equation)

$$J_i(x)/A = -u_i c_i(x)\, \mathrm{d}\tilde{\mu}_i/\mathrm{d}x = -u_i[RT\, \mathrm{d}c/\mathrm{d}x + z_i F c_i(x)\, \mathrm{d}\psi/\mathrm{d}x] \tag{64}$$

with u_i and A denoting, respectively, the mobility of the species in the membrane phase and the total membrane area. For a *steady state of transport*, J_i = constant, and Eqn. 64 can be integrated between $x1$ and $x2$ (see Fig. 1C) which yields

$$J_i = AP_i z_i\, \Delta\phi_m \frac{c_{i,1}(x1)\exp\{z_i\, \Delta\phi_m\} - c_{i,2}(x2)}{\exp\{z_i\, \Delta\phi_m\} - 1} \tag{65}$$

Here, $\Delta\phi_m = \phi(x1) - \phi(x2)$ is the difference in reduced electrical potential across the membrane (see Fig. 2). P_i is the permeability of the ith species,

$$P_i = RTu_i K_{pi}/d \tag{66}$$

where K_{pi} and d denote the partition coefficient of the species between membrane and aqueous phase (see Eqn. 24) and the thickness of the membrane, respectively.

The same flow, J_i, has to occur in the diffuse layers on both sides of the membranes and within the unstirred internal spaces which implies $\mathrm{d}\tilde{\mu}_i/\mathrm{d}x \approx 0$ in these domains. Provided that the mobility of the species in the aqueous phase is larger than in the membrane phase and that the species' concentration in the membrane is considerably lower due to $K_{pi} \ll 1$, the gradients of the electrochemical potential in the aqueous phases required to sustain J_i can become rather small. Hence, we approximate them by $\mathrm{d}\tilde{\mu}_i/\mathrm{d}x \approx 0$, which means no concentration gradient in the unstirred internal spaces, in line with the statement at the beginning of this section. Moreover, no gradients exist for uncharged species in the diffuse layers (as postulated in subsection III.A) while, in the case of a charged species, the diffuse layers are not perturbed by J_i. The concentrations on the membrane surfaces ($x = x1$ and $x2$) can then be expressed by Eqn. 34 and, in view of the relation (see Fig. 2)

$$\Delta\phi = \phi_1 - \phi_2 = \Delta\phi_m - \phi_{s1} + \phi_{s2} \tag{67}$$

Eqn. 65 is transformed into

$$J_i = AP_i z_i\, \Delta\phi_m \frac{c_{io,1}\exp\{z_i\, \Delta\phi\} - c_{io,2}}{\exp\{z_i(\phi_{s1} + \Delta\phi)\} - \exp\{z_i\phi_{s2}\}} \tag{68}$$

Some special cases are worth mentioning. The denominator of Eqn. 68 can be expanded into the Taylor series $z_i\, \Delta\phi_m \exp\{z_i\phi_{s2}\}\,[1 + z_i\, \Delta\phi_m/2 \ldots]$ which yields for an *uncharged species*

$$J_i = AP_i(c_{io,1} - c_{io,2}), \quad z_i = 0 \tag{68a}$$

and for a charged species in the case of no potential drop across the membrane per se

$$J_i = AP_i(c_{io,1}\exp\{z_i\, \Delta\phi\} - c_{io,2})/\exp\{z_i\phi_{s2}\}, \quad \Delta\phi_m = 0 \tag{68b}$$

If $\phi_{sk} \approx 0$, i.e., the surface potentials are negligibly small, $\Delta\phi_m \approx \Delta\phi$ (cf. Eqn. 67) and Eqn. 68 adopts the form

$$J_i = AP_i z_i\, \Delta\phi \frac{c_{io,1}\exp\{z_i\, \Delta\phi\} - c_{io,2}}{\exp\{z_i\, \Delta\phi\} - 1}, \quad \phi_{sk} \approx 0 \tag{68c}$$

usually found in the literature.

The effect of surface potentials on the permeation of charged species becomes apparent when comparing Eqns. 68 and 68c for $\Delta\phi = 0$. In the absence of surface potentials (or if they are neglected), Eqn. 68c is reduced to Eqn. 68a, i.e., permeation is uniquely driven by the difference in bulk phase concentrations. If surface potentials are present, Eqn. 68 reads

$$J_i = AP_i z_i(\phi_{s1} - \phi_{s2}) \frac{c_{io,1} - c_{io,2}}{\exp\{z_i\phi_{s1}\} - \exp\{z_i\phi_{s2}\}}, \quad \Delta\phi = 0 \tag{68d}$$

which is reduced to Eqn. 68b with $\Delta\phi = 0$ if $\phi_{s1} = \phi_{s2}$. In the latter case, J_i is larger (smaller) than expected from the concentration difference for $z_i\phi_{s2} < 0$ ($z_i\phi_{s2} > 0$) due to the accumulation (depletion) of the ith species at the membrane surfaces. This effect is augmented if $z_i\phi_{s2} < z_i\phi_{s1}$, and diminished if $z_i\phi_{s2} > z_i\phi_{s1}$.

IV.C-2. Transport through pores

An essential factor for permeation through membranes is the partition coefficient K_{pi} of the transported species (see Eqn. 66) which can become rather small depending on hydrophilicity and charge of the species. A device which constitutes a hydrophilic path through the membrane can greatly accelerate permeation for such species. In this *simplest model of a pore* the flow is still described by Eqn. 68. The characteristics of the pore such as the area of its cross section as compared to the total membrane area, its restrictions with respect to size of the species which can enter the pore, or the abundance of pores in the membrane are all included in the permeability, P_i. Eqn. 68 sets no limits to the magnitude of the flow through pores, in contrast to what is observed experimentally [47], and hence is applicable only in a limited range for the difference in concentration or membrane potential.

A comprehensive treatment of transport through pores was given by Läuger [48]. We shall adopt here a

simplified version which suffices to bring out the essentials. The pore provides a sequence of sites where the transported species can reside on its way through the pore. The transitions between sites are governed by the usual transition probabilities. We assume that the probabilities for transitions in the pore comply with the condition necessary to allow the reduction of states (see Appendix A.I-4) so that only two sites are left in the pore.

The pore can be treated as if it were an enzyme which adopts the four conformations depicted in Fig. 7A. Substrate and product are equivalent, respectively, to the transported species on that side of the membrane where transport in the positive direction starts and ends. The transitions $1 \rightleftarrows 2$, $3 \rightleftarrows 4$, and $1 \rightleftarrows 3$, $2 \rightleftarrows 4$ represent binding of substrate and product, respectively. The transition $2 \rightleftarrows 3$ is equivalent to the chemical reaction which, in the case of transport, consists of a transfer of the species between the two binding sites open to one (the 'substrate') or the other (the 'product') side of the membrane. The analysis of the diagram in Fig. 7B yields for the flow of the ith *uncharged species or if* $\Delta\phi = \phi_{sk} = 0$ (see Appendix A.II-4)

$$J_i = N_p \frac{\alpha_{32}}{\Sigma_p}\left[K_{23}\frac{c_{io,1}}{K_1} - \frac{c_{io,2}}{K_2}\right](1 + B_p), \quad z_i = 0 \tag{69}$$

The quantity Σ_p (see Eqn. A34) is a sum of four terms comprising also the concentrations $c_{io,1}$ and $c_{io,2}$ in the bulk phase of compartment 1 and 2, respectively. N_p denotes the mole number of pores. K_{23} is the equilibrium constant of the transition where the transfer of the species between binding sites occurs *, while α_{32} is its transition probability from state 3 to state 2. K_1 and K_2 are the dissociation constants for binding of the species from compartment 1 in transition $1 \rightleftarrows 2$ and from compartment 2 in transition $1 \rightleftarrows 3$, respectively. The term abbreviated by B_p (see Eqn. A35) reflects the relative contributions of the two cycles 1-2-3-1 (cycle 1) and 3-4-2-3 (cycle 2 in Fig. 7C) to the overall transport.

It is evident from Eqns. 69 and A34 that permeation through a pore is a 'saturable process' like any other enzyme-catalyzed reaction. When we try to cast these equations into the 'Michaelis-Menten form' by setting either $c_{io,2} \approx 0$ or $c_{io,1} \approx 0$, we encounter the same problems as in the case of random binding of two substrates to an enzyme (see subsection IV.B-2). For sufficiently small concentrations, Michaelis-Menten parameters can be found (Eqns. A38), and Eqn. 69 then adopts the form

$$J_i = N_p \frac{k_{cat1}(1 + b_p c_{io,1}/K_1)c_{io,1}}{K_{m1} + c_{io,1}[1 + (1 + \tau_3 K_{23})b_p c_{io,1}/(K_1 D_1)]} \quad \text{for } c_{io,2} \approx 0 \tag{70}$$

where b_p, τ_4 and D_1 are given in Eqns. A36, A37, and A38a, respectively. A similar relation also holds for J_i if $c_{io,1} \approx 0$. As long as $b_p c_{io,1}/K_1 \ll 1$, cycle 2 in Fig. 7C is not operative, and J_i yields linear plots in any of the conventional techniques for analysis of the Michaelis-Menten relation [15]. With increasing $c_{io,1}$, however, the above condition no longer holds, cycle 2 in Fig. 7C comes into play and eventually fully overrides cycle 1 in Fig. 7C if $b_p c_{io,1}/K_1 \gg 1$. This causes an increasing deviation from the linear relation in the aforementioned plots [47]. It is worth mentioning that this behavior of the pore does not disappear if all $\tau_i \approx 0$, in contrast to the case of random binding of substrates (see subsection IV.B-3). In the general case none of the concentrations on both sides of the membrane vanishes but they vary due to J_i. Thus, the permeation of the species through a given pore may 'slide' through a whole range of kinetic regimes.

For the permeation of a *charged species*, we can expect that the probabilities for the transitions $2 \rightarrow 4$ and $3 \rightarrow 4$ are very small because of electrostatic repulsion. Hence, $b_p \approx 0$ and also $B_p \approx 0$ (see Eqns. A35 and A36). The diagram of the pore then becomes formally

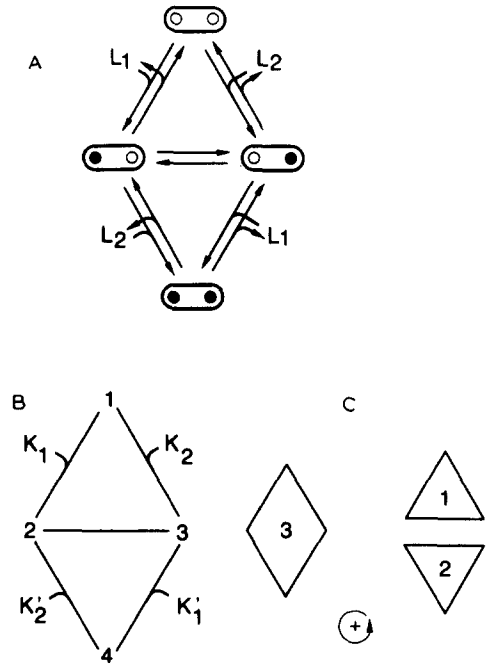

Fig. 7. Kinetic scheme (A), diagram (B) and cycles (C) for transport of species L through a pore with two binding sites. Open and closed circles in (A) represent free and occupied binding sites, respectively, while the index of L indicates from which compartment the species enters the pore. For further explanations see text.

* Although one would expect intuitively that $\alpha_{23} = \alpha_{32}$ for the barrier in the pore, i.e., $K_{23} = 1$, this condition applies only when the two sites in the pore have equal dissociation constants K_1 and K_2 (cf. Eqn. 79a, and see also [48]).

identical with that for an enzyme-catalyzed isomerization reaction in the absence of an inhibitor (see Fig. 4B), which suggests a relation for J_i like that in Eqn. 55. This, however, is true only when no drop in electrical potential across the membrane exists, a rather unlikely condition in view of the transport of a charged species. Including the effect of an electrical potential difference on the transition probabilities (see Appendix A.I-3 and A.II-4) yields

$$J_i = N_p \frac{\alpha_{32}}{\Sigma_{p^*}} \left[K_{23} \frac{c_{io,1}}{K_1} \exp\{ z_i \, \Delta\phi \} - \frac{c_{io,2}}{K_2} \right] \tag{71}$$

The terms in the quantity Σ_{p^*} are dependent on the surface potentials and the potential drop $\Delta\phi_m$ across the membrane (see Eqn. A41a). In case of a constant membrane potential $\Delta\psi$, the discussion of Eqn. 71 is straightforward and similar to that of the isomerization reaction. However, the Michaelis-Menten parameters are dependent on the electrical potentials. If $\Delta\psi$ varies, the behavior of J_i becomes too complex to be discussed here. Also, the analysis is often restricted to small potentials where exponentials can be linearized [48]. We conclude the discussion of pores by referring to the considerations of Cooper et al. [49] who have reviewed the transport through pores (or channels) in a broader context. Moreover, the procedures for 'testing simple pores' presented by Lieb and Stein [50] may prove to be useful for the analysis of experimental data.

IV.C-3. Carrier-mediated transport

A carrier is usually envisaged as a molecule which shuttles back and forth in the membrane and which binds a given species from the aqueous phase on either side of the membrane. It thus enables this species to cross the membrane without being exposed to the hydrophobic environment in the membrane. Valinomycin transporting K^+ or Rb^+ ions is the classical example for this mechanism [51]. However, a relatively small carrier molecule which actually moves within the membrane is the less frequent case and is suitable only for the transport of small species. Most carriers are integral membrane proteins able to adopt at least two conformations. The conformations differ in the accessibility and most likely the position of a binding site for the transported species, which faces and is open to the aqueous phase on one or the other side of the membrane. Note that the transition between the two conformations with bound species requires the displacement of the latter within the protein. This may cause substantial strains in the protein, particularly for bulky species, which translates into a high activation energy and low transition probabilities (see also Ref. 42).

Both schemes, i.e., mobile carrier and conformational model, result in the same diagram (Fig. 6E). Its analysis (see Appendix A.II-5) yields for the flow of the ith *uncharged species or if* $\Delta\phi = \phi_{sk} = 0$:

$$J_i = N_c \frac{\alpha_{32}}{\Sigma_c} \left[K_{23} K_{41} \frac{c_{io,1}}{K_1} - \frac{c_{io,2}}{K_2} \right], \quad z_i = 0 \tag{72}$$

where N_c denotes the mole number of the carrier. K_1 and K_2 are the dissociation constants for binding of the transported species to the carrier from compartment 1 and 2 with bulk phase concentrations $c_{io,1}$ and $c_{io,2}$, respectively. K_{23}, K_{41} and α_{32} denote the equilibrium constants and the transition probability for the transitions indicated by the indices, respectively. Inspection of the quantity Σ_c given in Eqn. A43 shows that it is formally identical with Σ_{r1} in Eqn. A18 for the isomerization reaction without inhibitor ($c_1 = 0$) except for the additional term comprising $c_{io,1}c_{io,2}$. This term vanishes if $\tau_3 \approx 0$, i.e., if the transition of the free carrier is much faster than that of the loaded carrier (cf. Eqns. A43 and A44), and the four-state diagram could be reduced to a three-state model like that in Fig. 4B. The term with the product of both concentrations also vanishes when one of the concentrations is zero, which enables us to define Michaelis-Menten parameters in the usual way (see Eqns. A45). Lieb and Stein [52] have discussed the testing of such 'simple carriers'.

The situation becomes considerably more complex if the *transported species and/or the carrier are charged*. Eqn. 72 is then converted to (see Appendix A.II-5)

$$J_i = N_c \frac{\alpha_{32}}{\Sigma_{c^*}} \left[K_{23} K_{41} \frac{c_{io,1}}{K_1} \exp\{ z_i \, \Delta\phi \} - \frac{c_{io,2}}{K_2} \right] \tag{73}$$

with Σ_{c^*} comprising the effect of the potential drop $\Delta\phi_m$ across the membrane and the surface potentials ϕ_{sk} (see Eqn. A47). The discussion of transport of charged species through pores applies as well to the carrier-mediated transport in the presence of electrical potentials and therefore need not be repeated.

V. Connection between kinetics and thermodynamics

Thermodynamics tells us in which direction a process proceeds spontaneously; however, it does not indicate how fast the process runs. On the other hand, a kinetic scheme of a process comprises all information about rates and seemingly does not require any thermodynamic elements. In fact, a *properly formulated kinetic scheme* takes care of thermodynamics by itself. The attribute 'properly formulated' implies that the kinetic scheme complies with the frame set by thermodynamics or, in other words, does not violate thermodynamic laws. As we shall see in the following section, this condition gives rise to restrictions imposed on the rate constants or transition probabilities in enzyme kinetics.

V.A. Microscopic reversibility, detailed and thermokinetic balancing

The twin concepts of microscopic reversibility and detailed balancing pertain to the same phenomenon and are often used interchangeably. They relate to the fact that all flows have to vanish in the equilibrium state where all parameters of a system no longer change in time (see subsection II.E-1). The conditions derived from this fact depend on the level of description of the system. In order to avoid confusions, it was therefore suggested [53] that the concept of *microscopic reversibility* should be used exclusively in a microscopic description of the system in terms of statistical mechanics. *Detailed balancing* then applies to the macroscopic (or phenomenological) level of description in terms of rate constants which arise from but are not identical to the transition probabilities pertinent to transitions between states of a system in the microscopic description [53]. These transition probabilities should not be confused with the transition probabilities α_{ij} pertinent to the transitions between states of an enzyme as introduced in the Appendix A.I-1.

The vanishing of all flows at equilibrium required by detailed balancing leads to a well-known relation between forward and backward rate constant and the equilibrium constant, K_c, of a chemical reaction. Thus, for the ith reaction in Eqn. 45 (cf. Eqns. 46 and 26)

$$k_i/k_{-i} = K_{ci} = [c_{Pi}/(c_{Si,1}c_{Si,2})]_{eq} \tag{74a}$$

where the subscript eq indicates the concentrations of product and substrates at equilibrium. Similarly, for the reaction in Eqn. 48

$$k_j/k_{-j} = K_{cj} = [c_{Pj,1}c_{Pj,2}/(c_{Sj,1}c_{Sj,2})]_{eq} \tag{74b}$$

For a sequence of two reactions where the product of the first reaction is a substrate of the second reaction

$$k_ik_j/(k_{-i}k_{-j}) = K_{ci}K_{cj} = K_{cij}$$

$$= [c_{Pj,1}c_{Pj,2}/(c_{Si,1}c_{Sj,1}c_{Sj,2})]_{eq} \tag{75}$$

where K_{cij} denotes the equilibrium constant for the overall reaction in Eqn. 52. This can be easily extended to sequences of several reactions. Detailed balancing then imposes the condition that the product of forward rate constants divided by the product of backward rate constants is equal to the product of the equilibrium constants for each reaction in the sequence, which in turn is equal to the equilibrium constant for the overall reaction emerging from the sequence. It is important to note that the relations between rate constants and equilibrium constants always hold irrespective of the reactions being at equilibrium or a sequence of reactions being in a steady state.

Detailed balancing applied to the kinetic scheme of an enzyme-catalyzed reaction leads to the general condition given in Eqn. A14 which is valid at, close to, or far from equilibrium. It is an extension of detailed balancing for enzyme diagrams and was given the name *thermokinetic balancing* [53] in order to distinguish it from detailed balancing which, in the case of enzyme cycles, applies only when the catalyzed reaction is at equilibrium. The reader may find Eqn. A14 a little bit hard to read, and he or she may become better acquainted with this important relation when we apply it to the examples discussed in Section IV. It should be added that the Haldane relations [54] also arise from thermokinetic balancing but are expressed in terms of the Michaelis-Menten parameters.

Thermokinetic balancing for the only cycle in the diagram of the enzyme-catalyzed isomerization reaction (Fig. 4B) yields

$$K_{23}K_P/K_S = K_c \quad \text{for } S \rightleftarrows P \tag{76}$$

where K_c denotes the equilibrium constant of the reaction in Eqn. 54. Note that no relation involving K_{Ii} is obtained, in line with the requirement that a change in catalytic activity due to inhibitors should not alter the energetics of the catalyzed reaction. Cycles 1 and 3 in the diagram (Fig. 5C) of the enzyme catalyzing the formation of one product from two substrates (cf. Eqn. 61) yield

$$K_{45}K_P/(K_{S1}K_{S2}) = K_c \quad \text{for } S_1 + S_2 \rightleftarrows P, \tag{77a}$$

and

$$K'_{S1}K'_{S2}/(K_{S1}K_{S2}) = 1 \tag{77b}$$

The ratio of dissociation constants in Eqn. 77b is unity because no chemical reaction is involved with cycle 3 (see Appendix A.I-5). Note that thermokinetic balancing for cycle 2 does not add a new relation, it can be obtained by substituting $K_{S1}K_{S2}$ in Eqn. 77a from Eqn. 77b. The full cycle in Fig. 6A for a redox reaction complies with

$$K_{45}K_{81}K_{67}K_{Do}K_{Ar}/(K_{32}K_{Dr}K_{Ao}) = K_c \tag{78a}$$

The reduction of states and the definition of the condensed constants K_D^* and K_A^* In Eqn. A32a reduces Eqn. 78a to

$$K_{45}K_{81}K_A^*/K_D^* = K_c \quad \text{for } D_r + A_o \rightleftarrows D_o + A_r \tag{78b}$$

Thermokinetic balancing applied to the cycles in the diagrams for transport through a pore yields for cycle 1 in Fig. 7C

$$K_{23}K_2/K_1 = 1 \tag{79a}$$

and for cycle 3 in Fig. 7C

$$K_1'K_2/(K_1K_2') = 1 \tag{79b}$$

Again, the condition for cycle 2 can be obtained from Eqns. 79a and 79b. Finally, for the cycle in the diagram for a carrier (Fig. 6E)

$$K_{23}K_{41}K_2/K_1 = 1 \tag{80}$$

The ratio of constants in Eqns. 79 and 80 is unity for the reasons explained in Appendix A.I-5.

V.B. Flow-force relations

The analysis of the kinetic scheme of a process results in a relation indicating how the flow of the process depends on the concentrations of the reactants or the transported species. On the other hand, the thermodynamic force of a process is defined in terms of electrochemical potentials which implicitly comprise these concentrations. Making the concentrations explicit by virtue of Eqn. 20 yields from Eqn. 12, in view of Eqns. 26a and 26b,

$$\exp\{X_i/RT\} = K_{ci}/\left[\prod_r c_{Ri,r}^{\nu_{Ri,r}}\right] \tag{81a}$$

for a chemical reaction. Note that the terms $z_{Ri,r}F\psi$ in Eqn. 20 are cancelled because $\Sigma\nu_{Ri,r}z_{Ri,r} = 0$ for a chemical reaction. Moreover, the stoichiometric coefficients $\nu_{Ri,r}$ have to be taken with signs according to the convention introduced in subsection II.D-1. Similarly, from Eqn. 15 and by virtue of Eqn. 26c,

$$\exp\{X_i/RT\} = K_{ci}\rho_{Di}^{1/n_{Di}}/\rho_{Ai}^{1/n_{Ai}} \tag{81b}$$

For a transport process, we obtain from Eqn. 17,

$$\exp\{X_i/RT\} = \exp\{z_i\,\Delta\phi\}\,c_{io,1}/c_{io,2} \tag{81c}$$

where $\Delta\phi = \phi_1 - \phi_2$ is the difference in reduced potential (see Eqn. 25) between the compartments. When writing Eqns. 81, we have set either $f_{i,k} = 1$ or $f_{i,1} = f_{i,2}$, in line with the policy adopted in this review *.

Inspection of the expressions for the flows given in Section IV (Eqns. 46, 53, 55, 62, 63, 68, 69, 71–73) shows that, in view of the pertinent relations for detailed balancing (Eqns. 74 and 75) and thermokinetic balancing (Eqns. 76–80), the flow is in every case related to the force by

$$J_i = [\exp\{X_i/RT\} - 1]/\boldsymbol{F}(c_i) \tag{82}$$

$\boldsymbol{F}(c_i)$ is the abbreviation for a generally quite complex function which comprises the concentrations of the reactants ($c_i = c_{Ri,r}$) or the transported species ($c_i = c_{i,k}$). It is equivalent to a reciprocal flow and can be read from the pertinent equations listed above. Eqn. 82 evidently fulfils the condition $J_i = 0$ for $X_i = 0$ as required by thermodynamics for the equilibrium state (see subsection II.E-1). This is not surprising because we have taken care of this condition by means of detailed or thermokinetic balancing.

The flow of a process is not unequivocally defined by its thermodynamic force. As evident from Eqns. 81 there is a multitude of concentrations c_i which constitute the same force but yield different $\boldsymbol{F}(c_i)$. Essig and Caplan [55] have set forth conditions which make the flow a unique function of the force. The system has to follow what the authors called a 'proper path', but it is not easily intelligible what factors would set the constraints which guide the system on such a path.

Other constraints almost invariably introduced by the design of an experimental system as discussed in subsection II.A is an interrelation between the concentrations of some of the species involved in the processes. In fact, due to mass balance (cf. Eqns. 10 and 16), the mole numbers of substrates and products in a chemical reaction or those of a transported species in the two compartments cannot vary independently in an isolated system. Moreover, when choosing such conditions that a steady state of the system can be attained (see subsection II.E-2) we set the initial concentration and the chemical capacity for some reactants high enough in order to prevent an appreciable change in their concentration. These constraints and their effect on the flows of the processes in the system were first realized by Rottenberg [8] and later extended by Van der Meer et al. [9].

V.B-1. Chemical reactions under constraints

The above-mentioned constraints applied to the isomerization reaction specified in Eqn. 54 read

$$c_S + c_P = c_t = \text{const.} \tag{83a}$$

which, by virtue of Eqn. 81a, is transformed into

$$c_P = c_t/(1 + \exp\{X/RT\}/K_c) \tag{83b}$$

The function $\boldsymbol{F}$ in Eqn. 82 then becomes

$$\boldsymbol{F}(c_i) = \exp\{X/RT\}/J_+ + 1/J_- \tag{84}$$

* In Eqn. 81c the bulk phase concentration $c_{io,2}$, may be fictitious if interfacial domains dominate in compartment 2 (cf. Fig. 3). Moreover, $f_{i,2} = f_{i,1}$ and $\mu_{i,2}^o = \mu_{i,1}^o$ may be an oversimplification in this case because of the different properties of water in interfacial domains as compared to bulk phase water.

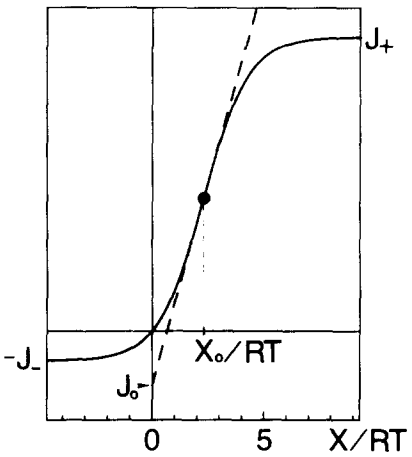

Fig. 8. Dependence of flow J on thermodynamic force X for a reaction or transport under constraints. The curve is the hyperbolic tangent and the broken line the tangent in its inflection point located at X_o. For large positive and negative forces the curve converges to the limits determined by the extreme flows J_+ and J_-, respectively. J_o indicates the intercept of the tangent on the ordinate. Flows are given in arbitrary units.

where the flows J_+ and J_- are the extreme flows for $c_S = c_t$, $c_P = 0$ and $c_S = 0$, $c_P = c_t$, respectively. For a reaction not catalyzed by an enzyme, they amount to

$$J_+ = Vk_1c_t \quad \text{and } J_- = Vk_{-1}c_t \tag{85a}$$

with k_1 and k_{-1} denoting the forward and backward rate constant, respectively. For an enzyme-catalyzed reaction the extreme flows can be expressed in terms of the Michaelis-Menten parameters (see Eqns. A20 and A21),

$$J_+ = (K_{mS}/c_t + 1)/(N_e k_{catS})$$

and

$$J_- = (K_{mP}/c_t + 1)/(N_e k_{catP}) \tag{85b}$$

By virtue of Eqns. 84 and 85, Eqn. 82 can be reformulated as

$$J = \frac{J_+ + J_-}{2} \tanh\left[\frac{X}{2RT} - \tfrac{1}{2}\ln\frac{J_+}{J_-}\right] + \frac{J_+ - J_-}{2} \tag{86}$$

Fig. 8 shows a plot of the now unambiguous flow-force relation in Eqn. 86. It thus appears that even a non-catalyzed chemical reaction displays saturation properties under the constraint specified in Eqn. 83a. The hyperbolic tangent has an *inflection point* when its argument is zero. Hence, from Eqn. 86

$$X_o/RT = \ln\{J_+/J_-\} \text{ (inflection point)} \tag{87}$$

which is equal to $\ln K_c$ for a non-catalyzed reaction. In the case of enzyme-catalysis, however,

$$X_o/RT = \ln\left[K_c \frac{1 + c_t/K_{mP}}{1 + c_t/K_{mS}}\right] \tag{88}$$

The argument in square brackets varies between K_c if $1 \gg c_t/K_{mX}$ (X = S and P) and $K_c K_{mS}/K_{mP} = k_{catS}/k_{catP} = K_{23}[1 + \tau_1(1 + K_{23})]/[1 + \tau_2(1 + K_{23})]$ (cf. Eqn. A20 and A21) if $1 \ll c_t/K_{mX}$. The location of the inflection point thus depends on c_t, and a substantial offset of X_o due to a large or small K_c can be partially or fully balanced by a large enough concentration c_t provided that K_{23}, τ_1 and τ_2 have appropriate values.

The hyperbolic tangent deviates less than 10% from its tangent in the inflection point if the argument varies within the range from -0.71 to 0.71 around this point. Hence, we can reasonably approximate Eqn. 86 by the linear relation

$$J \approx \left[\frac{J_+ - J_-}{2} - \frac{J_+ + J_-}{4}(X_o/RT)\right] + \frac{J_+ + J_-}{4}(X/RT) \tag{86a}$$

(see Fig. 8) which, in terms of X, covers the range of ± 1.75 kJ/mol around X_o. Note that the intercept on the J-axis, which is enclosed in square brackets in Eqn. 86a, also goes to zero when X_o approaches zero.

The same flow-force relation (Eqn. 86) emerges if c_S or c_P is constant with $J_- = N_e k_{catP}$ or $J_+ = N_e k_{cat}$ while the other extreme flow is given by Eqns. 85b with c_t representing the constant concentration, respectively. However, the non-catalyzed reaction no longer complies with Eqn. 86 under these conditions.

Appropriate constraints for the reaction where two substrates are converted into one product (Eqn. 61) are

$$c_{S1} + c_P = c_t = \text{const}, \quad c_{S2} \approx c_o = \text{const} \tag{89}$$

The flow of the non-catalyzed reaction is then again represented by Eqn. 86 with extreme flows

$$J_+ = Vk_1c_tc_o \quad \text{and } J_- = Vk_{-1}c_t \tag{90}$$

The same extreme flows pertain for $c_{S1} \approx c_o$ and $c_{S1} + c_P = c_t$. For the enzyme-catalyzed reaction, however, the situation is more complex. The function $F(c_i)$ adopts the form given in Eqn. 84 only if the reaction does not deviate from the simple 'Michaelis-Menten law' which, as discussed in subsection IV.B-3, requires either fast binding steps (i.e., $\tau_i \approx 0$, see Eqns. A25a) or ordered binding (i.e., $B_r \approx 0$ in Eqn. 62). The extreme flows then become in terms of the Michaelis-Menten parameters in Eqns. A27 and A28 (rewritten for the forementioned conditions),

$$J_+ = N_e k_{catS1}(c_o)/[1 + K_{mS1}(c_o)/c_t)]$$

and

$$J_- = N_e k_{catP}/[1 + K_{mP}/c_t + D(c_o)] \tag{91a}$$

The abbreviation $D(c_o)$ in Eqn. 91a reads

$$D(c_o) = c_o K_{mP}/(c_t K'_{S1}) \tag{91b}$$

for random binding, and

$$D(c_o) = \tau_1 c_o / K_{S2}[1 + K_{45}(1 + K_P/c_t)]/D_P \tag{91c}$$

for ordered binding (for D_p see Eqn. A28). In contrast to the non-catalyzed reaction, the relations for the extreme flows are not invariant with respect to an exchange of c_{S1} and c_{S2} in Eqn. 89. In fact, $\boldsymbol{F}(c_i)$ then includes the additional term $\tau_1 \exp\{X/RT\}/[\exp\{X/RT\} + c_o K_c](c_t/K_{S2})(1 + K_{45})/(N_e \alpha_{54})$ in the case of ordered binding which can be neglected under the conditions given in parentheses in Eqn. 92. Then,

$$J_+ = N_e k_{catS2}(c_o)/[1 + K_{mS2}(c_o)/c_t)]$$

and

$$J_- = N_e k_{catP}[1 + (K_{mP}/c_t)(1 + c_o/K_{S1})]$$

$$\text{for } c_{S1} \approx c_o, \quad c_{S2} + c_P = c_t, \quad (\tau_1 \approx 0 \text{ or } c_t \ll K_{S2}) \tag{92}$$

The position of the inflection point according to Eqn. 87 is also determined by c_o in addition to c_t and becomes for random binding under the constraints specified in Eqn. 89

$$\frac{X_o}{RT} = \ln\left[c_o K_c \frac{1 + c_t/K_P + c_o/K'_{S1}}{1 + (1 + c_o/K_{S2})c_t/K_{S1} + c_o K'_{S1}/(K_{S1}K_{S2})}\right] \tag{93}$$

An offset of X_o due to a large or small K_c can then be compensated by both concentrations. The constraints given in Eqn. 92 yield the same relation for X_o but with K_{S1} replacing K'_{S1} in the numerator, and c_o and c_t being swapped in the denominator. The relations for random binding have a similar structure but shall be omitted here because of their complexity.

The situation is somewhat different in the case of redox reactions. Mass balance requires only that

$$c_{Xr} + c_{Xo} = c_{Xt} = \text{constant} \quad \text{for X = D and A} \tag{95}$$

which does not provide a relation between ρ_D and ρ_A. Additional constraints are necessary which can arise from high enough concentrations and capacities for the species of one of the redox couples (e.g., the couple H_2O/O_2) yielding either ρ_A constant or $\rho_D \approx$ constant. Then, $\boldsymbol{F}(c_i)$ adopts the form of Eqn. 84 with extreme flows

$$J_+ = N_e \alpha_{54} K_{45}, \quad J_- = N_e \alpha_{54} \rho_A / [K_A^* (1 + K_{81})],$$

and

$$J_+/J_- = K_{45}(1 + K_{81}) K_A^*/\rho_A$$

$$\text{for } \rho_A \approx \text{const.}, \quad \tau_i \approx 0 \tag{95}$$

Analogous equations for the flows in the case $\rho_D \approx$ constant exist, and similar but more complex relations are obtained if $\tau_i \neq 0$. Thus, provided that the affinity of the electron is varied just by changing ρ of one of the couples under the constraints in Eqn. 94 while ρ of the other couple is approximately constant, the flow of electrons depends on the affinity according to the hyperbolic tangent (Eqn. 86) and the inflection point may be near $A_e = 0$ for suitable values of the fixed ρ (and c_t in case of $\tau_i \neq 0$).

V.B-2. Transport under constraints, and the kinetic inequivalence of chemical and electrical potential

Mass balance in the case of transport between two compartments requires that

$$V_1 c_{io,1} + V_2 c_{io,2} = N_{ti} = c_{ti} V_t = \text{const.} \tag{96a}$$

where N_{ti} is the total mole number of the ith species, and c_{ti} is the total concentration defined with respect to the total volume $V_t = V_1 + V_2$. In most cases the volume of the suspending medium is much larger than that of the combined interior spaces of the vesicles, i.e., $V_1 \gg V_2$ Hence, the chemical capacity (cf. Eqn. 29) in compartment 1, particularly if supported by suitable buffers, is also much larger than that in compartment 2, and

$$c_{io,1} \approx \text{const.} \tag{96b}$$

is then the most likely additional constraint. For the transport of an *uncharged species or if* $\Delta\phi = \phi_{sk} = 0$, the function $\boldsymbol{F}(c_i)$ adopts the form given in Eqn. 84 under the constraints specified in Eqns. 96 in the case of permeation (cf. Eqn. 68a) and carrier-mediated transport (Eqn. 72). This is also true for the transport through a pore provided that double occupancy of the pore can be excluded (Eqn. 69 with $b_p = B_p \approx 0$). The extreme flows read for permeation

$$J_+ = AP_i N_t / V_1 \quad \text{and } J_- = AP_i N_t / V_2 \tag{97a}$$

while for carrier-mediated transport (index x = c) or transport through a singly occupied pore (index x = p)

$$J_+ = N_x k_{cat1}/[1 + (V_1/V_t)c_t/K_{m1}]$$

and

$$J_- = N_x k_{cat2}/[1 + (V_2/V_t)c_t/K_{m2} + D_x] \tag{97b}$$

The additional term D_x is for a pore and carrier, respectively,

$$D_p = 0 \quad \text{and } D_c = \tau_3 \frac{c_1}{K_1} \frac{K_{41}(1 + K_{23})}{1 + \tau_1(1 + K_{23}) + \tau_3 K_{41}} \tag{97c}$$

It vanishes also for a carrier if $\tau_3 \approx 0$, i.e., if the transition of the empty carrier is much faster than that of the loaded carrier. Transport under the above-specified

constraints and conditions thus complies with the unambiguous flow-force relation of Eqn. 86. Its inflection point is very much offset from the origin in the case of permeation since (cf. Eqns. 87 and 97a) $X_o/RT = \ln\{V_2/V_1\}$ which is rather negative because of $V_2/V_1 \ll 1$ (see above). This is not so for the transport mediated by a pore or a carrier. In these cases, the location of the inflection point is determined mainly by c_t with respect to the binding constants and the equilibrium constants for the translocation steps. Assuming for the moment that all $\tau_i \approx 0$ and $V_2/V_t \approx 0$ while $V_1/V_t \approx 1$, $X_o/RT \approx K_{23}/(1 + K_1/c_t)$ for a pore and $X_o/RT \approx K_{23}/[1 + K_1/c_t(1 + 1/K_{41})]$ for a carrier.

Let us now turn to the other extreme, where only an electrical potential difference exists across the membrane but the concentrations in both compartments are equal, i.e., $c_{io,1} = c_{io,2} = c_{it}$. Obviously, $J_i = 0$ for an uncharged species. For a charged species with valence z_i, $X_i/RT = z_i\,\Delta\phi$ (cf. Eqn. 81c) and, with the simplifying assumption of equal surface potentials on both sides of the membrane,

$$J_i = X_i A P_i c_{it}/(RT \exp\{z_i\phi_{s1}\}), \quad \phi_{s2} = \phi_{s1} \tag{98}$$

for permeation (cf. Eqns. 67 and 68). The flow is always proportional to its conjugated force, in strong contrast to the other extreme case (viz. no electrical potential but a concentration difference) where it was at most linear over a limited range of force. We thus encounter the unpleasant situation that the *chemical and electrical potential which are thermodynamically equivalent in determining the force are kinetically not equivalent.* This is in general also true for transport mediated by a carrier or a pore. The effect of an electrical potential concerns all transitions in a cycle where a displacement of charges takes place, i.e., whose $\zeta_{ij} \neq 0$ (see Appendix A.I-3), while different concentrations in the compartments affect only the association probabilities in the binding transitions (cf. Eqns. A41 and A47). On the other hand, a surface potential merely alters the concentration on the membrane surface as compared to the concentration in the adjacent bulk phase, and hence influences also only the association process in binding. However, if a pore or a carrier are built in such a way that electrical potential and concentration operate essentially on the same transitions, the two terms in the force have the same effect on transport, and such devices are said to display kinetic equivalence of electrical and chemical potential. For a further discussion of this concept see Refs. 56,57.

V.C. Energetics of enzymes

The cycle diagram method of Hill also provides insight into the energetics of the enzyme states. This will allow us to address among other topics the question of 'rate-limiting steps' and the controversial point of 'energy transfer' between reactants.

V.C-1. Standard, basic and gross free energy levels

The equilibrium constants defined in Eqns. A15 and A16 for each transition in a diagram can be interpreted in terms of *standard free energies*, in full analogy to the equilibrium constants for reactions in solution (cf. Eqns. 26). Each transition from state i to state j is then associated with a change in standard free energy, $G_i^o - G_j^o$, of the states. In fact, we could also say a difference in standard chemical potential, $\mu_i^o - \mu_j^o$, of the states but will retain G^o to avoid confusion with μ^o for reactants. Thus, from Eqn. A15,

$$G_j^o = G_i^o - RT \ln K_{ij} \tag{99a}$$

for a transition due to a conformational change (see subsection IV.B-1), and from Eqn. A16

$$G_{j(\mathrm{Rr})}^o = G_i^o + RT \ln K_{\mathrm{Rr}} \tag{99b}$$

for a transition pertinent to binding of reactant R_r where j is the state with bound reactant as indicated. By virtue of Eqns. 99, we can construct a diagram for the levels of the standard free energies of the states in each cycle. These levels are with respect to an arbitrarily chosen reference state which usually is the state of the enzyme (or pore or carrier) without bound reactants, inhibitors or any other ligand.

Fig. 9A shows an example of a standard free energy level diagram for an enzyme catalyzing the isomerization reaction (see Eqn. 54 and Fig. 4) in the absence of an inhibitor. In the presence of an inhibitor, an additional level is added to each state according to Eqn. 99b written for the dissociation constant, K_{Ii}, of inhibitor binding to state i, as indicated by the broken lines in Fig. 9A. The last level in Fig. 9A, representing again the free enzyme, is displaced from the reference level by $-\Delta G^o = \mu_S^o - \mu_P^o = RT \ln K_c$ because going around the cycle in the positive direction causes P to be formed from S. This is another expression of thermokinetic balancing (see Eqn. 76) which relates the equilibrium constants of the transitions in a cycle to the equilibrium constant of the reaction associated with a turn around the cycle.

The standard free energy levels set the absolute frame or the 'scaffold' in which the enzyme can move. As evident from the example in Fig. 9A, they can go 'up and down' and thus do not lend themselves to decide in which direction an enzyme cycle will turn. In fact, they are modified by the actual concentrations of the reactants in a steady state of the system. Including these concentrations leads to what Hill has termed the *basic free energy*, G', of the enzyme states [12]. Conforma-

tional transitions are obviously not affected by concentrations of reactants, hence

$$G'_j = G'_i - RT \ln K_{ij} \tag{100a}$$

but for a transition with binding of a reactant,

$$G'_{j(\mathrm{Rr})} = G'_i + RT \ln\{K_{\mathrm{Rr}}/c_{\mathrm{Rr}}\} \tag{100b}$$

Fig. 9B depicts the basic free energy levels obtained from the standard free energy levels in Fig. 9A for two different steady states. The difference between reference and final level is now equal to the thermodynamic force of the reaction $S \rightleftarrows P$ for the given concentrations c_S and c_P (see Eqn. 81a). The basic free energies define the levels attainable by the enzyme states in a given steady state of the system, and still can go 'up and down'. The enzyme so to speak 'diffuses back and forth' between these levels which causes the probabilities, p_i, of the states (see Appendix A.I-1) to eventually adopt such values that the flow J_{ij} for each transition in a cycle (cf. Eqn. A7) is the same at the *steady state of the enzyme*.

Similarly as we have related the thermodynamic force of a reaction to the concentrations of the reactants by means of the equilibrium constant (see Eqn. 81a), we

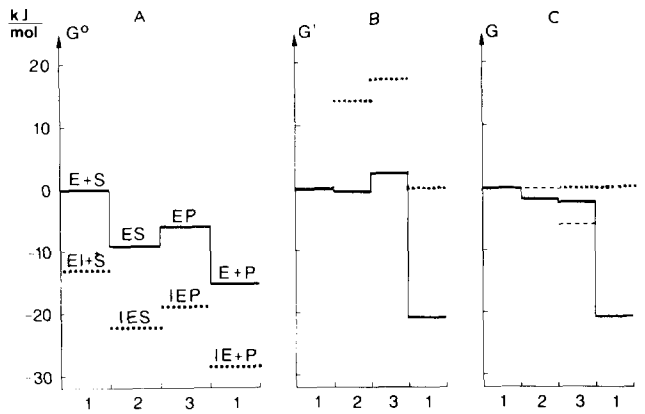

Fig. 9. Standard (A), basic (B) and gross free energy levels (C) for an enzyme catalyzing the isomerization reaction specified in Eqn. 54 (cf. Fig. 4). $G°$ was calculated with Eqns. 99 and $K_S = 0.025$ M, $K_{23} = 0.25$, $K_P = 50$ M which yields $K_c = 500$. Broken lines indicate $G°$ for bound inhibitor with $K_I = 0.005$ M (noncompetitive inhibition, see Eqn. 59), and are omitted in (B) and (C). G' in (B) was calculated according to Eqns. 100 for $c_S = 36$ mM, $c_P = 4$ mM (solid line), and for $c_S = 0.08$ mM, $c_P = 39.92$ mM (dotted line) pertinent to equilibrium (constant $c_t = c_S + c_P = 40$ mM). G in (C) was calculated according to Eqns. 101 and the following values for p_1, p_2, and p_3 obtained from the analysis of the diagram in Fig. 4B: 0.5364, 0.3863, and 0.0773 for $\tau_1 = 20$, $\tau_2 = 4$ (solid line); 0.4098, 0.5770, and 0.0132 for $\tau_1 = \tau_2 = 0.1$ (broken line); 0.9960, 0.0032 and 0.0008 for either set of τ_i values (dotted line). The former two cases pertain to $c_S = 36$ mM, $c_P = 4$ mM and have relative flows $J/(N_e\alpha_{32})$ of 0.019 and 0.131, respectively, while the latter case is at equilibrium ($J = 0$) with equal G for all states. The numbers on the bottom indicate the states of the enzyme (cf. Fig. 4B).

can define a thermodynamic force for each transition by means of the state probabilities and the pertinent equilibrium constants. The force is equal to the difference in what Hill calls the *gross free energy*, G, of the enzyme states [12]. Hence,

$$G_j = G_i - RT \ln\{K_{ij} p_i / p_j\} \tag{101a}$$

and

$$G_{j(\mathrm{Rr})} = G_i + RT \ln\{K_{\mathrm{Rr}} p_j / (c_{\mathrm{Rr}} p_i)\} \tag{101b}$$

The state probabilities, p_i, are determined by the transition probabilities, α_{ij}, and can be calculated as outlined in the Appendix. Fig. 9C then presents the gross free energy levels for the two steady states, calculated with the parameter values given in the legend. Note that the difference between final and reference level of the gross free energy is still equal to the force of the reaction, in line with the notion that catalysis does not change the energetics of the catalyzed reaction. The force for each transition has now the same sign, it indicates the net turnover direction of the cycle which results from stochastic backward and forward movement of the enzyme between the states analogous to the diffusion of molecules down a concentration (or free energy) gradient [12].

The above considerations were made for an enzyme in solution. They apply as well to membrane bound enzymes but then have to include the effect of a membrane potential on the transition probabilities and the possible deviation of the concentrations on the membrane surface from that in the bulk phase due to surface potentials. This simply adds the term $\zeta_{ij} F \Delta\phi_m / RT$ in Eqns. 100a and 101a, while the term for Eqns. 100b and 101b reads $F[\zeta_{ij} \Delta\phi_m + z_{\mathrm{Rr}}\phi_{sk}]/RT$. The membrane potential shifts the basic and gross free energy levels for those transitions which involve a charge displacement (see Appendix A.I-3) and contributes to the thermodynamic force of the transmembrane processes (cf. Eqn. 81c); however, it does not affect the standard free energy levels.

V.C-2. Relevance of free energies to enzyme performance

The standard free energy levels reflect the interaction of the enzyme with the reactants. Thus, in the example shown in Fig. 9, there is a strong interaction between substrate S and the enzyme E, while the opposite is true for the product P. These interaction energies should be considered in the context of the purpose for which the enzyme is designed, i.e., the concentrations of substrate and product which it encounters in situ. The relevant quantities are then the basic free energy levels shown in Fig. 9B. Assuming that $c_t = 40$ mM is a typical total concentration for reactants for our hypothetical enzyme

we find K_S to be well adjusted for values of c_S where a substantial flow of the reaction occurs, while binding of S to the enzyme hardly occurs at equilibrium of the reaction. On the other hand, the conditions for the product are such that little binding occurs at any circumstances. This principle is particularly evident in the example of the Ca^{2+}-transporting ATPase of the sarcoplasmic reticulum discussed by Walz and Caplan [53]. The dissociation constants are roughly 2 μM and 2 mM for the release of these ions into the cytoplasm and the lumen of the reticulum, respectively, and well adjusted to the Ca^{2+}-concentrations typical for the two spaces.

A frequently used approach is to declare one transition in a kinetic scheme to be the rate-limiting step which should legitimate the assumption that all other transitions are at (or very close to) equilibrium. Such close to equilibrium transitions are recognizable by a vanishing difference between the gross free energy levels of the pertinent states, which immediately brings us to the following conclusions. *The* rate limiting step in a scheme hardly exists, because G is determined by G', which in turn depends on the concentrations of the reactants (cf. Eqns. 100 and 101). Hence, only in an exceptional case will the variation in G' be balanced by a suitable adjustment of the state probabilities such that G remains constant and about equal for all states before and after the 'rate-limiting step' while the varying thermodynamic force of the reaction appears fully as a difference in G for the states adjacent to the 'rate-limiting step'. Such a situation indeed occurs if all $\tau_i \approx 0$ in a given scheme (see Appendix). Otherwise, transitions with a very small difference in G can occur (see Fig. 9C) but this condition does not have to persist when the concentrations of the reactants vary (cf. Fig. 4 in Ref. 53). Under no circumstances can a 'rate-limiting step' be inferred from the standard free energy levels. As evident from the example in Fig. 9, the 'high affinity' for the binding of S does not cause the pertinent transition to be 'rate-limiting', and the 'low affinity' for the binding of P does not help to reduce the drop in G for this transition. The relevant parameters are the relative transition probabilities as expressed by the τ_i values together with the G' levels.

It is important to note that the change in G^o for a given transition primarily reflects the variation in the interaction of the enzyme with bound reactants. Hence, an attempt to interpret such changes as a 'transfer of free energy' between the reactants of two coupled processes [58] is bound to fail. Besides the fact that the assignment of a change in G^o to a given bound reactant is highly ambiguous in the presence of other bound reactants [53,59], the enzyme would then merely play the role of an 'inert matrix'. Such a view would be hard to reconcile with the high affinities and specificities involved in the binding of reactants to enzymes (see also Ref. 42).

VI. Coupled processes and energy conversion

A coupling between two processes in general terms means that they cannot proceed independently, although all necessary reactants are present. This definition includes a number of cases which we usually do not qualify as coupled processes. Thus, a reaction occurring in one compartment with reactants being transported across the membrane into the other compartment would be coupled processes since, at steady state, transport and reaction rates are strictly interrelated. Similarly, the flow of electrons through a redox enzyme whose donating redox couple is the accepting couple of another redox enzyme (cf. subsection IV.B-4) is equal to the electron flow through the preceding enzyme at steady state. This situation is known as electron transport through a chain of redox enzymes rather than coupling of two independent electron transferring processes. We therefore restrict the notion of coupling to those cases where the coupled processes are either two reactions of different type, or a reaction and a transport where the latter does not pertain to the reactants of the former, or two transports of different species.

Coupling, i.e., a strict relation between the flows of the processes, can occur only if *the processes share a common element which has attained a steady state*. Note that the steady state in this statement concerns only the common element and not the whole system. The common element can be rather diverse in nature ranging from a simple chemical species in solution to a dipole-dipole interaction of components in a membrane. The strict relation between flows can cause the flow of one process to run against its thermodynamic force (cf. subsection II.D-3), and an *energy conversion* then takes place from the process whose flow is in the direction determined by its force, which is called the driving process, to the process whose flow runs against its force called the driven process. Which process is driving and which is the driven one is not inherent to the coupling mechanism but depends on the conditions imposed on the system (clamping of forces, chemical capacities etc., see subsection VI.E).

Inherent in the notion of coupling is the possibility of uncoupling the processes by any suitable means which causes the interrelation between the flows to be changed or totally broken. The mechanisms by which such an uncoupling in general terms is brought about are as diverse as is the nature of the common element. This has created some confusion with respect to terminology because, for historical reasons, it has become customary to restrict the notation uncoupling (and uncouplers for the means causing uncoupling) to a particular mechanism. I shall try to avoid the confusion by choosing different notations for uncoupling in the general sense depending on the mechanism involved. Moreover, I will divide the discussion of coupling

according to the nature of the common element and the level of description.

VI.A. Electroneutrality and the membrane potential

It may appear somewhat unusual that this subject is dealt with under the topic of coupling. However, the condition of electroneutrality introduces a strict relation between the flows of charged species across a membrane, and the membrane potential (or the capacitance associated with the membrane) constitutes the common element. The condition of electroneutrality expresses the fact that an imbalance of charges in an aqueous phase cannot exist except for the very thin diffuse layers on the membrane surfaces (see subsection III.B). Hence, for the bulk phase in the kth compartment

$$\sum_i z_i N_{i,k} = 0 \text{ (electroneutrality)} \tag{102}$$

where the sum includes all charged species. Taking the time derivative of Eqn. 102 and introducing the flows according to Eqn. 16 yields

$$\sum_i z_i J_i = 0 \tag{103}$$

which is the interrelation of flows referred to above. Note that Eqn. 103 remains valid even when the flow of some of the charged species in the compartments vanishes.

According to our general concept of coupling, the common element has to be in a steady state. This means that Eqn. 103 is not obeyed as long as the composition of the diffuse layers on the membrane surfaces varies substantially or, in other words, as long as a charging of the membrane capacitance takes place. Let us therefore investigate whether this process can relax to a steady state before one of the compartments has reached such a state. To this end, we compare the change in voltage across the membrane capacitance, $\mathrm{d}U$, with the corresponding changes in concentration of charged species, $\mathrm{d}c_{io,k}$, in the bulk phase of the compartments. Recognizing that $\mathrm{d}Q_i = Fz_i\,\mathrm{d}N_i$ charges are transferred across the membrane concomitantly with the transfer of $\mathrm{d}N_i$ moles of a charged species, we obtain from Eqns. 42 in view of Eqn. 27,

$$\mathrm{d}U = \sum_i z_i\,\mathrm{d}c_{io,k}[FC_{ci,k}/(AC_m)] \tag{104}$$

The terms in square brackets determine how the changes in concentration are translated into a change in voltage. Taking the volume, V_k, of a compartment as the lower limit for the chemical capacity $C_{ci,k}$ (cf. Eqn. 29) these terms become identical for all species and amount to $FV_k/(C_mA)$, where A is the total membrane area included because C_m is the capacitance per unit membrane area. We can evaluate this term for thylakoids, since data on the specific surface, $\bar{o} = A/N_{chl}$, are available [60]. The term then reads $F\bar{v}_k/(C_m\bar{o})$ where $\bar{v}_k = V_k/N_{chl}$ is the specific volume of compartment k and N_{chl} denotes the mole number of total chlorophyll contained in the thylakoid membranes. With $\bar{o} \approx 1$ $\mathrm{m}^2/\mu\mathrm{mol}$, $\bar{v}_2 \approx 20$ l/mol, and $C_m \approx 1$ $\mu\mathrm{F/cm}^2$, $F\bar{v}_2/(C_m\bar{o}) \approx 200$ mV/mM while $F\bar{v}_1/(C_m\bar{o}) \approx 10^5$ mV/mM whereby $\bar{v}_1$ is approximated by V_{tot}/N_{chl} and given a value of 10^4 M^{-1}. Similar results are most likely obtained for other vesicular suspensions. We thus find that changes in the range of tenth of millimolar in the smaller compartment * suffices to build up typical values for a large membrane potential, and therefore conclude that charging of the membrane capacitance indeed relaxes (and thereafter adapts) fast enough to attain (and remain in) a steady state before this occurs for the two compartments (see subsection II.E-2).

Having established the validity of Eqn. 103 we can exploit it to estimate the membrane potential which is the difference of the electrical potentials in the bulk phase of the compartments, $\Delta\psi = \psi_1 - \psi_2$. We just have to substitute the flows in Eqn. 103 by the appropriate relations worked out for transport in subsection IV.C, but then we realize that transcendental equations emerge which comprise sums of exponentials of the membrane potential. Hence, an explicit solution does not exist in general but is possible for special cases. If only one charged species (which is given the index p for permeable) can move across the membrane Eqn. 103 is simplified to $J_p = 0$ and, independent of the mode of transport or the presence of surface potentials,

$$\Delta\psi = (RT/z_iF)\ln\{c_{po,2}/c_{po,1}\} \tag{105}$$

This relation is known as the Nernst equation and could as well be derived from the equilibrium condition $X_p = 0$, since $J_p = 0$ (cf. Eqns. 17 and 20).

If only univalent ions permeate through the membrane, and if the surface potentials are negligibly small or else are equal but have opposite signs, we obtain by virtue of Eqn. 68 the relation which is known as the Goldman equation,

$$\Delta\psi = \frac{RT}{F}\ln\left[\frac{\Sigma_+ P_i c_{io,2} - \Sigma_- P_i c_{io,1}}{\Sigma_+ P_i c_{io,1} - \Sigma_- P_i c_{io,2}}\right]$$

$$\text{for } z_i = \pm 1, \quad \phi_{s2} = -\phi_{s1} \quad \text{or } \phi_{sk} \approx 0 \tag{106}$$

* Note that this compartment is treated as if bulk phase conditions would apply while in many cases interfacial domains are dominant (cf. Fig. 3). This does not invalidate the conclusion about the fast relaxation for charging of the membrane capacitance but has consequences for the formation of X_H to be discussed in subsection VI.C-1.

where Σ_+ and Σ_- indicates summation over all positive and negative species, respectively. Provided that all transport processes can be approximated by the linear flow-force relations to be discussed in subsection VI.D-1 (see Eqns. 111), the solution for $\Delta\psi$ is straightforward and reads in the case of no coupling

$$\Delta\psi = -\left[\sum_i z_i L_i \Delta\mu_i\right] \Big/ \left[F\sum_i z_i^2 L_i\right] \tag{107}$$

where $\Delta\mu_i$ is the difference in chemical potential (cf. Eqn. 22). There are additional special cases which I leave to be figured out by the reader as a challenge.

VI.B. Coupling on the molecular level by enzymes

Two processes become coupled if they are catalyzed by the same enzyme and when the enzyme has attained a steady state. The enzyme thus constitutes the common element. Enzyme-catalyzed group translocating reactions could then be considered as coupled processes. They usually occur by the so-called ping-pong mechanism in Cleland's notation [40] where the moiety (or group) to be translocated is first transferred onto the enzyme by one substrate/product pair and taken over from the enzyme by the other pair. In this respect, the electron transfer between a donating and accepting redox couple via a redox enzyme discussed in subsection IV.B-4 could also be considered as a 'group (the electron) translocating reaction'. However, I shall exclude such cases from the present discussion for two reasons. The translocated group can often not exist as a free entity, as in the case of the electron in redox reactions or the methylene group in transmethylation reactions; the 'coupled processes' are then at most 'half reactions', as specified in Eqn. 13 for redox couples, which cannot proceed independently. In cases where the group exists as free entity (e.g., the phosphate group) the type of reaction is the same for both processes which, according to the policy set at the beginning of this section, is considered as a flow of a species through a sequence of steps (like in electron transport).

VI.B-1. Antiport of species, and the concepts of slipping and multiple inflection point

We can construct what is generally called a cotransport of species by hooking two carriers together. Depending on which states in the cycle pertinent to transport of one species (cf. Fig. 6E) are common to the cycle for the other species, we end up with what is termed *antiport* if the two states of the unliganded enzyme are shared (see Fig. 10A) or *symport* if the states liganded with one species are identified with the 'free' enzyme states in the (isolated) cycle for the other species. We postpone the discussion of symport to the next subsection and concentrate here on antiport, which

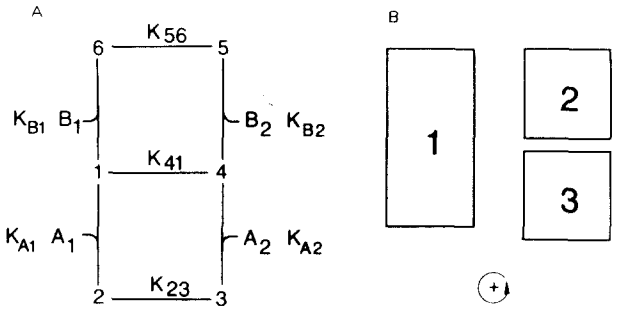

Fig. 10. Diagram (A) and cycles (B) for an antiport carrier. A and B denote the species with index 1 and 2 indicating the compartment from which they are bound to the carrier. For an explanation of symbols see legend to Fig. 4.

allows us to introduce the important concepts of slipping and multiple inflection point by means of 'relatively simple' relations. Before doing so we note that coupled transport could as well be achieved by hooking two pores together. In this case, a given state of one pore (see Fig. 7) has to interact with the states of the other pore but to a quite different extent (for an assessment of interaction see Hill [12,14]). The diagram emerging from this treatment is similar to that for a coupled carrier.

The analysis of the diagram for antiport shown in Fig. 10A yields two flows whose positive direction is from compartment 1 to compartment 2. For *uncharged species A and B or if* $\Delta\phi = \phi_{sk} = 0$, the flow for species A becomes in terms of the thermodynamic forces X_A and X_B of the species (cf. Eqn. 17)

$$J_A = \frac{1}{F(c_i)}\left\{\exp\left\{\frac{X_A - X_B}{RT}\right\} - 1 + \tau_{sA}\frac{K_{B1}}{c_{B,1}}\left[\exp\left\{\frac{X_A}{RT}\right\} - 1\right]\right\} \tag{108a}$$

while that for species B reads

$$J_B = \frac{-1}{F(c_i)}\left\{\exp\left\{\frac{X_A - X_B}{RT}\right\} - 1 + \tau_{sB}\frac{K_{A2}}{c_{A,2}}\left[\exp\left\{\frac{X_B}{RT}\right\} - 1\right]\right\} \tag{108b}$$

In Eqns. 108, $c_{A,2}$ and $c_{B,1}$ denote the concentrations of species A and B in the bulk phase of compartment 2 and 1, respectively. K_{B1} and K_{A2} are the dissociation constants as indicated in Fig. 10A (cf. Eqn. A16). The term $F(c_i)$ (compare Eqn. 82) as well as the quantities τ_{sA} and τ_{sB} can be found in the Appendix (Eqns. A50 and A53).

It is evident from Eqns. 108 that both flows are driven by the composite force, $X_A - X_B$ which expresses the coupling between the flows due to the common element, i.e., the enzyme. The composite force is the difference of the individual forces because of the antiport mechanism of coupling and, for the same reason, the negative sign appears in front of Eqn. 108b. In addition and depending on the values of τ_{sA} and τ_{sB},

each flow is also driven by its conjugate force alone. Inspection of Eqns. A52 and A53 shows that τ_{sA} and τ_{sB} are proportional to the ratios α_{14}/α_{65} and α_{14}/α_{32}, respectively, which measure how fast the transition between the states of the free carrier (states 1 and 4) is with respect to those between the states with bound species B (states 5 and 6) and A (states 2 and 3, see Fig. 10A). The part of the flow of any species driven by its conjugate force alone is obviously not coupled to the flow of any other species. We thus recognize that the *transition 1 ⇄ 4 causes the flows to be not tightly coupled.* This partial uncoupling (or even full uncoupling if τ_{sA} and $\tau_{sB} \gg 1$) is an intrinsic property of the enzyme and hence was called 'intrinsic uncoupling' [61–63]. In order to clearly distinguish this case from 'classical uncoupling' (see subsection VI.C) I suggest using the notation of *a slip in the enzyme* or *slipping*. This refers to the fact that the enzyme can occasionally or frequently 'slip' through cycles 2 and 3 (see Fig. 10B) besides going around the 'coupled cycle' 1. The frequency of this slipping is governed by τ_{sA} and τ_{sB} which, for this reason, have been given the index s.

The function $\boldsymbol{F}(c_i)$ written in terms of forces under the constraints

$$c_{A,1} \approx c_A = \text{const} \quad \text{and } c_{B,1} \approx c_B = \text{const} \tag{109}$$

comprises X_A and the composite force $X_A - X_B$ (see Eqn. A54). Provided that the transition of the carrier with bound A is much slower than the transition with bound B (i.e., $\tau_5 \approx 0$), the terms with force X_A can be neglected and $\boldsymbol{F}(c_i)$ adopts the form of Eqn. 84 with X being replaced by the composite force. Eqns. 108 then read:

$$J_A = \frac{\exp\{(X_A - X_B)/RT\} - 1}{1/J_- + \exp\{(X_A - X_B)/RT\}/J_+} + \tau_{sA}\frac{K_{B1}}{c_B}\frac{\exp\{X_A/RT\} - 1}{1/J_- + \exp\{X_A/RT\}/[J_+ \exp\{X_B/RT\}]}$$

$$\text{for } \tau_5 \approx 0 \quad \text{and } c_A = \text{const}, \quad c_B = \text{const} \tag{110a}$$

and

$$J_B = -\frac{\exp\{(X_A - X_B)/RT\} - 1}{1/J_- + \exp\{(X_A - X_B)/RT\}/J_+} - \tau_{sB}\frac{K_{A2}}{c_A}\exp\{X_A/RT\} \times \frac{\exp\{-X_B/RT\} - 1}{1/J_- + \exp\{-X_B)/RT\}/[J_+ \exp\{-X_A/RT\}]}$$

$$\text{for } \tau_5 \approx 0 \quad \text{and } c_A = \text{const}, \quad c_B = \text{const} \tag{110b}$$

The extreme flows J_+ and J_- are given by Eqns. A55 in the Appendix. Let us start the discussion of Eqns. 110 with the case of no slipping, i.e., $\tau_{sA} = \tau_{sB} = 0$. Then, $J_A = -J_B$ as expected. Moreover, both flows are determined by the same extreme flows, which is not trivial at all and possible only because we can neglect the terms comprising X_A in $\boldsymbol{F}(c_i)$ due to $\tau_5 \approx 0$. It means that we get the same hyperbolic tangent function (cf. Eqn. 86) when we clamp, say, X_B and vary X_A as when we do the opposite. Rothschild et al. [64] referred to this situation as the coupled processes having a 'multiple inflection point', and have worked out conditions to be fulfilled by a system for such points to exist.

For an antiport carrier with a slip, i.e., $\tau_{sA} \neq 0$ and $\tau_{sB} \neq 0$, the second terms in Eqns. 110 contribute to J_A and J_B. Each of these terms can also be expressed by a hyperbolic tangent but with respect to the conjugate force X_A and X_B only and with extreme flows depending on the force of the other species. Moreover, the term for species B is proportional to $\exp\{X_A/RT\}$ but not vice versa, and in general $\tau_{sA} \neq \tau_{sB}$, as exemplified by the present case *. The symmetry with respect to forces found in the case without slip can then at most approximately hold for a small slip and sooner or later breaks down with increasing slipping. It should be noted that, even if the 'slip cycles' 2 and 3 (see Fig. 10B) fully override the coupled cycle 1 due to a very fast transition 1 ⇄ 4, J_A and J_B are not totally independent because the transport of both species is still mediated by the same enzyme for which the two species compete. Only in the absence of one species is the transport of the other one through a coupled carrier with a slip identical to the transport through a non-coupled carrier (as can be verified by rewriting Eqns. A48 and A50 with the concentration of one species set to zero).

The above considerations apply to uncharged species or to charged species in the absence of a membrane potential and of surface potentials. If the latter condition is dropped we encounter the complex situation already discussed for an uncoupled carrier (see subsection IV.C-3). Again, if the *carrier displays kinetic equivalence of chemical and electrical potential* (see subsection V.B-2) it behaves very similar to the carrier without potentials. A carrier with kinetic equivalence for the coupled cycle 1 in Fig. 10B can be constructed if both transported species have the same valence. The carrier then has the same charge with opposite sign residing at such a position with respect to the binding sites that $\zeta_{23} = \zeta_{56} = 0$ (see Appendix A.I-3). However, this causes $\zeta_{14} \neq 0$ and slipping becomes dependent on the membrane potential. I leave it to the reader to expand this view to the possible consequences and other cases of a slippy carrier with charged species.

* Since $\tau_5 \approx 0$, $\tau_7 < \tau_6$, hence $\tau_{sA} <$ (or $\ll$) τ_{sB} depending on b_1, b_2 and K_{41} (cf. Eqns. A51–A53).

VI.B-2. Symport of species, and the effect of coupling on the Michaelis-Menten parameters

In the case of symport it is not determined a priori which of the cotransported species binds to the free carrier, and the general case therefore involves *random binding* (see Fig. 11) exactly as in the case of the enzyme-catalyzed reaction with two substrates (see subsection IV.B-2). I refrain here from writing the flow-force equations because they are rather complex though straightforward. Instead I comment on the effect of coupling on the Michaelis-Menten parameters. I use the example of lactose permease residing in the cell membrane of *Escherichia coli* which catalyzes the symport of one lactose molecule with one H^+ ion [65].

Most investigations concern the transport of lactose under energized conditions ($X_H \neq 0$) or for $X_H = 0$. Depending on the direction of transport, a clear-cut difference for the effect of X_H on the Michaelis-Menten parameters is observed. For transport out of the cell or vesicle (efflux) the system obeys a 'simple Michaelis-Menten law' with a predominant effect of X_H on k_{cat} and a minor effect on K_m. Moreover, kinetic equivalence of the two terms in X_H is found [66,67]. Efflux for $X_H = 0$ is strongly dependent on pH in the suspending medium with an apparent pK of about 8.5 [68]. Transport into the cell or vesicle (influx) follows a 'simple law' only if $X_H = 0$ or $\Delta\psi > 130$ mV (with $\Delta\mu_{H^+} \approx 0$). For intermediate values of X_H strong deviations from a 'simple law' are observed [69,70]. Kinetic inequivalence is found, since the same phenomenon is not detectable if the predominant term in X_H is $\Delta\mu_{H^+}$ [65]. It is interesting to note that the data on lactose influx measured by Page et al. on a high time resolution show the 'loading' of the carrier (see Fig. 2B in [65] where the initial rise turns into a slower rise around 20

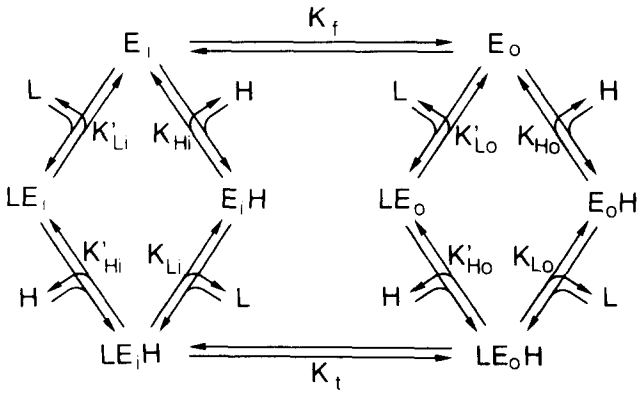

Fig. 11. Kinetic scheme for a symport carrier. The scheme is written for a symport of lactose (L) and H^+ ions (H) as performed by lactose permease. Indices i and o pertain to enzyme conformations whose binding sites are accessible, respectively, from the inner and the outer space of the cell. K_{Xy} and K'_{Xy} are the dissociation constants for binding of species X to conformation y of the enzyme, while K_f and K_t denote the equilibrium constant for the transition of the free carrier from i to o and the loaded carrier from o to i, respectively.

nmol lactose taken up per mg protein; 1 mg protein corresponds to 21.5 nmol lactose permease).

The deviation from linearity for influx upon energization points to a random binding of substrates from the suspending medium, while binding of ligands from the inside should either be ordered or much faster than the conformational change of the carrier (cf. subsection IV.B-2). Simulations based on the scheme in Fig. 11 with arbitrarily assigned values for the rate constants [70] indeed mimic the observed behavior for influx. On the other hand, Kaback and coworkers [67,68] interpreted their data as indicating an ordered binding of substrates which requires a regulation of the permease by X_H. The most puzzling observations, however, pertain to those experiments where the exchange of labelled versus unlabeled lactose is measured. Exchange flows were found to be totally independent of X_H or pH in the suspending medium [66–68], which is hardly conceivable in view of the other transport data. Thus, by applying what we have learned from the study of the thermokinetic behavior of enzymes in the preceding sections, we can conclude that the scheme in Fig. 11 cannot account for all experimental data. A possible extension of the scheme which may remove the inconsistencies will be presented in subsection VI.E.

VI.B-3. Transport coupled to a chemical reaction

A device which couples transport to a chemical reaction is usually called a pump. In analogy to coupling of two transport processes, we can construct a pump by merging an enzyme which catalyzes the reaction with a pore or a carrier. The combination of a pore with an enzyme was excellently reviewed by Läuger [71]; it would be superfluous to reiterate here his presentation, for anything here could be at most a faint summary. The behavior of proton pumps (i.e., chemical reactions coupled to the transport of H^+ ions) has been extensively treated by Pietrobon and Caplan [61]. It therefore suffices to summarize the essential points.

Again, in full analogy to the case of coupled transport, it is not determined a priori whether reactants or the transported species bind first to the free enzyme. A general scheme then has to include random binding of reactants and transported species as shown in Fig. 12. A three-dimensional representation in perspective is chosen, and the resulting diagram may be recognized as the general form of what 'insiders' sometimes like to call the 'Wikström cube'. Horizontal transitions indicate binding of the transported species, while vertical transitions are pertinent to the binding of reactants. Note that the latter would be replaced by a rhombus for those transitions which involve random binding of two substrates. The transitions in the third dimension then represent the conformational changes of the enzyme which open the binding site of the transported species to one or the other side of the membrane. Transitions

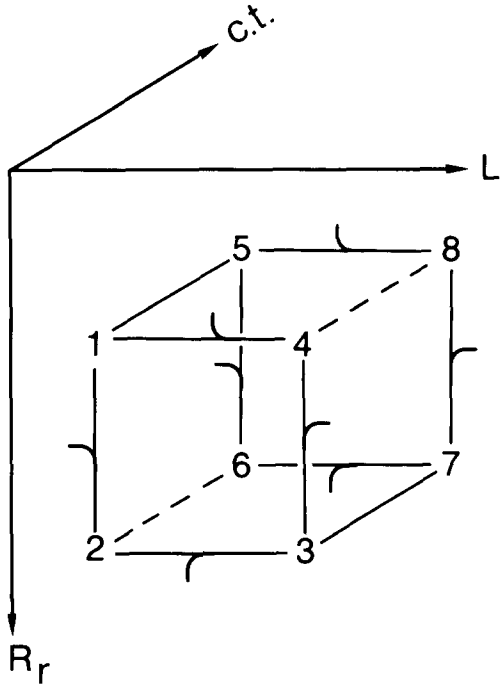

Fig. 12. Diagram for a transport coupled to a chemical reaction. Horizontal transitions indicate binding of the transported species L while vertical transitions pertain to binding of reactants R_r. Transitions in the third dimension are conformational changes of the enzyme (c.t.) which alter the accessibility of the binding sites for L (and possibly R_r in case of redox reactions) from one compartment to the other. Broken lines indicate transitions which cause a slip for the coupled processes.

marked by broken lines in Fig. 12 introduce slipping. The scheme deliberately does not specify which reaction takes place at which transitions in order to remain general. The reader who has had the endurance to follow my presentation up to this point will now most likely be so familiar with the diagram representation that he or she will be able to project his or her own view into the general diagram.

For the same reasons discussed in the context of random binding for an enzyme catalyzed formation of one product from two substrates (see subsection IV.B-3), we can assume that the enzyme follows a predominant cycle (which simplifies matters without loss of essentials). Pietrobon and Caplan [61] have chosen the cycle 1-4-3-7-8-5-1 in Fig. 12 with the slip 4-8 as the predominant cycle, and have exchanged the sequence of the transitions 3-7 and 7-8. Let us choose instead the cycle 1-2-3-7-6-5-1 with the slip 2-6 as the predominant cycle and spread it into two dimensions. We then can easily map it onto the diagram shown in Fig. 10 and identify species A as the transported species. When we choose a redox reaction as the coupled chemical reaction, it is equivalent to a transport of electrons (see subsection IV.B-4) and the transported species B is simply replaced by another transported species, viz. the electron. Depending on where we put the electron-donating couple D (cf. Fig. 6C) we arrive at a symport of H^+ ions and electrons (D in compartment 1), which is equivalent to a Mitchellian proton-redox loop, or an antiport. The latter case could be a minimal scheme for cytochrome oxidase which transports H^+ ions out of the mitochondrion upon electron transfer from cytochrome *c* (which is D) on the outer membrane surface to oxygen from the inside [72].

Based on the mapping of cycles, we can anticipate the same characteristics of the flow-force relations for the redox-driven transport as we have found for the antiport system discussed in subsection VI.B-1. The reader who takes the effort to work through the pertinent equations (which are more complex than in the case of antiport) will find this anticipation confirmed. In other words, conditions under suitable constraints can be found which give rise to a multiple inflection point, in limited ranges for the forces though. The inflection point can even be close to the origin (i.e., $X_o \approx 0$, cf. Eqn. 87). This applies to pumps without or with only a small slip, and increasing the slip breaks the symmetry of flows with respect to the two forces. Moreover, which slip cycle becomes predominant depends on the forces (besides the values of τ_s, cf. Eqns. 110). A rigorous proof for these statements can be found in the detailed treatment of pumps by Pietrobon and Caplan [61].

A comment on the kinetic equivalence of electrical and chemical potential in pumps should be added. It does exist as experimentally demonstrated for the H^+-ATP synthase in chloroplasts [73]. We have discussed in subsection VI.B-1 how an antiport carrier could comply with kinetic equivalence, and another example is given in Ref. 61. These considerations do not apply to the antiport of H^+ ions and electrons where the two transported species obviously have opposite signs. Besides the difficulties in devising a scheme with kinetic equivalence, this antiport displays some interesting new features of the flow-force relations in response to a membrane potential whose discussion, however, is beyond the scope of this review.

VI.B-4. Coupling due to direct interaction of enzymes, and the notion of decoupling

We have already invoked interaction when constructing a cotransport of species or a pump by means of pores. In these cases, however, the two constituents of the coupling device are continuously in close contact; they are so to speak glued together. What is meant here is an interaction between separate enzymes which are freely movable in a membrane. The discussion of this phenomenon has to remain vague because it has mainly been inferred from a phenomenological description of coupling (see subsection VI.D) [74] and possible mechanistic clues are just starting to emerge [75]. The following mechanisms are therefore hypothetical but reasonable.

Suppose a membrane contains two types of pump which transport the same species but coupled to different chemical reactions, the obvious example being a redox-driven H^+-pump and the H^+-ATP-synthase. Let us assume that the transported species does not leave a pump directly into or enter it directly from the adjacent aqueous phase but via an additional binding site (or sites) on the enzyme which, besides being accessible to the aqueous phase, can be accessed from the more polar domain of the membrane facing the aqueous phase. We then have additional states in the scheme of the pump with given probabilities (see Appendix A.I-1). If we further assume that the transported species can be exchanged between the pumps when they come close enough for a sufficiently long time interval, we have the direct interaction between the enzymes referred to above. We thus arrive at a situation where the transported species has two parallel routes. Depending on the 'collision' frequency of the pumps and the probabilities of the additional binding sites (which is also determined by the collision frequency in a steady state for the pumps) the species either hops from one type of pump to the other or enters and leaves the pumps via the aqueous phase. It is conceivable that agents or conditions can be found which decrease the probability of the former route and make the latter more favorable. As proposed by Rottenberg [74], *such conditions and the agents creating them should be called decoupling and decouplers*, respectively, in order to distinguish them from 'classical' uncoupling (see subsection VI.C-1).

Another direct interaction of enzymes was discussed by Kamp et al. [76]. These authors focus attention on the possible displacement of charges associated with the conformational changes of enzymes (see Appendix A.I-3). As discussed in subsection III.E-2, charges in the membrane create large electric fields which vary concomitantly with their displacement. As a consequence, any enzyme carrying itself charges will react if possible with a conformational change which reduces the strain created by the altered electric field. Kamp et al. considered two charges with opposite sign (i.e., a dipole) in two different enzymes and incorporated the dipole-dipole interaction arising from the electric field of each dipole into the transition probabilities of the pertinent conformational changes associated with a reorientation of the dipoles.

When comparing the two postulated mechanisms for direct interaction of enzymes, we recognize that their characteristics are rather different. A dipole-dipole interaction is nonspecific and effective over relatively large distances. Any enzyme carrying charges could be coupled to any other charged enzyme even if they are not in close proximity. In contrast, direct exchange of species occurs only when the pumps are close enough for a sufficient period of time and only between pumps which transport the same species.

VI.C. Coupling due to a common thermodynamic force

Two processes which share a thermodynamic force become coupled when this force has attained a steady state and then constitutes the common element. This is also true if the two processes themselves involve coupling and the shared force is one of the coupled forces in each process. The common force can be either that of a chemical reaction or that of a transport process. Thus, in a cell in which the thermodynamic force for the reaction where ATP is formed from ADP and phosphate (often called the 'phosphate potential') has reached a constant value, any two processes which involve this reaction in either direction (i.e., synthesis or hydrolysis of ATP) are in principle coupled. Most readers are probably more familiar with the cases where the common element is the force of a transport process, particularly if the transported species is the H^+ ion. Although the interrelation of flows arising from a common thermodynamic force is more conveniently assessed by the phenomenological description to be discussed in subsection VI.D, a few aspects are worth being considered here.

VI.C-1. Chemiosmosis, and the concept of 'classical' uncoupling

Mitchell [77] was the first who realized that the thermodynamic force for H^+ ions can serve as a common element in energy-converting organelles and formulated what is known as the chemiosmotic mechanism (previously hypothesis) of coupling, in short chemiosmosis. In general, chemiosmosis is not restricted to the H^+ ion but usually refers to it if the transported species is not specified. Mitchell introduced the notation 'protonmotive force' for the quantity X_H/F which, however, will not be used here because I feel that the conversion of X_H into electrical units does not warrant a new name.

X_H, as any other force for a transport process, comprises two terms (cf. Eqns. 17 and 20), one which pertains only to the H^+ ion and consists of the difference in chemical potential, $\Delta\mu_{H^+}$ (cf. Eqn. 22), and one arising from the membrane potential $\Delta\psi$ which affects all charged species. The steady state for X_H implies that the charging of the membrane capacitance has also reached such a state (see subsection VI.A). The voltage built up across this capacitance depends on the flows contributing to the charging. One of these flows is obviously the *net flow* of H^+ ions which is determined by the algebraic sum * of the flows pertinent to the H^+-pumps. However, the sum almost invariably in-

* Algebraic sum means that the flows have to be summed up as they appear according to the sign convention and irrespective of the direction in which they actual occur.

cludes an additional term due to the permeability of the membrane or any other mechanism creating an uncoupled transport for H^+ ions. Usually, we refer to permeability and/or other mechanisms collectively as the *leak of the membrane* for H^+ ions. When the net flow of H^+ ions is the only substantial flow occurring in the system (as, for example, in mitochondria, see also subsection VI.D), $\Delta\psi$ reached at steady state is the major part of $\Delta\tilde{\mu}_{H^+}$ because of the rather large chemical capacities for H^+ ions due to buffering (cf. subsections II.E-2 and VI.A). When additional flows take place, e.g., because the membrane is also permeable to other charged species (as in the case of thylakoids), $\Delta\psi$ at steady state may become rather small, since it is in part converted into a $\Delta\mu$ of the other permeant species, and $\Delta\mu_{H^+}$ is then the dominant term in $\Delta\tilde{\mu}_{H^+}$.

Unfortunately, there exists no simple algorithm for quantifying the above qualitative statements, at least not for energy-converting organelles. As shown in subsection VI.A for thylakoids, the chemical capacities in the internal space of the organelles are not so much larger than the electrical capacitance of the membrane that a negligibly small variation in the concentrations of species would occur during charging of C_m. Therefore, a quantitative solution can be found only by integrating the non-linear differential equations which emerge from the relations describing the flows (see Sections IV and VI.B) upon insertion of the time-dependent $\Delta\psi$, and in most cases only a numerical integration is possible (e.g., by means of a network simulating program [18,78]). It is worth adding that this problem does not exist for systems with considerably larger volumes of the internal spaces (e.g., nerve cells). The membrane potential can then be assessed by any relation (cf. Eqns. 105–107) appropriate for the system under consideration.

Any agent or manipulation of the system which affects X_H causes a change in coupling of the pumps, and a *diminution of X_H is an uncoupling in the 'classical' sense*. The latter notation refers to the fact that Mitchell's hypothesis could for the first time explain the action of uncouplers, which seems to have been so convincing that many people still almost automatically associate the notion of uncoupling with the following mechanism. An agent which increases the leak of the membrane for H^+ ions is an uncoupler because it induces a flow of these ions which competes with the flows of the pumps and eventually abolishes X_H if a large enough leak is generated. The leak-inducing agent can either introduce a pore (e.g., gramicidin) or operate as a carrier for H^+ ions as in the case of the protonophores (e.g., FCCP). Depending on which part of $\Delta\tilde{\mu}_{H^+}$ is dominant, there are additional ways of manipulating X_H. An antiport carrier exchanging H^+ for another monovalent cation, e.g., K^+ in the case of nigericin, converts $\Delta\mu_{H^+}$ into $\Delta\mu_{K^+}$ to an extent which is determined by the chemical capacities of the two species. Alternatively, increasing the permeability for a charged species (e.g., K^+ by means of valinomycin) reduces $\Delta\psi$ in a system where this part of $\Delta\tilde{\mu}_{H^+}$ is dominant. This primarily would not suffice for uncoupling, since the decreased X_H could be compensated by the pumps but in terms of $\Delta\mu_{H^+}$ rather than $\Delta\psi$. Thus, a mitochondrion would adopt the behavior of a thylakoid. However, this is largely prevented by H^+/substrate cotransporters (e.g., the phosphate carrier) which effectively clamp $\Delta\mu_{H^+}$. Hence X_H indeed decreases in parallel to $\Delta\psi$. In addition, the change in volume associated with the flow of K^+ ions and substrates may eventually impair the functioning of the mitochondria.

VI.C-2. 'Localized' versus 'delocalized' chemiosmosis

It has been postulated (see, for example, Westerhoff et al. [35]) that H^+ ions released from one type of pump may first enter a 'local domain' in the membrane from which they are either picked up by the other type of pump or else move into the bulk of the adjacent aqueous phase. This so-called 'localized' chemiosmosis was invoked in order to explain an imbalance of forces, which seems to exist in certain experiments, and to account for 'missing' H^+ ions in pulse experiments. 'Delocalized' chemiosmosis then pertains to a system without local domains and therefore a direct release of H^+ ions into the bulk phases. The concept of localized chemiosmosis is rather controversial, and some general comments without going into details may be helpful.

Evidence for or against localized chemiosmosis is based in the first place on a reliable estimation of the thermodynamic forces. As discussed by Ferguson [79], a critical review of the data used in support of localized chemiosmosis seems to be necessary. The force X_H is particularly vulnerable to experimental errors. Besides the difficulties introduced by the binding of markers to membranes, the tight folding of membranes in mitochondria and chloroplasts can falsify a straightforward estimation of $\Delta\tilde{\mu}_{H^+}$ by conventional techniques (see subsection III.D). It may be added that, depending on conditions, X_H values calculated in the conventional way for thylakoids can be in error by several kJ/mol (Ref. 23 and more refined but unpublished results by Walz and Ziemke).

The analysis of a scheme describing localized chemiosmosis such as the analog electric network presented in Ref. 35 is hampered by the lack of information on the H^+-permeability of the barrier separating the local domains from the bulk phase. Moreover, the scheme should be devised such that it accounts for the experimental conditions it is intended to simulate. Thus, representing the force of the ATP synthesizing reaction by a constant voltage source (or battery) is illegitimate because this force is usually not clamped but only the force of the redox process. Another aspect concerns the action of inhibitors of the pumps on the 'coupling units' (i.e., the

combination of the two types of pumps connected by the local domains). Westerhoff et al. [35] assumed that inhibition of either pump knocks out the whole unit, which seems rather unrealistic. This author has analyzed a similar circuit which, however, includes capacitors representing localized and delocalized X_H as well as the concentrations of ATP, ADP and phosphate. The circuit thus accounts for the evolvement of the non-clamped forces during the system's progress from initial conditions to the stationary state. The unpublished results of this investigation (performed by means of the network simulating program mentioned in the preceding subsection) did generally not confirm the conclusions drawn by Westerhoff et al., which exemplifies that fallacies can be inherent in an inappropriately devised model.

The existence of local domains cannot be denied a priori. In fact, structures which could serve as such domains were experimentally demonstrated on the inner surface of thylaksid membranes [80,81]. They can sequester H^+ ions in non-energized thylakoids which then are not equilibrated with the bulk phase. Upon energization, however, the sequestering is removed as soon as the capacity of these structures for H^+ ions is exhausted, and the barrier causing the sequestering seems to vanish [80]. H^+ ions may then still be channeled through these structures, but the relevant point is how many of them are picked up by the H^+-ATP synthase before they leave the structures into the adjacent bulk phase. The reader may have noticed that these considerations converge to the discussion of a direct interaction of enzymes (see subsection VI.B-4). We thus realize that the concept of localized chemiosmosis could as well be abandoned, while the explanation of the phenomena for which it was invoked could be possibly found in an appropriately formulated scheme for direct interaction. The thermodynamic treatment of local domains by Westerhoff and Chen [82] can then be considered as a first step in this direction.

VI.D. Phenomenological description of coupled processes

In the preceding subsections, we have derived flow-force relations based on kinetic schemes. But what should we do if the system under consideration is a black box in the sense that we have little or no information on molecular mechanisms, let alone a reasonable kinetic scheme. We then would appreciate a tool which relates the flows to the forces in such general terms as is the definition of these quantities in thermodynamics (see subsection II.D). Although such a tool could only provide a phenomenological description, it would have the advantage of not being restricted to a particular mechanism and would merely require the assignment of coupling between flows.

VI.D-1. Non-equilibrium thermodynamics and linear flow-force relations

Provided that the force of a process is small, i.e., $X/RT \ll 1$, the higher order terms in a Taylor expansion of $\exp(X/RT)$ in Eqn. 82 can be neglected. A linear relation between flow and force is thus obtained because, under the aforementioned condition, the function $\boldsymbol{F}$ in Eqn. 82 can be approximated by the constant $\boldsymbol{F}(c_{i,eq})$, which is its value at equilibrium ($X = 0$). The same procedure can also be applied to coupled processes *without slipping* (cf. Eqns. 108 and [61]). It is important to note that, in the latter case, the conjugate force for each of the coupled processes can be rather large, and only the composite force has to be small (i.e., $X_A - X_B \ll RT$ in Eqn. 108). The state of the coupled processes where the composite force vanishes is called *static head* because it is characterized by the maximal force attainable by one of the processes when the force of the other one is clamped. It is a true equilibrium state, despite the arguments put forward by Naftalin [83] against the existence of such a state, which have been disproved [18].

Because the particularities of a given kinetic scheme appear exclusively in the function $\boldsymbol{F}(c_i)$ (cf. Eqns. 82 and 108 with $\tau_{si} = 0$) which was approximated by a constant value, the linearized flow-force relations are in fact independent of a kinetic scheme. Hence,

$$J_i = L_i X_i \quad \text{for } |X_i| \ll RT \tag{111a}$$

for the ith process, and for the ith pair of coupled processes

$$J_{i,1} = L_i X_{i,1} + n_i L_i X_{i,2}$$

$$J_{i,2} = n_i L_i X_{i,1} + n_i^2 L_i X_{i,2}$$

$$\text{for } |X_{i,1} + n_i X_{i,2}|/RT \ll 1 \quad \text{and no slip} \tag{111b}$$

where n_i is the stoichiometry of the coupled flows ($n = -1$ for the antiport discussed in subsection VI.B-1). The coefficients $L_i = [RT\boldsymbol{F}(c_{i,eq})]^{-1}$ are called generalized permeabilities and are of course dependent on $c_{i,eq}$ pertaining to the equilibrium state and the static head. They are therefore not characteristic constants of the processes as are the rate constants or the transition probabilities which also determine $\boldsymbol{F}$. Note that the 'linearized flow-force relations are fully symmetric with respect to the two forces, a property which is known as Onsager symmetry. Eqns. 111 were the starting point of what is called *linear non-equilibrium thermodynamics*, in short, linear NET.

The range of validity of linear flow-force relations can vastly exceed that expected form the validity of the above linearization near equilibrium or static head (at most 0.25 kJ/mol if we set the limit $|e^x - 1 - x| \leq 5\%$

and neglect changes in $\boldsymbol{F}$). Provided that the experiment is carried out under the proper constraints (cf. subsections V.B and VI.B-1), the flows are described by the hyperbolic tangent of the forces (Eqn. 86) which can be approximated by its tangent in the inflection point (Eqn. 86a),

$$J_i = L_i X_i + J_{io} \quad \text{for } |X_i - X_{io}|/RT \leq 0.71 \tag{112a}$$

and

$$J_{i,1} = L_i X_{i,1} + \gamma_i n_i L_i X_{i,2} + J_{io}$$

$$J_{i,2} = n_i L_i X_{i,1} + \gamma_i n_i^2 L_i X_{i,2} + n_i J_{io}$$

$$\text{for } |X_{i,1} + n_i X_{i,2} - X_{io}|/RT \leq 0.71, \quad \text{and no slip} \tag{112b}$$

The coefficient L_i and the additional term * J_{io} in Eqns. 112 are found to be (cf. Eqns. 86a and 87)

$$L_{io} = (J_{i+} J_{i-})/(4RT) \tag{113a}$$

and

$$J_{io} = (J_{i+} - J_{i-})/2 - \ln\{J_i + /J_{i-}\}(J_{i+} + J_{i-})/4 \tag{113b}$$

where J_{i+} and J_{i-} are the extreme flows for the ith process or pair of coupled processes under the given constraints (cf. Eqns. 85, 90–92, 95, 97, A55). The factor γ_i accounts for a kinetic inequivalence of the two forces [11,61] of coupled processes. It does not emerge from Eqn. 110 because we have chosen conditions (see subsection VI.B-1) which lead to a *multiple inflection point where* $\gamma_i = 1$. Hence, the flows still display Onsager symmetry irrespective of whether X_o (cf. Eqn. 87) is close to zero or not. In the general case the symmetry is broken, i.e., $\gamma_i \neq 1$.

For *coupled processes with slipping* a linearization of the flow-force relations which retains Onsager symmetry is possible only if both forces separately are small (in contrast to the case without slip where only the composite force had to be small, see above). Then

$$J_{i,1} = (L_i + L_{is,1}) X_{i,1} + n_i L_i X_{i,2}$$

$$J_{i,2} = n_i L_i X_{i,1} + n_i^2 (L_i + L_{is,2}) X_{i,2}$$

$$\text{for } |X_{i,1}|/RT \ll 1 \quad \text{and } |X_{i,2}|/RT \ll 1 \tag{114}$$

where $L_{is,1}$ and $L_{is,2}$ represent the contributions to the pertinent flows due to slipping which usually are not identical (i.e., $L_{is,1} \neq L_{is,2}$, cf. Eqns. 110). In the range of extended linearity around the inflection point of the hyperbolic tangent relating flows to forces under suitable constraints, Onsager symmetry breaks down and the 'extended range' may become considerably less extended. This shall be demonstrated by means of Eqns. 110 for the antiport of species. Linearizing the two terms in these relations according to Eqn. 86a yields

$$\begin{aligned} J_A &= [L + L_{sA}(X_B)] X_A - [L - J_{sA}/X_B] X_B + J_o \\ J_B &= -[L + J_{sB}/X_A] X_A + [L + L_{sB}(X_A)] X_B - J_o \end{aligned} \tag{115}$$

where L and J_o are according to Eqns. 113 with extreme flows J_+ and J_- given in Eqns. A55. The additional terms L_{sX} and J_{sX} (X = A and B) arise from slipping and read

$$L_{sA}(X_B) = \tau_{sA}(K_{B1}/c_B)(J_+ \exp\{X_B/RT\} + J_-)/(4RT) \tag{116a}$$

$$L_{sB}(X_A) = \tau_{sB}(K_{A2}/c_A)(J_+ + J_- \exp\{X_A/RT\})/(4RT) \tag{116b}$$

and

$$J_{sA} = \tau_{sA} \frac{K_{B1}}{c_B} \left[\frac{J_+ \exp\{X_B/RT\} - J_-}{2} - \frac{J_+ \exp\{X_B/RT\} + J_-}{4RT} X_{o,sA} \right] \tag{117a}$$

$$J_{sB} = \tau_{sB} \frac{K_{A2}}{c_A} \left[\frac{J_+ - J_- \exp\{X_A/RT\}}{2} - \frac{J_+ + J_- \exp\{X_A/RT\}}{4RT} X_{o,sB} \right] \tag{117b}$$

$X_{o,sA}$ and $X_{o,sB}$ in Eqns. 117 denote the position of the inflection points of the slip contributions to the flow of species A and B, respectively,

$$X_{o,sA} = X_o + X_B \quad \text{and } X_{o,sB} = X_o + X_A \tag{118}$$

while X_o ($= RT \ln\{J_+/J_-\}$, cf. Eqn. 87) is that of the coupled process. Evidently, the different inflection points do not coincide; hence only if $L \gg L_{sA}$, J_{sA}/X_B, L_{sB}, J_{sB}/X_A the latter quantities can be approximated by constants and the linearity of the coupled process expressed by L is preserved. Increasing the slip causes the range of linearity to be diminished and/or displaced, and eventually results in two essentially independent (but see subsection VI.B-1) flow-force relations if slipping overrides the coupled process (for a further discussion of this phenomenon see [61]).

Westerhoff and Van Dam [11] advocate the view that Eqn. 112a suffices to describe any possible non-coupled process while Eqn. 112b accounts for all coupled processes if it includes the terms $L_{is,1}$ and $L_{is,2}$ (in the same way as shown in Eqns. 114) in order to assess slipping. They call their procedure *mosaic NET* where 'mosaic' should refer to the fact that the description of a system, no matter how complex it may be, can be composed from building blocks based on Eqns. 112, like

* Westerhoff and Van Dam [10] use $\Delta G^{\#} = J_{io}/L_i$, while Pietrobon and Caplan [61] denote J_{io} by K_r.

the little stones in a mosaic. They have discussed a large number of such systems thus demonstrating the versatility of the algorithm. It may then be worth summarizing the conditions to be fulfilled in order that Eqns. 112 (including a slip) are useful approximations.

(1) The concentrations of the species involved in reactions and transport have to be restricted by suitable constraints. Such constraints are almost automatically introduced by the experimental system discussed in subsection II.A. Only in the case of redox reactions (see subsection V.B-1) do appropriate constraints have to be established by a proper experimental design.

(2) If charged species are involved in a (coupled or uncoupled) transport, the mechanism must display kinetic equivalence if both chemical and electrical potential in the force of the species are expected to vary (a unique correlation between the two as claimed in Ref. 11 does not suffice). Only if one of the parts is constant kinetic inequivalence can be tolerated, however, the flow-force relations can be altered if a different though constant value is chosen. Surface potentials should be negligibly small or else at least constant.

(3) Coupled processes should preferably display a multiple inflection point under the given constraints. This is not a necessity but makes the linear approximations a lot safer. The factors γ_i are then unity and, provided that the multiple inflection point is close to the origin (i.e., $X_o \approx 0$) the additional terms J_{io} can be neglected.

(4) Accounting for slipping in coupled processes by means of two additional generalized permeabilities ($L_{is,1}$ and $L_{is,2}$) holds at most for small slips. A linearization of the flow-force relations with substantial slip is in general not possible, and the approximation with two slip permeabilities is bound to fail.

VI.D-2. Degree of coupling and phenomenological stoichiometry

Kedem and Caplan [4] have introduced a normalization of the generalized permeabilities in the flow-force relations of a coupled process near equilibrium. In terms of the permeabilities in Eqns. 114,

$$q_i = 1/[(1 + L_{is,1}/L_i)(1 + L_{is,2}/L_i)]^{1/2} \tag{119a}$$

and

$$Z_i = n_i[(1 + L_{is,1}/L_i)/(1 + L_{is,2}/L_i)]^{1/2} \tag{119b}$$

The normalized quantities q and Z are called the degree of coupling and the phenomenological stoichiometry, respectively. As evident from Eqns. 119, q_i is bound by the limits 1 ($L_{is,1} = L_{is,2} = 0$) and 0 ($L_{is,1}$, $L_{is,1}$, $L_{is,2} \gg L_i$), and its actual value then indicates how much slipping occurs. Similarly, Z_i varies between n_i (which is the molecular stoichiometry of the coupled process) for $L_{is,1} = L_{is,2} = 0$, and $n_i[L_{is,1}/L_{is,2}]^{1/2}$ (which essentially indicates the relative rates of slipping of the two processes) if $L_{is,1}$, $L_{is,2} \gg L_i$. By means of q and Z, the efficiency of energy conversion, defined as the ratio of 'output' over 'input power', becomes for the ith coupled processes

$$\eta_i = -(J_{i,2}X_{i,2})/(J_{i,1}X_{i,1})$$

$$= -[q_i + Z_i X_{i,2}/X_{i,1}]/[q_i + 1/(Z_i X_{i,2}/X_{i,1})] \tag{120}$$

Unfortunately, these very general relations are valid only near equilibrium (cf. validity range of Eqns. 114). Caplan [61,84] has carefully investigated the meaning of q and Z in the extended ranges of linearity far from equilibrium discussed in the preceding subsection and came to the conclusion that the interpretation of both parameters, which is valid near equilibrium, in general no longer holds. Many coupled processes were analyzed by means of linear NET (reviewed in Ref. 7) and found to comply with Eqns. 114, particularly when the input force was clamped and only the output force was varied. This, however, does not justify the assumption that these systems behave like 'near equilibrium' while in fact being far from it. The investigations about optimization of energy conversion [11,85] should therefore be revisited and their physical meaning reinvestigated.

VI.D-3. Analysis of complex systems, and the 'non-ohmic' behavior of membrane leaks

Processes occurring in the internal space of organelles which usually elude an experimental assessment can be translated into fictitious processes involving only experimentally observable parameters in the suspending medium. The translation is performed by means of the dissipation function (see subsection II.D-3) and the conditions imposed on the flows by a steady state (see subsection II.E-2 and Eqn. 103). Linear flow-force relations have the advantage that the equations emerging from such a description can be handled by standard procedures of linear algebra.

Suppose we have a suspension of mitochondria respiring on succinate. At a steady state of the system we then observe that only the mole numbers of succinate, malate and oxygen change with time in the suspending medium (which is compartment 1 in our system, see Fig. 1). Hence, the dissipation function for this state is

$$\Phi = -[\tilde{\mu}_{S,1}\, dN_{S,1}\, dt + \tilde{\mu}_{M,1}\, dN_{M,1}\, dt + \tilde{\mu}_{O,1}\, dN_{O,1}\, dt] \tag{121}$$

where we have assumed that the capacities are large enough so that $\tilde{\mu}_{x,1} \approx$ constant for succinate (X = S), malate (X = M), and oxygen (X = O). The terms in Φ suggest that the mitochondria 'catalyze' the oxidation of succinate by oxygen in compartment 1 whereby malate is formed. However, we expect that this fictitious overall reaction arises from a set of processes which, if

expressed in terms of flows and conjugated forces, should yield the same Φ. Thus,

$$\Phi = J_e A_{e,2} + (J_{He} + J_{Hl}) X_H + J_h A_h + J_S X_S + J_M X_M + J_O X_O + J_u X_u + J_{Hu} X_{Hu} \quad (121a)$$

The forces X indicate transport of species across the membrane. The transport of H^+ ions associated with X_H involves two flows, one coupled to electron transport, J_{He}, and one due to the leak of the membrane, J_{Hl}. The last two terms in Eqn. 121a arise from a protonophoric uncoupler (if present) with indexes u and Hu denoting the unprotonated and protonated form, respectively. The affinity $A_{e,2}$ is equal to $\tilde{\mu}_{eD,2} - \tilde{\mu}_{eA,2}$, where D and A indicate the donating (succinate/fumarate) and accepting (water/O_2) redox couple (cf. Eqns. 15 and 23), and drives the electron transport, J_e (for the definition of $\tilde{\mu}_e$ in case of protonating redox couples see Ref. 17). J_h and A_h are pertinent to the hydration reaction of fumarate which yields malate.

The affinity of electron transport $A_{e,2}$ can be related to the affinity $A_{e,1}$ of the fictitious reaction taking place in compartment 1,

$$A_{e,1} = A_{e,2} - X_S/2 + X_M/2 - X_O/4 + A_h/2 \quad (122a)$$

where the factors $1/2$ and $1/4$ arise from the number of electrons exchanged by the two redox couples (see Eqn. 13). In Eqn. 122a we have assumed that $\tilde{\mu}_{w,k}$ ($k = 1$ and 2) for water is constant and $X_w = 0$, i.e., the transport of water is so fast that it is always very close to equilibrium. A similar assumption for the protonation reactions of the uncoupler in both compartments yields

$$X_H + X_u = X_{Hu} \quad (122b)$$

Upon insertion of Eqns. 122 into Eqn. 121a we obtain

$$\Phi = J_e A_{e,1} + (J_{He} + J_{Hl} + J_{Hu}) X_H + (J_h - J_e/2) A_h + (J_S - J_e/2) X_S + (J_M + J_e/2) X_M + (J_O - J_e/4) X_O + (J_u + J_{Hu}) X_u \quad (121b)$$

The steady state requires that the changes in mole number for all species in compartment 2 vanish due to a balancing of flows (see Eqn. 18b and subsection II.E-2). This means that each group of flows enclosed in parentheses in Eqn. 121b sums up to zero, and only the term $J_e A_{e,1}$ is left, which in fact describes the fictitious reaction inferred from Φ in Eqn. 121. Note that the balancing of flows in this case automatically fulfills the condition imposed by electroneutrality, i.e., $J_{He} + J_{Hl} - 2J_S - 2J_M + z_u J_u + (z_u + 1) J_{Hu} = 0$ (for a steady state where electroneutrality is needed as an additional condition see Ref. 86).

Writing linear flow-force relations for the processes expressed by Φ in Eqn. 121a and substituting Eqns. 122 yields a system of linear equations which, in matrix notation, can be represented by $\boldsymbol{J} = \boldsymbol{L}\boldsymbol{X}$ where $\boldsymbol{J}$ and $\boldsymbol{X}$ denote the vectors of flows (defined as the sums in parentheses) and forces given in Eqn. 121b, respectively, while $\boldsymbol{L}$ is a matrix comprising the generalized permeabilities. Matrix inversion of $\boldsymbol{L}$ and setting all flows which vanish at the steady state to zero in $\boldsymbol{J}$ yields all forces at this state, from which the dependence of the only non-vanishing flow J_e on the forces can be obtained. Thus [86],

$$J_e q Z = [L_e(c_I) Z^2 (1 - q^2) + L_{H,l} + L_{H,u}] X_H \quad (123)$$

at the steady state which is a static head for H^+-pumping. $L_e(c_I)$ is the permeability of the redox-driven H^+-pump and has the argument c_I to indicate that it depends on the concentration of an added electron transport inhibitor. $L_{H,l}$ and $L_{H,u}$ denote the permeabilities for H^+ ions due to the leak in the membrane and the added uncoupler, respectively [86]. Z and q are the quantities defined in Eqns. 119 and should be considered with due caution as discussed in the preceding subsection.

Two explanations have been proposed for the experimentally observed non-linear dependence of J_e on X_H upon gradual inhibition of electron transport by increasing c_I in the absence of an uncoupler ($L_{H,u} = 0$). Usually, pumps are considered to be tightly coupled, i.e., without a slip, hence $q = 1$ and $Z = n$ is assumed. The non-linearity has then to be accounted for by a non-linear dependence of $L_{H,l}$ on X_H as suggested for the first time by Nicholls [87], and the leak is said to have a 'non-ohmic behavior' (cf. Eqn. 123). Although such a behavior has been demonstrated in mitochondria, reconstituted proteoliposomes and lipid vesicles [88,89], it appears not to be sufficient to explain the non-linearity of J_e as function of X_H, particularly at high values of X_H [62]. The alternative explanation considers a slip in the pump and a constant $L_{H,l}$ [62,63,86]. The non-linear part of the $J_e(X_H)$ curve at high values of X_H is then due mainly to the inhibition of the 'slipping' pumps with a minor contribution from $L_{H,l}$, and the opposite is true for small X_H values where the curve converges to a linear dependence on X_H. This explanation also holds for experiments with a small concentration of a protonophoric uncoupler ($L_{H,u} \neq 0$, [86]) whereas the other explanation breaks down because the non-linearity of $L_{H,l}$ disappears in the presence of such uncouplers [88,89]. However, the conclusion that protonophoric uncouplers increase the slip [86], which was derived from the change in q and Z caused by the uncoupler, is probably untenable in view of the meaning of these parameters for slippy pumps far from equilibrium (see preceding subsection).

Brown [90] recently presented an argument against slips in redox-driven H^+-pumps which is not conclusive.

He compared J_e for electron transport from succinate to oxygen at a given X_H with that for the two segments succinate to ferricyanide and ferrocyanide to oxygen at the same X_H. He found the ratio of these flows independent of X_H within experimental error which he thinks "casts doubt on the original evidence for slip in the mitochondrial proton pumps" [90]. This analysis of flow ratios, as valuable as it may be as an experimental finding, is inappropriate for the intended purpose. First of all, electron transport through the segments occurs across the membrane and hence involves the so-called 'chemical' (or 'scalar') H^+ ions due to the redox reactions of donating and/or accepting redox couples. These should be separated from the really pumped H^+ ions because they are not subjected to slipping in the pumps [86]. Secondly, the flow ratios found deviate from integers, in contrast to what has to be expected for pumps without slips, and thus do indicate slipping rather than contradicting it. Finally, a slip in the pumps does not necessarily cause variable flow ratios, but constant flow ratios indicate an independence of the slip on X_H (which is not trivial, see subsection VI.B-1 and Caplan [84]). X_H is not imposed by the experimental conditions (and thus an independent quantity) but adjusts itself on the system's course to static head. Its relation to the constant affinity, $A_{e,1}$, is essentially determined by the term in square brackets in Eqn. 123 [86]; hence, it is not astonishing that the flows of different pumps at a given X_H maintain the same proportion for different values of X_H. This short discussion should show that an oversimplified approach to a complex system is inadequate and bears the risk of fallacies.

VI.E. Control and regulation of coupled processes

The unique flow-force relations for coupled processes arrived at under suitable constraints (see, for example, Eqns. 108) indicate that the flow of one process is also determined by the force of the other process. Hence, if one force is clamped while the other is zero but adjustable, we start from the state called *level flow* which is characterized by the maximal flows attainable under the given circumstances. The flow of the driven process, i.e., the one with the unclamped force, gives rise to an increasing force for this process which slows down both processes until the flow of the driven process vanishes. The state then attained is called *static head* and characterized by the maximal force for the driven process which can be reached under the given conditions. This effect of the forces may be summarized by the notion that the flows of coupled processes are under *thermodynamic control.* It also occurs in coupled processes with slipping unless the slip is so large that it fully overrides the coupling of the processes. In principle, the same static head can be generated by different concentrations for the reactants of the driven process (the clamped force being always the same), since forces are determined only by ratios of concentrations. However, besides probably changing the parameters of the constraints, the expected static head may not be observed at all because some of the concentrations which vary during the system's course to this state could adopt such values that the turnover of the enzyme cycles becomes rather small. Although theoretically the final state of the system is still static head which would be attained after a long (maybe infinite) period of time, the state practically reached is determined by kinetic properties of the enzyme, and the system is said to be under *kinetic control.*

Besides the two types of control inherent in coupled processes, additional effects controlling the flows can exist which may be collectively called *regulations.* A typical example for a regulation is the H^+-ATP synthase in chloroplasts (and probably also in mitochondria) which is inactive in non-energized thylakoids. The enzyme is activated by one of its forces (X_H) and the activation (or regulation) itself depends on the redox state of the enzyme [91] which is regulated by electron transport via the thioredoxin system. The relevance of this 'regulated' activation to the performance of thylakoids is evident. Without activation, or rather deactivation of the enzyme in the dark, the ATP synthesized in the light would simply be hydrolyzed in the dark, as can be experimentally demonstrated when the light-activated enzyme is kept reduced by means of thiol reagents [91] and thus active in the dark.

Another regulation might be present in lactose permease in that the enzyme can perform two catalytic cycles, one as shown in Fig. 11 and a second one pertinent to, for example, a non-coupled carrier (see Fig. 6E). The activity of each cycle would then be determined by a regulatory binding site for lactose (most likely accessible only from the suspending medium, Lolkema et al., unpublished results), and an occupied binding site would favor the second cycle. A first requisite emerging from such a regulation pertains to the binding of substrates to lactose permease at equilibrium where both forces are zero, i.e., $c_{lo,1} = c_{lo,2}$ and $\Delta\psi = 0$. Then, each transition can be assessed by Eqns. A15 and A16, and collecting the states with bound L yields *one* overall dissociation constant for the scheme in Fig. 11 which can be expressed by means of the equilibrium constants for the transitions,

$$K_{L1}(c_H) = \langle K_L\rangle[1+\langle K_H\rangle/c_H]/[1+\langle K'_H\rangle/c_H] \quad \text{for}$$

$$c_{Ho,1} = c_{Ho,2} = c_H \tag{124a}$$

and with the substitions (cf. Fig. 11)

$$\begin{aligned}\langle K_L\rangle &= (K_{Lo} + K_t K_{Li})/(1+K_t)\\ \langle K_H\rangle &= (K_f+1)/(K_f/K_{Ho}+1/K_{Hi})\\ \langle K'_H\rangle &= (K'_{Ho} + K_t K'_{Hi})/(1+K_t)\end{aligned} \tag{124b}$$

The regulatory binding site together with the second cycle adds a second independent overall dissociation constant, K_{L2}. The analysis of the data for binding of the substrate analogue α-nitrophenyl β-D-galactopyranoside to lactose permease has indeed to include two overall dissociation constants (Lolkema and Walz, (1990) Biochemistry, in press) thus supporting the postulated regulation mechanism. The physiological significance of a regulated lactose uptake would relate to an economic expenditure of metabolic energy. If a cell faces a high enough lactose concentration, a carrier-catalyzed permeation suffices, and an uptake driven by X_H (which has to be generated by the cell) comes into play only when the lactose concentration in the surroundings becomes too small for permeation.

A very striking regulation of only one of two coupled processes by a system parameter can be deduced from the data published by Bamberger et al. [92] on light-driven electron transport in thylakoids. These authors found J_e to be linearly dependent on X_H expressed as ΔpH (since $\Delta\psi \approx 0$ [93]) provided that the pH in the thylakoids, pH_i, is constant (Fig. 13A). Although one could have some reservations about the experimental techniques employed * the linearity displayed by the data in Fig. 13A appears to be real and extends over a range of about 7.5 kJ/mol which is roughly twice that expected for an extended linear range around an inflection point (see subsection V.B-1). The straight lines representing the linear flow-force relation for different pH_i values are parallel but shifted to higher J_e values with decreasing pH_i. The intercepts of these lines on the ordinate which indicate J_e at level flow (i.e., $X_H = 0$) are plotted in Fig. 13B as a function of pH_i together with corresponding data pertinent to other experiments presented in [92]. Evidently, J_e, besides being under thermodynamic control, is regulated by pH_i in a complex way. For $pH_i \geq 5.2$, J_e at level flow (or L_e relating it to the constant A_e in a linear flow-force relation) increases with decreasing pH_i, and this dependence can be approximated by a curve pertinent to the fraction of the protonated species in an acid/base pair with $pK \approx 7$. For $pH_i < 5.2$, however, J_e steeply declines and probably approaches zero at $pH_i \approx 4$.

A constant pH_i is just the opposite of what happens when investigating isolated thylakoids where the pH in the suspending medium is approximately constant. Similarly, in whole chloroplasts, pH_i falls during illumination, while the pH in the stroma rises considerably less [94]. The behavior of J_e in illuminated thylakoids during the transition from level flow to static head with an approximately constant external pH_o is therefore quite different. If $pH_o = 6$, J_e starts at a high value and then decreases [92] which is caused by thermodynamic control (increasing X_H) but even more by the regulation shown in Fig. 13B when pH_i falls below 5. Hence, ΔpH at static head is less than expected from thermodynamic control [92] despite of the large amount of H^+ ions taken up which are almost totally buffered in the internal space of the thylakoids [95]. In contrast, at $pH_o = 8.5$, J_e starts at a lower value but hardly changes on the course to static head [92]. This is not due to a poor coupling of the redox-driven proton pumps at this pH_o (as sometimes erroneously claimed). In fact, ΔpH reached at static head is maximal, in line with thermodynamic control and despite of the smaller amount of H^+ ions taken up due to less internal buffering [95].

The regulation of J_e serves two purposes. Firstly, it prevents an over acidification of the internal space of thylakoids which would occur at high light intensities after exhaustion of the internal buffering capacity in case pH_o would adopt for some reasons a value below 7. Secondly, it makes J_e essentially independent of the rate of ATP synthesis at the physiological pH_o value (in strong contrast to mitochondria) which is important because J_e also generates NADPH. Both NADPH and ATP are needed for the dark reactions and can be formally exported from the chloroplasts by shuttle mechanisms (but not as actual species) [96]. A more or less fixed stoichiometry between ATP and NADPH production which would arise from a non-regulated J_e (as it exists in mitochondria for ATP synthesis and NADH oxidation though) would therefore be counterproductive. Note that X_H in thylakoids is additionally generated by the so-called cyclic electron transport [97] which keeps ATP synthesis going also in the case of a low J_e due to a high reduction state of the $NADPH/NADP^+$ couple. It should be added that part or all of what is attributed to regulation in the above discussion may eventually be recognized as kinetic control when future developments of the description of coupled processes in thylakoids will have provided us with a more detailed picture.

VII. Concluding remarks

The biothermokinetic description of processes and energy conversion in a system can be said to proceed through different stages. At an early stage when the system is still essentially a black box, its assessment is restricted to a phenomenological description. Linear flow-force relations are then a very useful tool, despite

* The measurement of ΔpH by means of 9-aminoacridine involves an overestimation of this quantity which depends on the magnitude of ΔpH [25]. Moreover, the photometric technique used to follow ferricyanide reduction includes some light scattering artifacts (Ziemke and Walz, unpublished results). In view of these arguments, the curves drawn by Bamberger et al. [92] in their Fig. 8 were replaced by straight lines for the replotted data in Fig. 13. This, however, should be considered only as a first approximation, and work is in progress in order to verify (or disprove) this assumption.

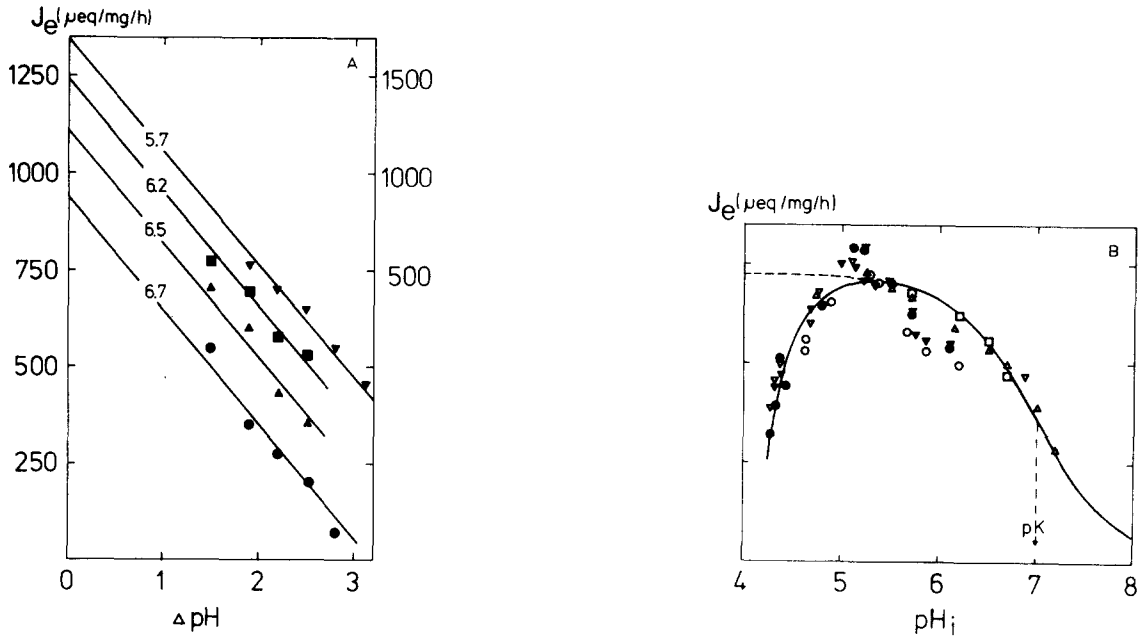

Fig. 13. Dependence of the flow of light-driven electron transport, J_e, in thylakoids on the force of H^+ ions (A) and on pH_i in the thylakoids at level flow (B). The data in (A) are replotted from Fig. 8 in Ref. 92 for a constant internal pH, pH_i, of 5.7 (▼), 6.2 (■), 6.5 (▲) and 6.7 (●). The force $X_H = \tilde{\mu}_{H,1} - \tilde{\mu}_{H,2} = RT\ln 10(pH_2 - pH_1) + F\Delta\Psi$ is represented by $\Delta pH = pH_o - pH_i$ (pH_o is the pH in the suspending medium) since $\Delta\Psi$ was assumed to be negligibly small. The data in (B) were obtained from the plots in (A) and additional data given in Ref. 92 for different experimental conditions (indicated by different symbols). The curve for $pH_i \geq 5.3$ which is continued as broken line for $pH_i < 5.3$ was calculated according to $J_e = J_{e,o}/(10^{pH-pK} + 1)$ with $J_{e,o} = 1450$ μequiv/mg per h and $pK = 7$.

their limited validity. They are in principle model-free and therefore do not preclude a possible mechanism which we may not have thought of in our attempt to compile a suitable description of the system. Moreover, they are relatively easy to handle, even for a complex system, and thus prove to be adequate for a situation where our limited knowledge of the system prevents the sketching of a refined picture. They can help us to design new experiments, particularly when we keep in mind what requirements are to be met for the existence of linear relations. Above all, and most important, however, is the fact that such relations are in accordance with thermodynamics which sets the frame for any description. On the other hand, the failure of a system to comply with linear relations does not necessarily indicate a violation of thermodynamics, since linearity is a special case which may not be encountered due to inappropriate boundary conditions.

In a later stage more information about the system will become available which should enable us to extend our description to the mechanistic level. The characteristics learned from the phenomenological description should find their expression in a kinetic scheme. Thus, a regulation detected in the former description (see subsection VI.E) should either be attributable to a kinetic control of the system under the given conditions or else be taken into account by a regulated mechanism. Since most likely not all parts of a system will have attained the same level of detailedness at a given stage we shall have to work with 'mixed' descriptions where molecular mechanisms are combined with still phenomenological relations. A consistent combination of the two is not always straightforward and can be rather tedious, which, however, should not deter us from doing it. A mechanistic description which disregards all other processes occurring in the system is in principle not experimentally challengeable. Similarly, a description in terms of linear flow-force relations has only a limited significance, despite its generality, if not eventually understood on a mechanistic basis. An extended range of linearity exceeding that expected from kinetic schemes under constraints (see subsection V.B) may arise from a complex and important regulation. Moreover, the interpretation of the degree of coupling and the phenomenological stoichiometry remains obscure as long as it is not proven that the meaning of these quantities which pertains to states close to equilibrium persists for states far from equilibrium (see subsection VI.D-2).

The increasing refinement of the description in successive stages sooner or later results in rather complex equations which are hardly interpretable. In this case, it is advisable to resort to computer simulations with assigned values for the parameters. This is not a difficult task, since the steady state of a kinetic scheme can usually be described by a set of linear equations whose solution is obtained by standard techniques (frequently found in software libraries or so-called user-oriented packages). The behavior of a given model or

description can then be explored by varying the values of the parameters and, provided that enough independent experimental data are available, some of the parameters can even be estimated by non-linear fitting algorithms.

Our considerations were deliberately restricted to steady states. Considerably more information about the kinetic behavior of a system can of course be obtained from the transients between steady states. This, however, requires that differential equations are solved under given boundary conditions, which in many cases does not result in a general solution, particularly because a set of non-linear differential equations is frequently encountered. A computer simulation by means of a suitable package (e.g., the network simulation program * mentioned in subsections VI.A and VI.C-2) is then almost inevitable. It should be added that an attempt to analyze the transient of, for example, a coupled transport by means of a unidirectional Michaelis-Menten type of 'rate law with product inhibition' [70] is inappropriate for the reasons discussed in subsection IV.B-1. Moreover, unpublished investigations of this author have shown that the time course of substrates and products are not uniquely determined by the Michaelis-Menten parameters, even for the simplest reaction (isomerization, cf. Eq. 56) in that a multitude of values for K_m and k_{cat} for substrate and product yield the same time-courses.

The reader who has had the patience and the endurance to follow me through all the calculations and considerations in this review will hopefully be rewarded by a deeper insight into the principles underlying the thermodynamics and kinetics of processes in biological systems and in particular of energy conversion. The theoretical treatment of complex biological systems presented here may appear, and in several cases is, too rigorous to be directly applicable to experimental data. However, one should keep in mind that it is more advantageous to start from a rigorous and detailed picture which is then reduced step by step until it lends itself to an experimental challenge (for an example of such an approach see Ref. 86). This makes the simplifications explicit and helps to avoid the risk of oversimplifications and fallacies inherent in an approach which starts from the other end, i.e., from simplest principles. I hope to have been able to evoke or increase the reader's interest in all the related topics which had to be left out in order to restrict this already lengthy review to a reasonable size. These are among others the conversion of light into chemical energy [11,12,71], cooperativity and allosteric regulation of enzymes [14], or the controversial aspects of 'double inhibitor titrations' [98,99]. Finally, new experimental findings such as a slip in the H^+-ATP synthase which seems to be regulated by the type of divalent cations present [100] or the intermediate states in cytochrome oxidase with transitions involving proton pumping [101,102] have to be incorporated into kinetic schemes which, in the latter case, leads to supercycles with interesting properties.

* A paper by Mikulecky, Walz, Scriven and Caplan which describes the modelling of biological systems and includes a manual for the use of the network simulation program SPICE will appear in Treatise on Bioelectrochemistry (Milazzo, G., ed.), Vol. 1.

Acknowledgements

Many colleagues have contributed to and influenced the presentation of the material in this review by stimulating discussions. In particular, the close and fruitful collaboration with S. Roy Caplan and the illuminating ideas of Terrell L. Hill were of invaluable help. I would like to thank H. Ronald Kaback, who introduced me to lactose permease, for hospitality and helpful discussions. I am also indebted to Jannette Rüsch for a critical reading of the manuscript, and to Wolfgang Ziemke, who skillfully prepared most of the figures. Financial support by the Swiss National Science Foundation is gratefully acknowledged.

Appendix

This section contains an outline of the cycle diagram method of Hill [12,13] and presents a short description of how the diagrams given in the text are analyzed.

A.I. The cycle diagram method of Hill

A.I-1. Probabilities of states and transitions

When all states of an enzyme and the transitions connecting them have been collected they are arranged in a *diagram* (for examples see Figs. 4B, 5B, 6C and E, 7B, 10A), and the states are numbered for identification in the subsequent analysis. The probability, p_i, of the ith state is then defined as

$$p_i = N_i / N_e \tag{A1}$$

where N_i and N_e are the mole number for enzyme in state i and for total enzyme, respectively. Obviously,

$$\sum_i p_i = 1 \tag{A2}$$

The transition between states i and j is governed by transition probabilities α_{ij} and α_{ji} for 'forward' ($i \rightarrow j$) and 'backward' ($j \rightarrow i$) direction, respectively, in close analogy to unidirectional chemical kinetics (cf. Eqn. 43). Forward and backward transitions are true first-order processes for a conformational change. For a transition arising from binding of reactant R_r to the enzyme, the unidirectional process describing dissocia-

tion (say $j \rightarrow i$) is still true first-order, but the association process is only pseudo-first-order, since its transition probability comprises the concentration of the reactant, c_{Rr}, according to

$$\alpha_{ij} = \alpha^{o}_{ij} c_{Rr} \quad \text{for association of } R_r \text{ with enzyme} \tag{A3}$$

where α^{o}_{ij} is a true second order transition probability (compare Eqn. 44 for unidirectional chemical kinetics).

The change of p_i with time arises from all transitions $i \rightleftarrows j$ in which state i is involved and amounts to

$$dp_i/dt = \sum_j (\alpha_{ji} p_j - \alpha_{ij} p_i) \tag{A4}$$

When the *enzyme has reached the steady state*, $dp_i/dt = 0$ for all states, and Eqns. A4 are reduced to a system of linear equations for the probabilities p_i at steady state. Since any one of these equations can be represented by a linear combination of the other equations in the system, it has to be replaced by Eqn. A2. The solution for p_i can then be obtained by conventional procedures of linear algebra. The change in concentration of reactant R_r arises from all the transitions pertinent to binding of R_r and amounts to

$$dN_{Rr}/dt = N_e \sum_j (\alpha_{ji} p_j - \alpha^{o}_{ij} c_{Rr} p_i) \tag{A5}$$

The time derivative in Eqn. A5 can be used to define the flow of the catalyzed reaction or the flow of a transported species according to Eqns. 11 or 16, respectively.

A.I-2. Partial diagrams and cycle flows

Hill [12] has developed an algorithm which allows us to write down the steady state solution for the probabilities p_i and for the flows J_{ij} for all transitions without solving the system of linear equations mentioned above. In a first step, following the rule of partial diagrams [12], a quantity pertinent to the ith state and abbreviated by * $\boldsymbol{\Sigma}_i$ is constructed which consist of a sum of products of transition probabilities. Then, $p_i = \boldsymbol{\Sigma}_i / \boldsymbol{\Sigma}$, where $\boldsymbol{\Sigma}$ is the sum of the $\boldsymbol{\Sigma}_i$ for all states.

In a next step, the cycles in the diagram are sorted out and numbered (or lettered) consecutively. A positive sense of rotation is arbitrarily chosen which applies to all cycles. The cycle flow, J_k, for the kth cycle is then calculated which has the form

$$J_k = N_e (\boldsymbol{\pi}_{k+} - \boldsymbol{\pi}_{k-}) \boldsymbol{\Sigma}'_k / \boldsymbol{\Sigma} \tag{A6}$$

* Bold-face is used for $\boldsymbol{\Sigma}$ and $\boldsymbol{\pi}$ in order to distinguish these quantities from the symbols indicating the sum of terms and number π, respectively.

The quantity $\boldsymbol{\pi}_{k+}$ is the product of the transition probabilities α_{ij} taken for the positive direction of all transitions in the cycle, and $\boldsymbol{\pi}_{k-}$ is the corresponding product for the negative direction. $\boldsymbol{\Sigma}'_k$ is a similar quantity for the cycle k as is $\boldsymbol{\Sigma}_i$ for the state i.

The flow through each transition at steady state, J_{ij}, is then given by

$$J_{ij} = N_e [\alpha_{ij} p_i - \alpha_{ji} p_j] = \sum_k s_{k,ij} J_k \tag{A7}$$

where $s_{k,ij} = 1$ and -1 for the transition $i \rightarrow j$ being in the positive and negative direction in cycle k, respectively, while $s_{k,ij} = 0$ if the transition $i \rightarrow j$ does not occur in cycle k. Eqn. A7 applied to all transitions which involve binding of the rth reactant R_r yields the *flow of reactant R_r out of the enzyme cycle(s)*. Let $n_{k,Rr}$ be a stoichiometric coefficient indicating the number of transitions in cycle k which involve binding of R_r. In determining $n_{k,Rr}$, a transition is counted as positive (negative) if its direction of dissociation (association) of R_r coincides with the positive direction. Then

$$J_{Rr} = \sum_k n_{k,Rr} J_k \tag{A8}$$

which is equal to the flow of a transport process or, after dividing by the stoichiometric coefficient of R_r (see subsection II.D-1), equal to the flow of the catalyzed reaction.

A.I-3. Effect of electrical potentials on transition probabilities

The change in conformation of the enzyme in the course of a cycle is in many cases accompanied by displacements of charges. An obvious example is the binding of a charged reactant to the enzyme. The charge carried by the reactant is displaced from the aqueous phase 'outside' the enzyme to the position 'inside' the enzyme where it is brought to when the reactant is bound. Displacements within the enzyme occur upon reorientation of charged reactants either due to chemical reactions or by shifting the accessibility of a binding site to a different domain on the enzyme. Less obvious are the cases in which the enzyme itself carries charged groups. A conformational change can then cause a displacement of charges also for the free enzyme or in the case of uncharged reactants.

The displacement of charges in a transition contributes to the energy barrier separating the two conformations and thus appears implicitly in the transition probabilities. Since electric fields strongly affect charge displacements, we have to expect an alteration of these probabilities when the enzyme is exposed to an electric field. No external electric field is present when the enzyme is suspended in an aqueous phase. However, the

rearrangement of charges in the enzyme (or the change of the intrinsic electric field within the enzyme) associated with the transitions may find its expression in a dependence of the transition probabilities on the ionic strength in the aqueous phase [103]. This is due to readjustments of the diffuse layer, which is present on the surface of a charged enzyme as it is on the surfaces of a charged membrane (see subsection III.B).

Membrane-bound enzymes are exposed to an electric field whenever a difference in electrical potential across the membrane exists. In the following, we assume that this electric field is constant, i.e., that the potential changes linearly within the membrane (see subsections III.B and E). The effect of the field on the transition probabilities follows from the theory of absolute reaction rates [38] and yields a correction factor comprising $\Delta\phi_m$, which is the difference of the reduced electrical potential (cf. Eqn. 25) across the membrane,

$$\alpha_{ij}^{*} = \alpha_{ij} \exp\{\zeta_{ij}\,\Delta\phi_m/2\} \quad \text{and} \quad \alpha_{ji}^{*} = \alpha_{ji} \exp\{-\zeta_{ij}\,\Delta\phi_m/2\} \tag{A9}$$

where α_{ij}^{*} and α_{ji}^{*} are the transition probabilities for $i \to j$ and $j \to i$, respectively, in the presence of the electric field. In Eqn. A9, we have assumed that the energy barrier separating the two states i and j is symmetric so that the effect of $\Delta\phi_m$ is split equally between forward and backward transition [12,71].

The quantity ζ_{ij} in Eqn. A9 is an operationally defined valence effective for the transition $i \to j$. Suppose that the conformation of the enzyme in state i has the kth charge with valence z_k at a position with coordinate $x_{k,i}$ on the x-axis shown in Fig. 1C. The conformational change associated with the transition $i \to j$ moves this charge to position $x_{k,j}$ and thus displaces it by $\Delta x_{k,ij} = x_{k,j} - x_{k,i}$. The effective valence ζ_{ij} is then defined as [71]

$$\zeta_{ij} = \sum_k z_k\,\Delta x_{k,ij}/d \tag{A10}$$

where d is the thickness of the membrane. The sum in Eqn. A10 has to be taken over all charges k including those associated with charged reactants which are bound or released or displaced when going from state i to state j. The ζ_{ij} values for a given cycle are subject to the condition

$$\Sigma_+ \zeta_{ij} = \Sigma_+ z_t \tag{A11}$$

where z_t is the valence of a species transported across the membrane when going around the cycle in the positive direction. $\Sigma_+ z_t$ then means that the sum has to be taken for all species transported by a given cycle and z_t has to be multiplied by 1 or -1 if the transport occurs in the positive or negative direction for flows, respectively. Similarly, $\Sigma_+ \zeta_{ij}$ means that the sum has to include all transitions of a given cycle, and that a ζ_{ij} has to be multiplied by 1 or -1 if the direction of the transition $i \to j$ coincides with the positive or the negative direction of the cycle, respectively. Eqn. All is the analogue to thermokinetic balancing (see subsection A.I-5) for electric terms.

A.I-4. Reduction of the number of states in a diagram

Some α_{ij} values may be much larger than the others in a certain sequence of transitions. Following a line of reasoning similar to that which lead to the overall reaction in Eqn. 52 in chemical kinetics, it is then found that the intermediate states in the sequence can be neglected, and that the whole sequence can be approximated by one transition [12].

Suppose we have a sequence of four states with the transitions $1 \rightleftarrows 2 \rightleftarrows 3 \rightleftarrows 4$. Provided that the transition $2 \rightleftarrows 3$ is much faster than transitions $1 \rightleftarrows 2$ and $3 \rightleftarrows 4$, states 2 and 3 can be combined into one state $2'$, and the new sequence $1 \rightleftarrows 2' \rightleftarrows 4$ has the transition probabilities

$$\alpha_{12} = \alpha_{12}, \quad \alpha_{2'1} = \alpha_{21}/(1+K_{23}) \quad \text{and}$$

$$\alpha_{2'4} = \alpha_{34}K_{23}/(1+K_{23}), \quad \alpha_{42'} = \alpha_{43}$$

$$\text{for } \alpha_{23}, \alpha_{32} \gg \alpha_{12}, \alpha_{21}, \alpha_{34}, \alpha_{43} \tag{A12}$$

where K_{23} is the equilibrium constant for the transition $2 \rightleftarrows 3$ (see Eqn. A15).

If one of the inequalities in Eqn. A13 below holds, the sequence can be condensed into one, i.e., $1 \rightleftarrows 4$, with transition probabilities

$$\alpha_{14} = \alpha_{12}\alpha_{23}\alpha_{34}/\langle\alpha\rangle \text{ and}$$

$$\alpha_{41} = \alpha_{21}\alpha_{32}\alpha_{43}/\langle\alpha\rangle$$

$$\text{with } \langle\alpha\rangle = \alpha_{21}\alpha_{31} + \alpha_{21}\alpha_{34} + \alpha_{23}\alpha_{34}$$

$$\text{for } \alpha_{21}, \alpha_{31} \text{ or } \alpha_{21}, \alpha_{34} \text{ or } \alpha_{23}, \alpha_{34} \gg \alpha_{12}, \alpha_{43} \tag{A13}$$

A.I-5. Thermokinetic balancing

Detailed balancing (see subsection V.A) applied to the kinetic scheme of an enzyme requires that all transition flows J_{ij} vanish. As evident form Eqn. A7, this condition is met if all cycle flows vanish, hence $\pi_+ = \pi_-$ for all cycles (cf. Eqn. A6). This condition clearly applies only to the equilibrium state, since pseudo-first-order transition probabilities include the concentration of reactants. Upon substitution of pseudo-first-order transition probabilities by virtue of Eqn. A3, the condition $\pi_{k+} = \pi_{k-}$ for the kth cycle is transformed into

$$\frac{\Pi_{k+}\alpha_{ij}\alpha^{\circ}_{kl}\alpha_{nm}}{\Pi_{k-}\alpha_{ji}\alpha_{lk}\alpha^{\circ}_{mn}} = \Pi K_{ij}\frac{\Pi K_{\mathrm{Rr}(mn)}}{\Pi K_{\mathrm{Rr}(lk)}} = \prod_r [c_{\mathrm{Rr}}^{n_{k,\mathrm{Rr}}}]_{\mathrm{eq}} = K_c \tag{A14}$$

In this equation the term $\Pi_{k+}\ \alpha_{ij}\alpha^{\circ}_{kl}\alpha_{nm}$ means the product of all transition probabilities in cycle k taken in the positive direction, where α_{ij}, α°_{kl} and α_{nm} stand for transitions with a conformational change, for transitions with association of a reactant R_r, and for transitions with association of a reactant R_r in the opposite direction, respectively. The term $\Pi_{k-}\alpha_{ji}\alpha_{lk}\alpha^{\circ}_{mn}$ is the corresponding product taken in the negative direction.

The quantities K_{ij} and K_{Rr} in Eqn. A14 are equilibrium constants, defined as

$$K_{ij} = \alpha_{ij}/\alpha_{ji} = [\,p_j/p_i\,]_{eq} \tag{A15}$$

for conformational transitions, and

$$K_{Rr} = \alpha_{ji}/\alpha^{\circ}_{ij} = [\,p_i c_{Rr}/p_j\,]_{eq} \tag{A16}$$

for transitions pertinent to binding. They also relate the probabilities p_i and p_j at equilibrium as indicated on the right-hand side of Eqns. A15 and A16. The second part of Eqn. A14 then means the product of all K_{ij} pertinent to conformational changes times the product of all dissociation constants for binding transitions whose dissociation coincides with the positive direction, divided by the product of dissociation constants for dissociation of R_r in the negative direction. The third part of Eqn. A14 is identical to the law of mass action (see Eqn. 26a) for a chemical reaction which converts all reactants with negative $n_{k,Rr}$ to all reactants with positive $n_{k,Rr}$. Obviously, K_c is the equilibrium constant for this reaction.

Note that $K_c = 1$ in Eqn. A14 if no chemical reaction is associated with a full turn around a given cycle, i.e., if all $n_{k,Rr} = 0$ (for an example see cycle 3 in Fig. 5C). $K_c = 1$ also holds if one turn of a cycle results only in a transport of species from one compartment to another, in line with the notion that the partition coefficient between two equal phases is unity (see subsection II.E-1).

A.II. Short description of the analysis of diagrams

A.II-1. The isomerization reaction

The diagram in Fig. 4B has six states and yields three partial diagrams. Hence, Σ has 18 terms, each consisting of a product of five transition probabilities α_{ij}. There is only one cycle whose dead-end branches cause $\Sigma'_1 = \alpha_{41}\alpha_{52}\alpha_{63}$ and whose cycle flow is

$$J_1 = N_e\alpha_{41}\alpha_{52}\alpha_{63}(\alpha_{12}\alpha_{23}\alpha_{31} - \alpha_{13}\alpha_{32}\alpha_{21})/\Sigma \tag{A17}$$

Since $n_{1,P} = -n_{1,S} = 1$, $J_c = J_p = -J_S = J_1$ (cf. Eqn. A8). When all pseudo-first-order α_{ij} are substituted by virtue of Eqn. A3 and the equilibrium constants defined in Eqns. A15 and A16 are introduced, Eqn. 55 is obtained with

$$\begin{aligned}\Sigma_{r1} = {} & [(1+\tau_1K_{23}+\tau_2)(1+c_1/K_{I1})] \\ & +[(1+\tau_2)(1+c_1/K_{12})+\tau_2K_{23}(1+c_1/K_{13})]c_S/K_S \\ & +[(1+\tau_1K_{23})(1+c_1/K_{13})+\tau_1(1+c_1/K_{12})]c_P/K_P\end{aligned} \tag{A18}$$

The quantities τ_i are relative transition probabilities defined as

$$\tau_1 = \alpha_{32}/\alpha_{21}, \quad \tau_2 = \alpha_{32}/\alpha_{31} \tag{A19}$$

The terms pertinent to S and P in Eqns. 55 and A18 can be condensed into quantities known as 'Michaelis-Menten' parameters [15]. A pseudo dissociation constant, K_{mS} ('Michaelis constant' and an overall first-order rate constant *, k_{catS}, (also known as 'turnover number'), both of which are dependent on the inhibitor concentration c_I, can be defined for the substrate S,

$$K_{ms}(c_I) = K_S(1+\tau_1K_{23}+\tau_2)(1+c_1/K_{I1})/D_S \tag{A20a}$$

and

$$k_{catS}(c_I) = \alpha_{23}/D_S = \alpha_{32}K_{23}/D_S \tag{A20b}$$

with the abbreviation

$$D_S = (1+\tau_2)(1+c_1/K_{12})+\tau_2K_{23}(1+c_1/K_{13}) \tag{A20c}$$

Similarly for the product P,

$$K_{mP}(c_I) = K_P(1+\tau_1K_{23}+\tau_2)(1+c_1/K_{I1})/D_P \tag{A21a}$$

and

$$k_{catP}(c_I) = \alpha_{32}/D_P \tag{A21b}$$

with the abbreviation

$$D_P = (1+\tau_1K_{23})(1+c_1/K_{13})+\tau_1(1+c_1/K_{12}) \tag{A21c}$$

A.II-2. Formation of one product from two substrates

The diagram in Fig. 5B has five states and yields 12 partial diagrams. Hence, Σ comprises 60 terms, each consisting of a product of four transition probabilities α_{ij}. Three cycles are present (see Fig. 5C), but the third cycle, which contains only transitions with binding of S_1 and S_2, does not contribute to J_c because $n_{3,S1} = n_{3,S2} =$

* If the mole number of enzyme, N_e, is not known, the maximal velocity $v_{maxX} = N_e k_{catX}/V$ (X = S or P) is used, where V is the volume of the compartment in which the reaction takes place.

$n_{3,P} = 0$. For the remaining two cycles, $n_{k,P} = 1$, and the sum of their flows constitutes J_c. We then obtain

$$J_c = N_e[(\alpha_{12}\alpha_{24}\alpha_{45}\alpha_{51} - \alpha_{21}\alpha_{42}\alpha_{54}\alpha_{15})(\alpha_{31} + \alpha_{34}) + (\alpha_{13}\alpha_{34}\alpha_{45}\alpha_{51} - \alpha_{31}\alpha_{43}\alpha_{54}\alpha_{15})(\alpha_{21} + \alpha_{24})]/\Sigma \quad \text{(A22)}$$

Upon substitution of pseudo-first-order α_{ij} terms according to Eqn. A3 and introduction of the equilibrium constants (Eqns. A15 and A16), Eqn. 62 is obtained with

$$\begin{aligned}\Sigma_{r2} = {} & [(1+\tau_3)(1+B_r) + \tau_2 K_{45}] \\ & + [1 + \tau_3 + \tau_2 K_{45} + B_r(1+\tau_3)]c_{S1}/K_{S1} \\ & + \{\tau_1 K_{45} + [(1+\tau_3)(1+B_r) + \tau_5 K_{45}]K'_{S1}/K_{S1}\}c_{S2}/K_{S2} \\ & + [1 + \tau_2(1+K_{45}) + \tau_1 + B_r(1+\tau_4)]c_P/K_P \\ & + [1 + \tau_3(1+K_{45})](1+B_r)c_{S1}c_{S2}/(K_{S1}K_{S2}) \\ & + \tau_1(1+K_{45})c_{S2}c_P/(K_{S2}K_P)\end{aligned} \quad \text{(A23)}$$

and the abbreviation

$$B_r = \beta_1 \frac{\beta_2 + c_{S2}/K_{S2}}{1 + \beta_3 c_{S1}/K'_{S1}} \quad \text{(A24)}$$

The quantities τ_i and β_i are relative transition probabilities defined as

$$\tau_1 = \alpha_{54}/\alpha_{21}, \quad \tau_2 = \alpha_{54}/\alpha_{42}, \quad \tau_3 = \alpha_{54}/\alpha_{51}, \quad \tau_4 = \alpha_{54}/\alpha_{31}, \quad \tau_5 = \alpha_{54}/\alpha_{43} \quad \text{(A25a)}$$

and

$$\beta_1 = \alpha_{43}/\alpha_{21}, \quad \beta_2 = \alpha_{21}/\alpha_{42}, \quad \beta_3 = \alpha_{43}/\alpha_{31} \quad \text{(A25b)}$$

Note that $K'_{S1}/K_{S1} = \beta_1\alpha^\circ_{12}/\alpha^\circ_{34}$. Moreover, Eqn. 77b was used in the above equations.

If the terms c_{S1}/K'_{S1} or c_{S2}/K_{S2} in Eqn. A24 can be neglected, i.e., if

$$\begin{aligned}&\beta_3 c_{S1}/K'_{S1} \ll 1 \quad \text{for } c_{S2} = \text{constant}, \quad \text{or} \\ &c_{S2}/K_{S2} \ll \beta_2 \quad \text{for } c_{S1} = \text{constant}\end{aligned} \quad \text{(A26)}$$

the flow of the reaction complies with the simple 'Michaelis-Menten law'. The corresponding parameters for S_1 are dependent on c_{S2} and vice versa,

$$K_{mS1}(c_{S2}) = K_{S1}[A_{11} + (\tau_1 K_{45} + A_{12})c_{S2}/K_{S2}]/D_{S1},$$

$$k_{catS1}(c_{S2}) = \alpha_{54}K_{45}(1+B_{r1})c_{S2}/(K_{S2}D_{S1})$$

$$\text{where } D_{S1} = A_{31} + A_{41}c_{S2}/K_{S2} \quad \text{(A27a)}$$

and

$$K_{mS2}(c_{S1}) = K_{S2}(A_{12} + A_{32}c_{S1}/K_{S1})/D_{S2},$$

$$k_{catS2}(c_{S1}) = \alpha_{54}K_{45}(1+B_{r2})c_{S1}/(K_{S1}D_{S2})$$

$$\text{where } D_{S2} = \tau_1 K_{45} + A_{22} + A_{42}c_{S1}/K_{S1} \quad \text{(A27b)}$$

The abbreviations A_{ij} and B_{rj} in Eqns. A27a and b read

$$A_{1j} = (1+\tau_3)(1+B_{rj}) + \tau_2 K_{45},$$

$$A_{2j} = [(1+\tau_3)(1+B_{rj}) + \tau_5 K_{45}]K'_{S1}/K_{S1},$$

$$A_{3j} = 1 + \tau_3 + \tau_2 K_{45} + B_{rj}(1+\tau_3),$$

$$A_{4j} = [1 + \tau_3(1+K_{45})](1+B_{rj})$$

$$j = 1 \text{ or } 2,$$

and

$$B_{r1} = \beta_1(\beta_2 + c_{S2}/K_{S2})$$

$$B_{r2} = \beta_1\beta_2/[1 + c_{S1}/K'_{S1}] \quad \text{(A27c)}$$

The Michaelis-Menten parameters for the product are

$$K_{mP} = K_P[(1+\tau_3)(1+\beta_1\beta_2) + \tau_2 K_{45}]/D_P,$$

$$k_{catP} = \alpha_{54}(1+\beta_1\beta_2)/D_P$$

$$\text{where } D_P = 1 + \tau_1 + \tau_2(1+K_{45}) + \beta_1\beta_2(1+\tau_4) \quad \text{(A28)}$$

A.II-3. Redox reactions

Provided that the association of redox species with the enzyme in the scheme of Fig. 6A is slow compared to the electron transfer transitions and/or some of the dissociations of the species, a reduction of the number of states (see subsection A.I-4) is possible. Thus, the transitions $1 \rightleftarrows 2 \rightleftarrows 3 \rightleftarrows 4$ can be condensed into a new transition $1 \rightleftarrows 4$ with transition probabilities

$$\alpha_{14} = \alpha'_{21}c_{Dr}/K_{Dr} \quad \text{and} \quad \alpha_{41} = \alpha'_{21}K_{32}c_{Do}/K_{Do}$$

$$\text{with } \alpha'_{21} = \alpha_{21}/[1 + \alpha_{21}/\alpha_{23} + K_{32}\alpha_{21}/\alpha_{34}]$$

$$\text{for } \alpha^\circ_{12}c_{Dr}, \alpha^\circ_{43}c_{Do} \ll \alpha_{21}, \alpha_{32} \quad \text{or } \alpha_{31}, \alpha_{34} \quad \text{or } \alpha_{23}, \alpha_{34} \quad \text{(A29a)}$$

Similarly for the transitions $5 \rightleftarrows 6 \rightleftarrows 7 \rightleftarrows 8$ which yield the new transition $5 \rightleftarrows 8$ with transition probabilities

$$\alpha_{58} = \alpha'_{78}K_{67}c_{Ao}/K_{Ao} \quad \text{and} \quad \alpha_{85} = \alpha'_{78}c_{Ar}/K_{Ar}$$

$$\text{with } \alpha'_{78} = \alpha_{78}/[1 + \alpha_{78}/\alpha_{76} + K_{67}\alpha_{78}/\alpha_{65}]$$

$$\text{for } \alpha^\circ_{56}c_{Ao}, \alpha^\circ_{87}c_{Ar} \ll \alpha_{65}, \alpha_{76} \quad \text{or} \quad \alpha_{65}, \alpha_{78} \quad \text{or} \quad \alpha_{67}, \alpha_{78} \quad \text{(A29b)}$$

Here, K_{32} and K_{67} are the equilibrium constants (cf. Eqn. A15) for the transitions $3 \rightleftarrows 2$ and $6 \rightleftarrows 7$, respectively. With these reductions, the scheme in Fig. 6A is transformed into a diagram with four states (Fig. 6C)

which has four partial diagrams. Σ then consists of 16 terms, each being the product of three transition probabilities.

There is only one cycle without dead-end branches, hence $\Sigma_1' = 1$. Moreover, $-n_{1,\mathrm{Dr}} = n_{1,\mathrm{Do}} = -n_{1,\mathrm{Ao}} = n_{1,\mathrm{Ar}} = 1$. The flow of the chemical reaction, which can be expressed in terms of a flow of electrons, J_e, is then

$$J_c = J_e/n_e = N_e(\alpha_{14}\alpha_{45}\alpha_{58}\alpha_{81} - \alpha_{41}\alpha_{54}\alpha_{85}\alpha_{18})/\Sigma \qquad \text{(A30)}$$

where n_e is the number of electrons which the enzyme exchanges with D (which of course is equal to the number of electrons exchanged with A). Upon substitution of the probabilities for the condensed transitions in Eqns. A29 and introduction of the equilibrium constants (Eqn. A15) for transitions 4 ⇄ 5 and 8 ⇄ 1, Eqn. 63 is obtained with

$$\begin{aligned}\Sigma_{\mathrm{rd}} = {} & (1+K_{81})[1+\tau_2 K_{\mathrm{Ao}}/c_{\mathrm{Ao}} + \tau_1 K_{45} K_{\mathrm{Do}}/c_{\mathrm{Do}}] \\ & + K_{81}[1+\tau_2(1+K_{45})K_{\mathrm{Ao}}/c_{\mathrm{Ao}} + \tau_3 K_{45}]\rho_{\mathrm{D}}/K_{\mathrm{D}}^{*} \\ & + [1+\tau_1(1+K_{45})K_{\mathrm{Do}}/c_{\mathrm{Do}} + \tau_3 K_{81}]\rho_{\mathrm{A}}/K_{\mathrm{A}}^{*} \\ & + \tau_3 K_{81}(1+K_{45})\rho_{\mathrm{D}}\rho_{\mathrm{A}}/(K_{\mathrm{D}}^{*}K_{\mathrm{A}}^{*}) \end{aligned} \qquad \text{(A31)}$$

In Eqn. A31, the combined equilibrium constants

$$K_{\mathrm{D}}^{*} = K_{32}K_{\mathrm{Dr}}/K_{\mathrm{Do}}, \quad K_{\mathrm{A}}^{*} = K_{67}K_{\mathrm{Ar}}/K_{\mathrm{Ao}} \qquad \text{(A32a)}$$

and the relative transition probabilities

$$\tau_1 = \alpha_{54}/(\alpha_{21}'K_{32}), \quad \tau_2 = \alpha_{54}/(\alpha_{78}'K_{67}), \quad \tau_3 = \alpha_{54}/\alpha_{81} \qquad \text{(A32b)}$$

are used. K_{Xr} and K_{Xo}, X = D or A, are the dissociation constants of the reduced and oxidized species, respectively, for the donating (X = D) or the accepting (X = A) redox couple.

A.II-4. Transport through pores

The diagram in Fig. 7B has four states and eight partial diagrams, which yields 32 terms for Σ each of which is a product of four transition probabilities α_{ij}. Three cycles are present but, similar to the case of two substrates (see subsection A.II-2), one cycle (the third in Fig. 7C) does not contribute to J_i. For the remaining two cycles, $n_{2,1} = -n_{2,2} = 1$ where index k,j indicates that the transported species dissociates from cycle j into compartment k. The flow of the ith *uncharged species or if* $\Delta\phi = \phi_{sk} = 0$, which is positive from compartment 1 to compartment 2, is then found to be (cf. Eqn. A8)

$$\begin{aligned} J_i = {} & N_{\mathrm{p}}[(\alpha_{12}\alpha_{23}\alpha_{31} - \alpha_{21}\alpha_{32}\alpha_{13})(\alpha_{42}+\alpha_{43}) \\ & - (\alpha_{24}\alpha_{43}\alpha_{32} - \alpha_{42}\alpha_{34}\alpha_{23})(\alpha_{12}+\alpha_{13})]/\Sigma \end{aligned} \qquad \text{(A33)}$$

When pseudo-first-order a_{ij} are substituted by virtue of Eqn. A3 and the equilibrium constants according to Eqns. A15 and A16 are introduced, Eqn. 69 is obtained in view of Eqn. 79b where

$$\begin{aligned} \Sigma_{\mathrm{p}} = {} & [1+\tau_1 K_{23} + \tau_2 + B_{\mathrm{p}}] \\ & + [1+\tau_2(1+K_{23}) + B_{\mathrm{p}}(1+\tau_3 K_{23})]c_{io,1}/K_1 \\ & + [1+\tau_1(1+K_{23}) + B_{\mathrm{p}}(1+\tau_4)]c_{io,2}/K_2 \\ & + [(1+B_{\mathrm{p}})K_1/K_1']c_{io,1}c_{io,2}/(K_1K_2) \end{aligned} \qquad \text{(A34)}$$

In Eqns. 69 and A34, the following substitutions were made

$$B_{\mathrm{p}} = b_{\mathrm{p}}[c_{io,1}/K_1 + (\alpha_{31}/\alpha_{21})c_{io,2}/K_2] \qquad \text{(A35)}$$

and

$$b_{\mathrm{p}} = (\alpha_{24}^{\circ}/\alpha_{13}^{\circ})/(1+\alpha_{42}/\alpha_{43}) \qquad \text{(A36)}$$

The quantities τ_i are relative transition probabilities defined as

$$\tau_1 = \alpha_{32}/\alpha_{21},\ \tau_2 = \alpha_{32}/\alpha_{31},\ \tau_3 = \alpha_{32}/\alpha_{42},\ \text{and}\ \tau_4 = \alpha_{32}/\alpha_{43} \qquad \text{(A37)}$$

Provided that $b_{\mathrm{p}}c_{io,1}/K_1 \ll 1$, the Michaelis-Menten parameters K_{m1} and k_{cat1} for $c_{io,2} \approx 0$ can be defined as

$$K_{\mathrm{m1}} = K_1(1+\tau_1K_{23}+\tau_2)/D_1 \quad \text{and} \quad k_{\mathrm{cat1}} = \alpha_{23}/D_1$$

$$\text{with } D_1 = 1+\tau_2(1+K_{23})+b_{\mathrm{p}} \qquad \text{(A38a)}$$

Similarly for $b_{\mathrm{p}}(\alpha_{31}/\alpha_{21})c_{io,2}/K_2 \ll 1$ and $c_{io,1} \approx 0$,

$$K_{\mathrm{m2}} = K_2(1+\tau_1K_{23}+\tau_2)/D_2 \quad \text{and} \quad k_{\mathrm{cat2}} = \alpha_{32}/D_2$$

$$\text{with } D_2 = 1+\tau_1(1+K_{23})+b_{\mathrm{p}}\alpha_{31}/\alpha_{21} \qquad \text{(A38b)}$$

If the species transported through the pore is charged, we can assume that only cycle 1 in Fig. 7C is operative, but its transition probabilities have to include the effect of the electrical potential across the membrane (cf. subsection A.I-3). The flow of the species then becomes

$$J_i = N_{\mathrm{p}}(\alpha_{12}^{*}\alpha_{23}^{*}\alpha_{31}^{*} - \alpha_{21}^{*}\alpha_{32}^{*}\alpha_{13}^{*})/\Sigma^{*} \qquad \text{(A39)}$$

with α_{ij}^{*} and α_{ji}^{*} according to Eqn. A9 which appear also in Σ^{*}. The condition in Eqn. A11 applied to cycle 1 reads

$$\zeta_{12} + \zeta_{23} + \zeta_{31} = z_i \qquad \text{(A40)}$$

where z_i is the valence of the transported species. Eqn. 71 is obtained by introducing dissociation constants and

equilibrium constants as usual, and by virtue of Eqns. 34, 67 and A40. The quantity Σ_{p*} in Eqn. 71 is

$$\Sigma_{p*} = \exp\{(\zeta_{23}/2+\zeta_{31})\Delta\phi_m\}[(1+\tau_1^*K_{23}^*+\tau_2^*)\exp\{z_i\phi_{s2}\} + [1+\tau_2^*(1+K_{23}^*)]c_{io,1}\exp\{z_i(\phi_{s2}-\phi_{s1}\}/K_1^* + [1+\tau_1^*(1+K_{23}^*)]c_{io,2}/K_2^*] \quad \text{(A41a)}$$

where

$$\tau_1^* = \tau_1\exp\{(\zeta_{12}-\zeta_{23})\Delta\phi_m/2\}, \quad \tau_2^* = \tau_2\exp\{-(\zeta_{31}+\zeta_{23})\Delta\phi_m/2\} \quad \text{(A41b)}$$

and

$$K_1^* = K_1\exp\{-\zeta_{12}\Delta\phi_m\}, \quad K_2^* = K_2\exp\{\zeta_{31}\Delta\phi_m\}, \quad K_{23}^* = K_{23}\exp\{\zeta_{23}\Delta\phi_m\} \quad \text{(A41c)}$$

A.II-5. Carrier-mediated transport

The diagram in Fig. 6E has four states and four partial diagrams, which yields 16 terms for Σ, each consisting of a product of three transition probabilities. There is one cycle without dead-end branches, hence $\Sigma_1' = 1$ and $-n_{1,1} = n_{2,1} = 1$, where the index k,j indicates that the transported species dissociates from cycle j into compartment k. The flow of the *ith uncharged species or a charged species if* $\Delta\phi = \phi_{Sk} = 0$, which is positive from compartment 1 to compartment 2, is then found to be (cf. Eqn. A8)

$$J_i = N_c(\alpha_{12}\alpha_{23}\alpha_{34}\alpha_{41} - \alpha_{21}\alpha_{32}\alpha_{43}\alpha_{14})/\Sigma \quad \text{(A42)}$$

where N_c denotes the mole number of carrier. Upon substitution of equilibrium constants according to Eqns. A15 and A16, Eqn. 72 is obtained with

$$\Sigma_c = [(1+K_{41})(1+\tau_1K_{23}+\tau_2)] + K_{41}[1+\tau_2(1+K_{23})+\tau_3K_{23}]c_{io,1}/K_1 + [1+\tau_1(1+K_{23})+\tau_3K_{41}]c_{io,2}/K_2 + \tau_3K_{41}(1+K_{23})c_{io,1}c_{io,2}/(K_1K_2) \quad \text{(A43)}$$

and the relative transition probabilities

$$\tau_1 = \alpha_{32}/\alpha_{21}, \quad \tau_2 = \alpha_{32}/\alpha_{34}, \quad \text{and } \tau_3 = \alpha_{32}/\alpha_{41} \quad \text{(A44)}$$

The Michaelis-Menten parameters found for the conditions $c_{io,2} \approx 0$ and $c_{io,1} \approx 0$ are, respectively,

$$K_{m1} = K_1(1+K_{41})(1+\tau_1K_{23}+\tau_2)/(K_{41}D_1), \quad k_{cat1} = \alpha_{23}/D_1 \quad \text{with } D_1 = 1+\tau_2(1+K_{23})+\tau_3K_{23} \quad \text{(A45a)}$$

and

$$K_{m2} = K_2(1+K_{41})(1+\tau_1K_{23}+\tau_2)/D_2, \quad k_{cat2} = \alpha_{32}/D_2 \quad \text{with } D_2 = 1+\tau_1(1+K_{23})+\tau_3K_{41} \quad \text{(A45b)}$$

If the transported *species is charged* with valence z_i, the α_{ij} terms have to be replaced by α_{ij}^* according to Eqns. A9 and A10. In view of the condition (cf. Eqn. A11)

$$\zeta_{12}+\zeta_{23}+\zeta_{34}+\zeta_{41} = z_i \quad \text{(A46)}$$

for the diagram in Fig. 6E, Eqn. A42 is transformed into Eqn. 73 with

$$\Sigma_{c*} = \exp\{(\zeta_{23}/2+\zeta_{34})\Delta\phi_m\} \times[(1+K_{41}^*)(1+\tau_1^*K_{23}^*+\tau_2^*)\exp\{z_i\phi_{s2}\} + K_{41}^*[1+\tau_2^*(1+K_{23}^*)+\tau_3^*K_{23}^*]\exp\{z_i(\phi_{s2}-\phi_{s1})\}c_{io,1}/K_1 + [1+\tau_1^*(1+K_{23}^*)+\tau_3^*K_{41}^*]c_{io,2}/K_2^* + \tau_3^*K_{41}^*(1+K_{23}^*)\exp\{z_i\phi_{s2}\}c_{io,1}c_{io,2}/(K_1^*K_2^*)] \quad \text{(A47a)}$$

where

$$\tau_1^* = \tau_1\exp\{(\zeta_{12}-\zeta_{23})\Delta\phi_m/2\}, \quad \tau_2^* = \tau_2\exp\{-(\zeta_{23}+\zeta_{34})\Delta\phi_m/2\}, \quad \tau_3^* = \tau_3\exp\{-(\zeta_{23}+\zeta_{41})\Delta\phi_m/2\}, \quad \text{(A47b)}$$

and

$$K_1^* = K_1\exp\{-\zeta_{12}\Delta\phi_m\}, \quad K_2^* = K_2\exp\{\zeta_{34}\Delta\phi_m\}, \quad K_{23}^* = K_{23}\exp\{\zeta_{23}\Delta\phi_m\}, \quad K_{41}^* = K_{41}\exp\{\zeta_{41}\Delta\phi_m\} \quad \text{(A47c)}$$

A.II-6. Antiport of species

The diagram in Fig. 10A has six states and 15 partial diagrams which yields 90 terms for Σ each consisting of a product of five transition probabilities. Three cycles are present (Fig. 10B) with $n_{A2,1} = -n_{B2,1} = -n_{B2,2} = n_{A2,3} = 1$, where the index X$k,j$ indicates that the transported species X (A or B) dissociates from cycle j into compartment k. The flows J_A and J_B, which are positive from compartment 1 to compartment 2, are then found to be for *uncharged species or charged species if* $\Delta\phi = \phi_{sk} = 0$ (cf. Eqn. A8)

$$J_A = (N_{ac}/\Sigma)[(\alpha_{12}\alpha_{23}\alpha_{34}\alpha_{45}\alpha_{56}\alpha_{61} - \alpha_{21}\alpha_{32}\alpha_{43}\alpha_{54}\alpha_{65}\alpha_{16}) + (\alpha_{65}\alpha_{54}+\alpha_{61}\alpha_{54}+\alpha_{61}\alpha_{56})(\alpha_{12}\alpha_{23}\alpha_{34}\alpha_{41} - \alpha_{21}\alpha_{32}\alpha_{43}\alpha_{14})] \quad \text{(A48a)}$$

and

$$J_B = (N_{ac}/\Sigma)[(\alpha_{21}\alpha_{32}\alpha_{43}\alpha_{54}\alpha_{65}\alpha_{16} - \alpha_{12}\alpha_{23}\alpha_{34}\alpha_{45}\alpha_{56}\alpha_{61}) + (\alpha_{23}\alpha_{34}+\alpha_{21}\alpha_{34}+\alpha_{21}\alpha_{32})(\alpha_{41}\alpha_{54}\alpha_{65}\alpha_{16} - \alpha_{14}\alpha_{45}\alpha_{56}\alpha_{61})] \quad \text{(A48b)}$$

where N_{ac} denotes the mole number of the antiport carrier. When we first introduce the equilibrium con-

stants for the transitions (see Fig. 10A and Eqns. A15 and A16) into Eqns. A48 and then the thermodynamic forces X_A and X_B of the species (cf. Eqn. 81c) we obtain Eqns. 108 in view of the relations arising from thermokinetic balancing

$$K_{A2}K_{B1}K_{23}K_{56}/(K_{A1}K_{B2}) = 1,$$
$$K_{B1}K_{56}/(K_{B2}K_{41}) = 1, \quad \text{and } K_{A2}K_{23}K_{41}/K_{A1} = 1 \tag{A49}$$

The factor $F(c_i)$ in Eqns. 108 reads

$$\begin{aligned} F = \{&[B_1 + B_2 c_{A1}/K_{A1} + B_3 c_{B2}/K_{B2}]K_{A2}K_{B1}/(c_{A2}c_{B1}) \\ &+ [B_4 + B_5 c_{A1}K_{B1}/(K_{A1}c_{B1})]c_{B2}K_{A2}/(K_{B2}c_{A2}) \\ &+ [B_6 c_{A1}/K_{A1} + B_8]K_{B1}/c_{B1} + B_7 + B_9 K_{A2}/c_{A2}\}/N_{ac}\alpha_{32} \end{aligned} \tag{A50}$$

where c_{Ak} and c_{Bk} denote, respectively, the concentrations of species A and B in the bulk phase of compartment k. The following substitutions have been made in Eqn. A50

$$\begin{aligned} &B_1 = \tau_7(1+K_{41})b_1b_2, && B_2 = \tau_5 b_2(K_{23} + \tau_6 b_4), \\ &B_3 = b_1(1+\tau_7 b_5), && B_4 = b_1(1+K_{56}), \\ &B_5 = K_{56}b_4 + \tau_5 K_{23} b_6, && B_6 = b_1(K_{56} + \tau_7 b_6), \\ &B_7 = b_3 + \tau_5 b_5, && B_8 = \tau_5 b_2(1+\tau_6 b_3), \\ &B_9 = \tau_5 b_2(1+K_{23}) \end{aligned} \tag{A51a}$$

with

$$\begin{aligned} &b_1 = 1 + \tau_1 K_{23} + \tau_2, && b_2 = 1 + \tau_3 K_{56} + \tau_4, \\ &b_3 = 1 + \tau_1(1+K_{23}), && b_4 = 1 + \tau_2(1+K_{23}), \\ &b_5 = 1 + \tau_3(1+K_{56}), && b_6 = 1 + \tau_4(1+K_{56}) \end{aligned} \tag{A51b}$$

The quantities τ_i and τ_s are relative transition probabilities defined as

$$\begin{aligned} &\tau_1 = \alpha_{32}/\alpha_{21}, && \tau_2 = \alpha_{32}/\alpha_{34}, && \tau_3 = \alpha_{65}/\alpha_{54}, \\ &\tau_4 = \alpha_{65}/\alpha_{61}, && \tau_5 = \alpha_{32}/\alpha_{65}, && \tau_6 = \alpha_{14}/\alpha_{32}, \\ &\tau_7 = \alpha_{14}/\alpha_{65} \end{aligned} \tag{A52}$$

while the parameters expressing the slip in Eqns. 108 are

$$\tau_{sA} = \tau_7 b_2 \quad \text{and } \tau_{sB} = \tau_6 K_{41} b_1 \tag{A53}$$

Under the constraints $c_{A1} \approx c_A = \text{const}$ and $c_{B1} = c_B = \text{const}$ (see Eqn. 109) $c_{A2} = c_A/\exp\{X_A/RT\}$, and $F(c_i)$ in Eqn. A50 can be transformed into

$$\begin{aligned} F = &[\exp\{(X_A - X_B)/RT\}[(B_3 + B_4 c_B/K_{B1})K_{A1}/c_A + B_5] \\ &/(K_{23}K_{56}) + \exp\{X_A/RT\}[(B_1 K_{A1}/c_A + B_2)K_{B1}/c_B \\ &+ B_9 K_{A1}/c_A]/(K_{23}K_{41}) + (B_6 c_A/K_{A1} + B_8)K_{B1}/c_B \\ &+ B_7]/(N_{ac}\alpha_{32}) \end{aligned} \tag{A54}$$

If $\tau_5 \approx 0$, $B_1 \approx B_2 \approx B_8 \approx B_9 \approx 0$ (see Eqns. A51) which allows us to rewrite Eqns. 108 in terms of extreme flows J_+ and J_- (see Eqns. 110) which are

$$\begin{aligned} J_+ &= N_{ac}\alpha_{23}K_{56}/[(B_3 + B_4 c_B/K_{B1})K_{A1}/c_A + B_5] \\ J_- &= N_{ac}\alpha_{32}/[B_6 c_A K_{B1}/(K_{A1}c_B) + B_7] \end{aligned} \tag{A55}$$

References

1 De Groot, S.R. and Mazur, P. (1962) Non-Equilibrium Thermodynamics, Elsevier, Amsterdam.
2 Katchalsky, A. and Curran, P.F. (1965) Nonequilibrium Thermodynamics in Biophysics, Harvard University Press, Cambridge, MA.
3 Prigogine, I. (1967) Introduction to Thermodynamics of Irreversible Processes, Interscience Publishers, New York.
4 Kedem, O. and Caplan, S.R. (1965) Trans. Faraday Soc. 61, 1897–1911.
5 Caplan, S.R. (1971) in Current Topics in Bioenergetics (Sanadi, D.R., ed.), Vol. 4, pp. 2-77, Academic Press, New York.
6 Wilson, D.F. (1980) Biochim. Biophys. Acta 616, 371–380.
7 Caplan, S.R. and Essig, A. (1983) Bioenergetics and Linear Nonequilibrium Thermodynamics: The Steady State, Harvard University Press, Cambridge, MA.
8 Rottenberg, H. (1973) Biophys. J. 13, 503–511.
9 Van der Meer, R., Westerhoff, H.V. and Van Dam, K. (1980) Biochim. Biophys. Acta 591, 488–493.
10 Westerhoff, H.V. and Van Dam, K. (1979) in Current Topics in Bioenergetics (Sanadi, D.R., ed.), Vol. 9, pp. 2–59, Academic Press, New York.
11 Westerhoff, H.V. and Van Dam, K. (1987) Thermodynamics and Control of Biological Free-Energy Transduction, Elsevier, Amsterdam.
12 Hill, T.L. (1977) Free Energy Transduction in Biology, Academic Press, New York.
13 Hill, T.L. (1989) Free Energy Transduction and Biochemical Cycle Kinetics, Springer Verlag, New York.
14 Hill, T.L. (1989) Cooperativity Theory in Biochemistry, Springer Verlag, New York.
15 Segel, I.H. (1975) Enzyme Kinetics, John Wiley & Sons, New York.
16 Atkins, P.W. (1986) Physical Chemistry, Oxford University Press, Oxford.
17 Walz, D. (1979) Biochim. Biophys. Acta 505, 279–353.
18 Walz, D. and Caplan, S.R. (1986) Biochim. Biophys. Acta 859, 151–164.
19 Overbeek, J.Th.G. (1952) in Colloid Science (Kruyt, H.R., ed.), Vol. 1, pp. 115–190 and 245–276, Elsevier, Amsterdam.
20 Walz, D., Bamberg, E. and Läuger, P. (1969) Biophys. J. 9, 1150–1159.
21 Müller, P. and Rudin, D.O. (1969) in Current Topics in Bioenergetics (Sanadi, D.R., ed.), Vol. 3, pp. 157–242, Academic Press, New York.
22 Ninham, B.W. and Parsegian, V.A. (1971) J. Theor. Biol. 31, 405–428.
23 Walz, D. (1984) in Advances in Photosynthesis Research (Sybesma, C., ed.), Vol. 2, pp. II.4.257–260, M. Nijhoff/W. Junk Publishers, The Hague.
24 Barber, J. (1979) Biochim. Biophys. Acta 594, 253–308.
25 Azzone, G.F., Pietrobon, D. and Zoratti, M. (1984) in Current Topics in Bioenergetics (Lee, C.P., ed.), Vol. 13, pp. 2–66, Academic Press, Orlando.

26 Pethig, R. (1975) Dielectric and Electronic Properties of Biological Materials, J. Wiley & Sons, New York.
27 Nelson, A.P. and McQuarrie, D.A. (1975) J. Theor. Biol. 55, 13–27.
28 Gräber, P. (1987) in Bioelectrochemistry (Milazzo, G. and Blanks, M., ed.), Vol. 2, pp. 379–425, Plenum Publishing, New York.
29 Walz, D. and Denis, M. (1984) in Charge and Field Effects in Biosystems (Allen, M.J. and Usherwood, P.N.R., eds.), pp. 69–76, Abacus Press, Tunbridge Wells.
30 McPherson, P.H., Okamura, M.Y. and Feher, G. (1988) Biochim. Biophys. Acta 934, 348–368.
31 Duniec, J.T. and Thorne, S.W. (1981) FEBS Lett. 126, 1–4; and (1983) Bull. Math. Biol. 45, 69–90.
32 Zimanyi, L. and Garab, G. (1982) J. Theor. Biol. 95, 811–821.
33 Klapper, I., Hagstrom, R., Fine, R., Sharp, K. and Honig, B. (1986) Proteins 1, 47–59.
34 Kamp, F., Chen, Y. and Westerhoff, H.V. (1988) Biophys. Chem. 30, 113–132.
35 Westerhoff, H.V., Melandri, B.A., Venturoli, G., Azzone, C.F. and Kell, D.B. (1984) Biochim. Biophys. Acta 768, 257–292.
36 Warshel, A., Russel, S.T. and Churg, A.K. (1984) Proc. Natl. Acad. Sci. USA 81, 4785–4789.
37 McLaughlin, S. (1977) in Current Topics in Membranes and Transport (Bonner, F. and Kleinzeller, A., eds.), Vol. 9, pp. 71–144, Academic Press, New York.
38 Glasstone, S., Laidler, K.J. and Eyring, H. (1941) The Theory of Rate Processes, McGraw-Hill, New York.
39 King, E.L. and Altman, C. (1956) J. Phys. Chem. 60, 1375–1378.
40 Cleland, W.W. (1963) Biochim. Biophys. Acta 67, 104–137.
41 Frauenfelder, H. and Wolynes, P.G. (1985) Science 229, 337–345.
42 Welch, G.R., Somogyi, B. and Damjanovich, S. (1982) Prog. Biophys. Mol. Biol. 39, 109–146.
43 Kamp, F. and Szabo, A. (1988) Cell Biophys. 12, 145–155.
44 Kamp, F., Welch, G.R. and Westerhoff, H.V. (1988) Cell Biophys. 12, 201–235.
45 Marcus, R.A. and Sukin, N. (1985) Biochim. Biophys. Acta 811, 265–322.
46 Richardson, I.W., Licko, V. and Bartoli, E. (1973) J. Membrane Biol. 11, 293–308.
47 Hladky, S.B. (1988) in Current Topics in Membranes and Transport (Agnew, W.S., Claudio, T. and Sigworth, F.J., eds.), Vol. 33, pp. 15–33, Academic Press, San Diego.
48 Läuger, P. (1973) Biochim. Biophys. Acta 311, 423–441.
49 Cooper, K., Jacobson, E. and Wolynes, P. (1985) Prog. Biophys. Mol. Biol. 46, 51–96.
50 Lieb, W.R. and Stein, W.D. (1974) Biochim. Biophys. Acta 373, 165–177.
51 Stark, G., Ketterer, B., Benz, R. and Läuger, P. (1971) Biophys. J. 11, 981–994.
52 Lieb, W.R. and Stein, W.D. (1974) Biochim. Biophys. Acta 373, 178–196.
53 Walz, D. and Caplan, S.R. (1988) Cell Biophys. 12, 13–28.
54 Haldane, J.B.S. (1930) Enzymes, Longmans, Green & Co., London (reprinted 1965, M.I.T. Press, Cambridge, MA).
55 Essig, A. and Caplan S.R. (1981) Proc. Natl. Acad. Sci. USA 78, 1647–1651.
56 Hansen, U.P. Gradmann, D., Sanders, D. and Slayman, C.L. (1981) J. Membr. Biol. 63, 165–190.
57 Chapman, J.B., Johnson, E.A. and Kootsey, J.M. (1983) J. Membrane Biol. 74, 139–153.
58 Tanford, C. (1981) Proc. Natl. Acad. Sci. USA 78, 270–273.
59 Hill, T.L. and Eisenberg, E. (1981) Q. Rev. Biophys. 14, 463–511.
60 Stolz, B. and Walz, D. (1990) in Current Research in Photosynthesis (Baltscheffsky, M., ed.) Vol. 2, pp. II.8.809–812, Kluwer, Dordrecht.
61 Pietrobon, D. and Caplan, S.R. (1985) Biochemistry 24, 5764–5776.
62 Zoratti, M., Favaron, M., Pietrobon, D. and Azzone, G.F. (1986) Biochemistry 25, 760–767.
63 Pietrobon, D., Zoratti, M., Azzone, G.F. and Caplan. S.R. (1986) Biochemistry 25, 767–775.
64 Rothschild, K.J., Elias, S.A., Essig, A. and Stanley, H.E. (1980) Biophys. J. 30, 209–230.
65 Page, M.G.P., Rosenbusch, J.P. and Yamato, I. (1988) J. Biol. Chem. 263, 15897–15905.
66 Kaczorowski, G.J., Robertson, D.E. and Kaback, H.R. (1979) Biochemistry 18, 3697–3704.
67 Garcia, M.L., Viitanen, P., Foster, D.L. and Kaback, H.R. (1983) Biochemistry 22, 2524–2531.
68 Viitanen, P., Garcia, M.L., Foster, D.L., Kaczorowski, G. and Kaback, H.R. (1983) Biochemistry 22, 2531–2536.
69 Viitanen, P., Garcia, M.L. and Kaback, H.R. (1984) Proc. Natl. Acad. Sci. USA 81, 1629–1633.
70 Page, M.G.P. (1987) Biochim. Biophys. Acta 897, 112–126.
71 Läuger, P. (1984) Biochim. Biophys. Acta 779, 307–341.
72 Krab, K. and Wikström, M. (1987) Biochim. Biophys. Acta 895, 25–39.
73 Gräber, P., Junesch, U. and Schatz, G.H. (1984) Ber. Bunsenges. Phys. Chem. 88, 599–608.
74 Rottenberg, H. (1985) in Modern Cell Biology (Satin, B., ed.), Vol. 4, pp. 47–83, Alan R. Liss, New York.
75 Pick, U., Weiss, M. and Rottenberg, H. (1987) Biochemistry 26, 8295–8302.
76 Kamp, F., Astumian, R.D. and Westerhoff, H.V. (1988) Proc. Natl. Acad. Sci. USA 85, 3792–3796.
77 Mitchell, P. (1961) Nature 191, 144–148.
78 Mikulecky, D.C. (1979) Biophys. J. 25, 323–340.
79 Ferguson, S.J. (1985) Biochim. Biophys. Acta 811, 47–95.
80 Dilley, R.A., Theg, S.M. and Beard, W.A. (1987) Annu. Rev. Plant Physiol. 38, 348–389.
81 Theg, S.M. and Junge, W. (1983) Biochim. Biophys. Acta 723, 294–307.
82 Westerhoff, H.V. and Chen, Y. (1985) Proc. Natl. Acad. Sci. USA 82, 3222–3226.
83 Naftalin, R.J. (1984) Biochim. Biophys. Acta 778, 155–175.
84 Caplan, S.R. (1981) Proc. Natl. Acad. Sci. USA 78, 4314–4318.
85 Stucki, J.W. (1980) Eur. J. Biochem. 109, 269–283.
86 Walz, D. (1983) in Biological Structures and Coupled Flows (Oplatka, A. and Balaban, M., eds.), pp. 45–60, Academic Press, New York.
87 Nicholls, D.G. (1974) Eur. J. Biochem. 50, 305–315.
88 O'Shea, P.S., Petrone, G., Casey, R.P. and Azzi, A. (1984) Biochem. J. 219, 719–726.
89 Krishnamoorthy, G. and Hinkle, P.C. (1984) Biochemistry 23, 1640–1645.
90 Brown, G.C. (1989) J. Biol. Chem. 264, 14704–14709.
91 Junesch, U. and Gräber, P. (1987) Biochim. Biophys. Acta 893, 275–288.
92 Bamberger, E.S., Rottenberg, H. and Avron, M. (1973) Eur. J. Biochem. 34, 557–563.
93 Rottenberg, H., Grunwald, T. and Avron, M. (1972) Eur. J. Biochem. 25, 54–63.
94 Heldt, H.W., Werdan, K., Milovancev, M. and Geller, G. (1973) Biochim. Biophys. Acta 314, 224–241.
95 Walz, D., Goldstein, L. and Avron, M. (1974) Eur. J. Biochem. 47, 403–407.
96 Krause, G.H. and Heber, U. (1976) in The Intact Chloroplast (Barber, J., ed.), pp. 171–214, Elsevier, Amsterdam.
97 Gimmler, H. (1977) in Encyclopedia of Plant Physiology: Photosynthesis I (Trebst, A. and Avron, M., eds.), Vol. 5, pp. 448–472, Springer-Verlag, Berlin.
98 Pietrobon, D. and Caplan, S.R. (1986) Biochemistry 25, 7682–7696.

99 Pietrobon, D. and Caplan, S.R. (1987) Biochim. Biophys. Acta 895, 241–258.
100 Gromet-Elhanan, Z. and Weiss, S. (1989) Biochemistry 28, 3645–3650.
101 Wikström, M. (1987) Chem. Scr. 27B, 53–58.
102 Wikström, M. (1989) Nature 338, 776–778.
103 Tollin, G., Meyer, T.E. and Cusanovich, M.A. (1986) Biochim. Biophys. Acta 853, 29–41.